博士論文

論文題目

Molecular analyses of *Toxoplasma gondii* protein kinase signals in parasite growth and differentiation

(トキソプラズマの増殖および分化に関わる

原虫プロテインキナーゼシグナルの分子生物学的解析)

氏名

杉　達紀

Contents

Preface: Aims and scope of the thesis 5

General Introduction 7

Toxoplasmosis 7

Toxoplasma gondii life cycle 8

Current status of Toxoplasmosis prevention 8

Bradyzoite differentiation 10

MAPK signal in *T. gondii* 11

Chapter 1 13

Abstract 14

Introduction 15

Materials and Methods 17

Results 23

Discussion 27

Figure legends 29

Figures 31

Chapter 2 34

Abstract 35

Introduction 36

Materials and Methods 37

Results and Discussion 39

Conclusion 42

Figure legends 43

Figures 44

Chapter 3 46

Abstract 47

Introduction 49

Materials and Methods 51

Results 60

Discussion 67

Tables 73

Figure legends 87

Figures 93

Chapter 4 99

Abstract 104

Introduction 105

Materials and Methods 107

Results 111

Discussion 114

Figure legends 116

Figures 118

General Conclusion 123

Acknowledgments.....127

References 128

List of publications 143

Summary in Japanese 146

Preface: Aims and scope of the thesis

Toxoplasma gondii (T. gondii) is a causative pathogen of the Toxoplasmosis. Because of the feasibility of genetical manipulation and in vitro culture systems, *T. gondii* is also an important model organisms for the study of the Apicomplexan pathogens including *Plasmodium*, *Neospora* and *Cryptosporidium*.

For the treatment of toxoplasmosis, several good drugs such as antifolate, spiramycine and clindamycine are used nowadays. However, parasites evade drug treatment by differentiating to bradyzoite in the tissue cyst and latently infect. Atovaquon and endochin-like quinolones have been reported to eradicate the tissue cyst in the mouse infection model so far, but conventional drug treatment cannot eradicate the tissue cyst. Therefore, to serve the new drug target and reveal the mechanisms for the bradyzoite differentiation are needed for the further anti-*T. gondii* treatment.

Protein kinase of parasite is one of the new druggable target. Several inhibitors have been reported to suppress parasite growth and genomic analysis showed the unique protein kinases which are not conserved in the mammalian genomes, are encoded in the parasite genome. Protein kinase signal is also implicated in the stress responses and bradyzoite differentiation of parasites. Therefore, protein kinases are the promising study target for the drug target validation and also for the mechanisms of the latent infection. Previous works used inhibitors to elucidate the role of protein kinase signals in the parasite life cycle; however, target genes are remained to be unidentified. Unraveling the target signals with the chemical genetics approach will uncover the mechanisms underlying parasite elaborate life cycle, and furthermore, will lead to identification of drug target.

In the present thesis, the author described molecular mechanisms of *T. gondii* protein kinase signals in parasite growth and differentiation, primarily with regard to the drug target validation of the parasite protein kinase signals.

In the **General Introduction**, diseases caused by the *T. gondii* and characteristics in the bradyzoite differentiation, which is one of the key problems for the treatment of parasite, are summarized. Known and suggested functions of the parasite protein kinases in bradyzoite differentiation are overviewed for the background of the present thesis.

In **Chapters 1 and 2** in this thesis, the author characterized and evaluated the parasite specific drug class of protein kinase analog, bumped kinase inhibitor (BKI). The author also described the new protein kinase analysis tools in *T. gondii* by the use of BKI.

In **Chapter 3**, in order to evaluate the drug potential of BKI, the author studied the mechanisms of resistance acquisition. By the use of random mutagenesis, the author established parasites clones resistant to 4-Amino-1-tert-butyl-3-(1′-naphthylmethyl)pyrazolo[3,4-d]pyrimidine (1NM-PP1), which is one of the bumped kinase inhibitors. The author identified the gene, *T. gondii* mitogen-activated protein kinase 1 (TgMAPK1), which is responsible for the resistance and is one of the targets by the BKI.

In **Chapter 4**, the author characterized the resistant parasite clones and revealed the cell division retardant effect by 1NM-PP1 was decreased in the resistant clones. By the use of parasite clones with mutation in TgMAPK1, the author analyzed the role of TgMAPK1 in switching cell division and cell differentiation from tachyzoite to bradyzoite.

In **General Conclusion,** the author summarized the data in the thesis collectively and remarked the conclusion.

General Introduction

Toxoplasmosis

Toxoplasmosis is a disease caused by the infection of protozoan pathogen, *Toxoplasma gondii* (*T. gondii*).

Infection rate of parasites to host animals including humans (Pappas et al., 2009) and domestic animals (Jones and Dubey, 2012; Tenter et al., 2000) is high all over the world. In Japan, Sakikawa *et al.* reported that 10.3% human pregnant woman assayed were seropositive for the *T. gondii* (Sakikawa et al., 2012).

Acute infection with *T. gondii* to humans usually goes to asymptomatic infection (Remington, 1974). Infected parasites differentiated from fast replicating tachyziote to dormant bradyzoite in cyst and infect latently (Black and Boothroyd, 2000).

When the infection or reactivation of latent infected parasites occurs in immunocompromized host, such as HIV-infected patients, organ transplanted patients and infants, the parasites causes acute Toxoplasmosis accompanied by the encephalitis, penumonitis and chorioretinitis (Wulf et al., 2005).

Transplacental infection of parasites to infants leads to congenital Toxoplasmosis. Symptoms are dependent on when the parasites infected infants. Patients with severe congenital toxoplasmosis have retinochoroiditis (common), hydrocephalus, microcephaly convulsions or intracranial calcification (rare) (Alford et al., 1974).

Domestic animals are also infected with *T. gondii*. Toxoplasma infection is important because of the pathogenesis such as abortion in sheep and goats and diarrhea in domestic cats. Not only animals themselves affected by the parasite, but also latent infected parasites in the meat production animals (tissue cyst), and oocyst shed from

infected cat are also important for the source of infection.

Toxoplasma gondii life cycle

To prevent the Toxoplasmosis in humans and animals, understanding of life cycle of *T. gondii* is very important. *T. gondii* sexual stage is observed only in the intestine of the definitive host cat and oocysts are excreted in infected cat feces (Dubey et al., 1970; Frenkel et al., 1970). Sporulated oocyst can infect divergent intermediate host animals from mammals to birds (Miller et al., 1972). Parasites undergo asexual stage in the infected host. Asexual stage consists of fast replicating tachyzoite and dormant bradyzoite in the tissue cyst (Black and Boothroyd, 2000). In mouse infection models with oral infection, initial proliferation of tachyzoite is observed in intestinal tissue (Gregg et al., 2013). After initial replication, tachyzoite utilizes infected immune cells as the vehicle for the prevalence in the tissue among the whole body (Coombes et al., 2013; Unno et al., 2008). Tachyzoite can pass the placenta by the mechanisms not fully characterized and infect infants and cause congenital Toxoplasmosis (Alford et al., 1974). In the latent infection stage, tachyzoite turns in bradyzoite which replicates slowly in the tissue cyst (Black and Boothroyd, 2000) in the tissues including brain, skeletal muscle, heart and kidneys (Dubey, 1997). Bradyzoite in meat is needed for the efficient parasite infection to the next host animals (Jones and Dubey, 2012). When the host animals lose their immunocompetence, bradyzoite can reactivate to become tachyzoite causing Toxoplasmosis (Nissapatorn, 2009).

Current status of Toxoplasmosis prevention

Prevention of Toxoplasmosis is divided into two strategies: **1) prevention of infection**,

and **2) prevention of symptoms** by inhibiting parasites growth in the infected host.

1) Prevention of infection.

As described in '*Toxoplasma gondii* life cycle' section above, infections are occurred by the ingestion of oocyst in infected cat feces or tissue cyst in infected meat production animals. Therefore, public health improvement with the cat feces and food safety is undertaken. Tachyzoite in the pregnant maternal host can infect the infant. Therefore, anti-parasitic drug treatment is used for the prevention of intraplacental infection (McLeod et al., 2009). Vaccination of Toxopasmosis is not applicable for human so far. Successful live attenuated vaccine for prevention of Toxoplasmosis abortion in sheep is commercially available. S48 strain in live vaccine Toxovax® (MSD Animal Health, New Zealand) was reported to lose its capacity to form cyst in meat (O'Connell et al., 1988). And several reports showed that cystgenesis in meat was protected with Toxovax® vaccination (Innes et al., 2009).

2) Prevention of symptoms by inhibiting parasites growth in the infected host.

When the infection in the high risk patients, such as infants in pregnant women and immunocompromized patients is detected, treatment with spiramycine, pyrimethamine, sulfadiazine/trimethoprim, or clindamycin are undertaken dependent on the patients status (Petersen and Liesenfeld, 2007) to control tachyzoite replication. Toxoplasmosis in HIV-infected patients is well controlled with highly active anti-retroviral treatment (HAART), which prevents patients from the loss of immune system (Vidal et al., 2005). Risk of congenital Toxoplasmosis can be reduced by the anti-parasitic drug treatment (McLeod et al., 2009). Drug treatment should be accompanied with diagnostics at the appropriate periods (McLeod et al., 2009).

Bradyzoite differentiation

Bradyzoite differentiation is related to the latent infection and the production of tissue cyst which is the source of infection and reactivated acute Toxoplasmosis. Bradyzoite is also notorious for evading from the drugs usually used (Gormley et al., 1998) except for the atovaquon. Cell division remarkably decreases in bradyzoite stages, and bradyzoite is thought to be the differentiated cell state of G0 cell division cycle (Bohne et al., 1994). Recently, transcriptome aspect of bradyzoite differentiation was uncovered markedly (Behnke et al., 2008). In the time course of bradyzoite differentiation, several ApiAP2 transcription factors are reported to regulate the transcriptional transition between tachyzoite and bradyzoite (Radke et al., 2013; Walker et al., 2013). *In vivo* mechanisms of bradyzoite differentiation were not fully understood, however, tropism of tissue cyst in brain, skeletal muscle, kidney and lung (Dubey, 1997) suggests that some host or environmental factors may be sensed by parasites. *In vitro* bradyzoite inducing system uses environmental stresses such as high pH, NO radical treatment and nutrient depletion to make the parasite express bradyzoite specific transcription and to make the parasite replicate slowly (Bohne et al., 1994). Eukaryotic initiation factor 2 alpha signals are reported to bridge stress response to the bradyzoite differentiation (Narasimhan et al., 2008; Sullivan et al., 2004).

To elucidate the signals which regulate bradyzoite differentiation, inhibitor based studies revealed that protein kinases are related to the bradyzoite differentiation. The inhibitors of cAMP and cGMP signals (Eaton et al., 2006; Hartmann et al., 2013), and Mitogen-activated protein kinase (MAPK) inhibitors (Unno et al., 2009; Wei et al., 2002) induce parasites to differentiate to bradyzoite form. It remains unknown so far which parasite genes are the target of the inhibitors. Coccidian cyclic GMP dependent

protein kinase (PKG) specific inhibitor ‘compound 1’ also induces bradyzoite differentiation dependent on strain used (Radke et al., 2006). Radke *et al.* showed inhibition of the target signal in host cell by ‘compound 1’ results in human cell division autoantigen-1 (hCDA1) upregulation and subsequent bradyzoite differentiation of parasites (Radke et al., 2006).

MAPK signal in *T. gondii*

MAPKs function in other eukaryotes showed that the signals regulate cell proliferation, cell differentiation via post translational modification of the downstream transcriptional factors and leads to transcriptional changes, the cell cycle progression, cell differentiation, and stress responses (Zhang and Liu, 2002).

MAPK cascades are parallel signaling pathways that mediate the intracellular transmission of various cellular stimulations. MAPKs are conserved in eukaryotic cells from unicells to multicellular organisms. MAPK is activated by the 3 to 4 tier protein kinase cascade, called MAPK kinase (MAPKK), MAPKK kinase (MAP3K), and MAP3K kinase (MAP4K) (Zhang and Liu, 2002).

Inhibitor work using SB203580 and SB21090 targeting mammalian p38-alpha showed that MAPK signals are related to the bradyzoite differentiation (Wei et al., 2002). Wei *et al*. reported the resistant parasites to SB203580, suggesting the target protein kinase signal is in the *T. gondii* (Wei et al., 2002).

T. gondii have the 3 MAPK homolog coded in its genome. TgMAPK1 (TGME49_312570) was reported to be the stress responsible MAPK (Brumlik et al., 2004).Transcriptome analysis showed that no obvious changes in mRNA level by the stress condition (Behnke et al., 2008). TgMAPK2 (ERK7 like TGME49_233010) was

reported to have protein kinase activity *in vitro* (Huang et al., 2011). The other putative MAPK (TGME49_207820) has not been characterized yet.

Even though *T. gondii* has MAPK homologs, no upstream MAPKK is detected in the *T. gondii* genome (Miranda-Saavedra et al., 2012). This lack of the conserved MAPK cascade suggested the unique activation mechanisms of *T. gondii* MAPKs and attracts as the drug target.

To elucidate the MAPK function in cell proliferation regulation in parasite and evaluate it as the drug target, the author suggested that the need for the functional analysis of MAPK in parasite life cycle, which is lacked in former studies.

Chapter 1

Analysis of *Toxoplasma gondii* CDPK1 by the use of analog sensitive kinase allele (ASKA)-based gene inhibition (ASKA-GI)

Submitted and published in EUKARYOTIC CELL, Apr. 2010, p. 667–670

Abstract

When we analyze protein kinase function in the cells, the kinase specific inhibitors provide powerful tool. The technologies which enable such tools for any kinases are analog sensitive kinase allele (ASKA)-based gene inhibition (ASKA-GI). The objective of this chapter was application of ASKA-GI to *Toxoplasma gondii* (*T. gondii*) kinase analyses. First the author revealed that an ASKA specific inhibitor, 1NM-PP1, had the Toxoplasma inhibitory activity. To find the target of this inhibitor, the author analyzed kinase genes in genome of *T. gondii*. With computational analyses 114 kinases were found to have invariant amino acid for phosphorylation activity. With kinase subdomain structure assignment and simple amino acid sequence alignments, the author confirmed that *T. gondii* calmodulin-like domain protein kinase (TgCDPK1), which was the unique kinase having the smallest amino acid glycine at the amino acid site which determines inhibitor analog sensitivity. Wild type and mutated analog insensitive TgCDPK1G128M, were expressed as GST and 6 x histidine-tagged fusion proteins using the baculovirus expression system. GST-TgCDPK1 and GST-TgCDPK1G128M were inhibited by 1NM-PP1 with 50% inhibitory concentrations (IC_{50}, in μM) of 0.9 and 2,400, respectively. TgCDPK1G128M-expressing parasites successfully recovered the capacity in the host monolayer disruption, invasion and gliding motility assays. The author showed that ASKA-GI is applicable for *T. gondii* protein kinase analysis. By the use of ASKA-GI, the author showed that TgCDPK1 functions in the invasion step.

Introduction

Several reports have shown that kinases function at the *Toxoplasma gondii* (*T. gondii*)invasion steps, including attachment (Kieschnick et al., 2001), secretion of microneme and subsequent invasion (Carruthers and Sibley, 1999; Kato et al., 2008). Several factors in the invasion mechanism have been reported to be phosphorylated (Gilk et al., 2009; Green et al., 2008). However, the candidate kinases have not been completely described so far. As reverse genetic approaches of this pathogen to essential genes, several tools have been developed, including conditional knock-down using Tet-Off system (Meissner et al., 2002), RNAi (Al Riyahi et al., 2006), and conditional proteolysis-based gene suppressing (Herm-Gotz et al., 2007). These methods are very useful for analyzing indispensable genes. However, they have some weak points. The gene suppression was not so instant in the conditional knock-down (Meissner et al., 2002). The proteolysis knock-down is dependent on genes to be analyzed (Herm-Gotz et al., 2007). Therefore, in the present report, the author tried to use analog sensitive kinase allele (ASKA)-based gene inhibition (ASKA-GI) using small compound as a regulation trigger.

ASKA is a kinase, whose gate keeper amino acid which determines the susceptibility to the inhibitor analog, is replaced from a bulky amino acid (insensitive) to a small amino acid (sensitive) (Bishop et al., 2000). The mutated kinases have been reported to function normally except inhibitor susceptibility *in vivo* (Shokat and Velleca, 2002). Wild type protein kinases have bulky amino acid at the gatekeeper residue and insensitive to inhibitor analog. Therefore, inhibitor analog can target analog sensitive mutated kinase selectively. ASKA-GI has been reported to be used for kinase analysis in several species (Salomon et al., 2009) and the attempt to application of this method to *Plasmodium*

kinase was described in the review (Doerig, 2004). On application of ASKA-GI to *T. gondii,* one assumption is needed. That is, *T. gondii* should have no or few ASKAs in the genome ideally.

In this study, the author confirmed inhibitory effect on parasite growth by 1NM-PP1, PP1 analog specific to the ASKA. Next, the author analyzed the kinome of *T. gondii* with the viewpoint of application of ASKA-GI and found putative ASKA TgCDPK1. TgCDPK1 has been reported to be in the process of invasion (Kieschnick et al., 2001) and thought to play a role in Ca^{2+} signal transduction (Billker et al., 2009). Second the author characterized the inhibition of TgCDPK1 kinase activity by 1NM-PP1 using *in vitro* kinase assay. Finally the author revealed that TgCDPK1 was the target of 1NM-PP1 in the invasion step by using analog insensitive TgCDPK1 expressing parasites. The author suggested that ASKA-GI, which is powerful tool for the kinase research, is applicable for analyzing kinases of *T. gondii*.

Materials and Methods

T. gondii culture

Tachyzoites of *T. gondii* RH and RH/ht$^-$ (kindly provided by Dr. X. Xuen) strains were used in this study. The parasites were maintained in monolayers of Vero cells cultured in Dulbecco's modified Eagle's medium (DMEM) that contained 7.5% fetal calf serum (FCS), 2 mM L-glutamine, 20 mM HEPES (pH 7.5), streptomycin, and penicillin. The host Vero cells were maintained in the same medium.

T. gondii kinome analysis

T. gondii kinases were retrieved from *T. gondii* genome for the computational analyses as follows. Firstly, proteins which contains interpro domain IPR011009, hidden Markov model of Protein kinase-like (PK-like) superfamily, were retrieved from ToxoDB (Gajria et al., 2008). The resultant protein list was further evaluated for kinase domain with the threshold of SMART (Letunic et al., 2009). Finally, the kinases were checked if it has the catalytic aspartate by KinG (Krupa et al., 2004). The 2nd structures of kinases were predicted with Psipred (Jones, 1999) and were also taken into consideration when subdomain structures were predicted.

Plasmids

T. gondii RH strain total RNA was isolated from the infected Vero cells using the TRIZOL reagent (Invitrogen, Carlsbad, CA, USA) according to the manufacturer's instructions. The entire TgCDPK1 open reading frame (ORF) was amplified by RT-PCR using the parasite total RNA as a template and the following primers: forward,

5′-CCGCCTCGAGCGGGCAGCAGGAAAGCACTCT-3′ and reverse, 5′-CCCAAGCTTAGTTTCCGCAGAGCTTCA-3′. The amplified fragment was digested with *Xho*I/*Hin*dIII and cloned into the *Xho*I/*Hin*dIII sites of pBluescript II KS+ (Stratagene, La Jolla, CA, USA). The resultant plasmid was designated pBS-TgCDPK1-stop. The pAcGHLT-TgCDPK1 construct (Fig. 1B) was generated by inserting the *Xho*I-*Not*I fragment of pBS-TgCDPK1-stop into pAcGHLT-C (BD bioscience, San Jose, CA, USA) to express a glutathione S-transferase (GST) fusion protein. Analog insensitive kinase mutant, TgCDPK1^{G128M}, expressing vector pAcGHLT-ai-TgCDPK1 was constructed from pAcGHLT-TgCDPK1 using the QuickChange Site-Directed Mutagenesis Kit (Stratagene), according to the manufacturer's instructions (Fig. 1A). For the expression of TgCDPK1^{G128M} in parasites, a GFP coding sequence of pMini.GFP.ht (Karasov et al., 2005) (kindly provided by Dr. G. Arrizabalaga) was replaced with a 3xFlag sequence from the p3xFlag-CMV vector (Sigma, St. Louis, MO, USA) and designated as pMini.3xFlag.ht. The CDPK1^{G128M} ORF was amplified from pGST-CDPK1^{G128M} with the primers 5′-GAAGATCTGGGGCAGCAGGAAAGC-3′ and 5′-GGGGTACCGAGTTTCCGCAGAGCTTC-3′, and cut with *Bgl*II/*Kpn*I and inserted into the same site of pMini.3xFlag.ht before the 3xFlag coding sequence and designated as pMini.TgCDPK1^{G128M}.3xFlag.ht (Fig. 1C).

Parasite transfection

Transfection of expression plasmid to *T. gondii* RH/ht^{-} was performed as described previously (Karasov et al., 2005). Briefly, 30 μg of plasmid DNA was electroporated into 5.0 × 10^7 parasites with GenePulser X at 2000 V, 25 μF, 50 ohm. From 24 h after

transfection, parasites were selected by 50 μg/ml mycophenolic acid and xanthine. After the limited dilution, TgCDPK1^{G128M} stably expressing clone RH/TgCDPK1^{G128M}FLAG was used for the further analysis.

Generation of recombinant baculoviruses

pAcGHLT-TgCDPK1 or pAcGHLT-TgCDPK1^{G128M} was co-transfected with linearized baculovirus DNA BaculoGold (BD bioscience) into Sf9 cells using Cellfectin (Invitrogen), as described previously (Kato et al., 2001), to generate recombinant baculoviruses that were designated as Bac-GST-TgCDPK1 or Bac-GST-TgCDPK1^{G128M}, respectively. The recombinant viruses were subsequently amplified in Sf9 cells.

Purification of recombinant proteins

The purification of recombinant proteins expressed in Sf9 cells infected with Bac-GST-TgCDPK1 or Bac-GST-TgCDPK1^{G128M} was performed as described elsewhere (Sugi et al., 2009). Briefly, Sf9 cells (1.0×10^6) infected with each baculovirus in 0.5 ml of ice-cold buffer C (50 mM Tris-HCl pH 7.5, 100 mM NaCl, 5 mM $MgCl_2$, 0.1% Nonidet P-40, 10% glycerol and 1 mM PMSF) were lysed by ultrasonication. After insoluble material was removed by centrifugation, the supernatants were mixed with 150 μl of a 50% slurry of glutathione-Sepharose beads (BD bioscience) for 2 h. The beads were extensively washed with buffer C and eluted with elution buffer (10 mM glutathione and 500 mM Tris-HCl, pH 8.0). Next, the eluted supernatants were reacted with Ni^{2+}-NTA agarose beads (Qiagen, Hilden, Germany) for 1 h. The beads were then washed three times with buffer C and used for the *in vitro* kinase assay.

***In vitro* kinase assay**

The author carried out *in vitro* kinase assays as described previously (Sugi et al., 2009). Purified kinases captured on Ni^{2+}-NTA agarose beads was rinsed twice with washing buffer (50 mM Tris–HCl [pH 9.0], 2 mM DTT) and incubated for 10 min at 37 ºC in a 25µl reaction mixture containing 1uCi of [γ-^{32}P] ATP and the varying concentrations of 1NM-PP1 (Merck KGaA, Darmstadt, Germany) or DMSO in kinase buffer (50 mM Tris–HCl [pH 8.0], 200 mM NaCl, 50 mM MgCl2, 0.1% Nonidet P-40, 1 mM DTT, 5 mM ATP).

Invasion assay

T. gondii tachyzoites were purified with 5 µm pore filter (Millipore, Billerica, MA, USA) and treated with the varying concentrations of 1NM-PP1 or DMSO for 10 min before inoculation. Confluent Vero cells on the chamber slides were infected with $1.0*10^6$ parasites/ml for 30 min 37 ºC in the infectious medium (DMEM containing 2% FCS) with the varying concentrations of 1NM-PP1 or DMSO. After incubation, cells were fixed with 4% paraformaldehyde for 20 min at room temperature. Extracellular parasites were stained with α-SAG1 monoclonal antibody [TP3] (Hytest, Finland) 30 min at room temperature, washed three times with PBS(-), permeabilized with 0.1% Triton X-100/PBS(–) for 30 min at room temperature, and whole tachyzoites were reacted with rabbit α-tachyzoite polyclonal antibody. After reaction with the first antibody, slides were washed 3 times with PBS(-), and reacted with secondary antibody (Alexa 546-conjugated anti-rabbit IgG and Alexa 488-conjugated anti-mouse IgG) for 1 h at room temperature, followed by five washes with 0.1% Tween-20. The stained samples were dried at room temperature, mounted under a cover glass, and observed using a

confocal laser scanning microscope (Carl Zeiss, Oberkochen, Germany).

Microneme secretion assay

Excreted and secreted antigen (ESA) was obtained as previously reported (Carruthers et al., 1999) with some modifications. In brief, parasites were incubated at 18 ºC for 10 min with reagent tested, followed by incubation at 37 ºC for 30 min after the addition of 1% (v/v) ethanol. Cells were removed by centrifugation at 4,000 g and the supernatant was used for western blotting (WB). For the detection of ESA, anti-TgM2AP rabbit antibody (Rabenau et al., 2001) (kindly provided by Dr. V. Carruthers) were used.

Monolayer Disruption Assays

To check the tachyzoite life cycle overall, host cell monolayer disruption were measured as described previously (Roos et al., 1994). Briefly, 96 well plates with confluent Vero cells were inoculated with 1.0×10^4 parasites in 200μl infectious medium (DMEM with 2% FCS) containing the tested reagent or DMSO at each concentration. About 4 days after inoculation, wells were washed with PBS(-) 3 times and fixed methanol for 5 min, and stained using crystal violet.

Gliding motility assay

Gliding motility was observed as described previously (Wetzel et al., 2003). Slide glasses were coated with 50% FCS-PBS (-) for 30 min 37 ºC before used for the gliding motility assay. Purified parasites were incubated in the infectious medium with tested reagent for 10 min at room temperature, and applied to the coated slide glass. After 15 min incubation at 37 ºC, slides were fixed with 4% paraformaldehyde in PBS(-). Fixed

slides were stained with α-SAG1 monoclonal antibody [TP3] and Alexa488 anti-mouse IgG.

Results

Kinome of T. gondii

Feasibility of application of ASKA-GI to a species depends on how less wild type analog sensitive kinases (as-kinases) appear in kinome of the target species. Therefore, the author needed to know the functional kinase set of *T. gondii*. From the computational analysis, 114 genes having functional kinase domain were retrieved. First, the author selected the genes consisting protein kinase like superfamily, which have interpro domain IPR011009, from the *T. gondii* strain ME49 genome at ToxoDB (http://www.toxodb.org/). At this step, the author obtained 186 genes. Next, the obtained 186 genes were tested whether they had functional kinase domain or not, using KinG (http://hodgkin.mbu.iisc.ernet.in/~king/) and annotations of the genes in ToxoDB. The tested genes were categorized into three groups: 114 kinases which have catalytic aspartate residue [28] (functional kinases), 27 kinases which do not have catalytic aspartate residue (unfunctional kinases) and 45 genes which could not be detected any kinase domain by KinG or were annotated to have incomplete catalytic kinase domain in ToxoDB. The author used the resultant 114 functional kinases as *T. gondii* kinome below.

ASKA in the T. gondii kinome

The author next checked whether 1NM-PP1 (Fig. 2A), which is an analog of tyrosine kinase inhibitor PP1 and has been reported to be specific to ASKAs (Bishop et al., 2000), has toxoplasmocidal property or not. The author performed host monolayer disruption assay for the evaluation of whole life cycle of tachyzoite and 1NM-PP1 blocked the growth of parasites with $IC_{50} < 100$ nM (Fig. 2A), suggesting that wild type *T. gondii* had

ASKA in the genome. Next, the author searched ASKAs in *T. gondii* genome. The responsible residues for the gate keepers of the ATP binding pockets in the subdomain V (Salomon et al., 2009) were identified. Most of the kinases had bulky amino acid at the gate keeper residue and predicted to be insensitive to 1NM-PP1. Twelve kinases had the possibility of inhibitor sensitivity (having amino acid, threonine, serine, alanine or glycine at the gate keeper residue) (Fig. 2B). Among them, *T. gondii* calmodulin-like domain protein kinase TgCDPK1 (GenBank ID: AF333958) was unique. The gatekeeper residue of TgCDPK1 is the smallest amino acid glycine, and it is thought to be the most sensitive to 1NM-PP1.

Characterization of analog insensitive engineered kinases

Next, the author checked whether the predicted ASKA TgCDPK1 was susceptible to 1NM-PP1 in the *in vitro* kinase assay, or not. Firstly, mutated analog insensitive TgCDPK1^{G128M} was constructed by substitution of gate keeper residue 128 glycine to methionine residue (Fig. 1A). The kinases (TgCDPK1 and TgCDPK1^{G128M}) were expressed as GST fusion recombinant proteins using baculovirus expression system. GST-TgCDPK1 and GST-TgCDPK1^{G128M} were inhibited by 1NM-PP1 with 50% inhibitory concentrations (IC_{50}, in μM) of 0.9 and 2,400, respectively (Fig. 2C). These results showed that 1NM-PP1 had a potential of a specific inhibitor for TgCDPK1. And susceptibility of kinases to the 1NM-PP1 depended on the gate keeper residue Gly 128.

1NM-PP1 insensitive CDPK1 transgenic parasite

To confirm that TgCDPK1 was responsible for the activity of 1NM-PP1 in *Toxoplasma*, the author constructed the strain, which stably expresses TgCDPK1^{G128M}, designated as

RH/TgCDPK1^{G128M}FLAG. RH/TgCDPK1^{G128M}FLAG expressed TgCDPK1^{G128M} as C-terminal 3xFlag-tagged protein (Fig. 3A) and whole lysate of the infected Vero cells contained one major tagged protein with molecular mass of 60,000 as detected by WB with anti-M2-FLAG antibody, whereas no band was detected from whole lysate of mock infected Vero cell or parental strain RH/ht^{-} infected Vero cells (Fig. 3A). The author checked whether the sensitivity of parasites to the 1NM-PP1 was altered from parental strain RH/ht^{-} or not. Firstly the author checked host monolayer disruption capacity. RH/ TgCDPK1^{G128M}FLAG disrupted host cell monolayer when treated with 0.5 μM 1NM-PP1 (Fig. 3B), whereas RH/ht^{-} was not able to disrupt and host cell (Fig. 3B). Next, to confirm which step of infection was inhibited by 1NM-PP1, invasion of parasites to host cells was assayed. Treatment with 0.5 μM 1NM-PP1 reduced the invasion rate of RH/ht^{-} to less than 40%, whereas no apparent changes were detected with the RH/TgCDPK1G128MFlag strain in the 0.5 μM 1NM-PP1 treatment group (Fig. 3C). And treatment with 5 μM 1NM-PP1 reduced the invasion rate of RH/ht^{-} to less than 20%, whereas RH/TgCDPK1^{G128M}Flag retained invasion more than 60% (Fig. 3C).

To investigate which steps of the invasion were inhibited, the author next assayed the gliding motility, which enables parasites to penetrate into host cells. Without 1NM-PP1 treatment, RH/ht^{-} and RH/ TgCDPK1^{G128M}Flag showed no difference in the trail of gliding stained with anti-SAG1 antibody (Fig. 3D left panels). With 0.5 μM 1NM-PP1 treatment, however, RH/ht^{-} lost their gliding motility and no trail of gliding was seen (Fig. 3D right upper panel), whereas RH/ TgCDPK1^{G128M}Flag retained the motility (Fig. 3D right lower panel).

Finally the author checked whether ethanol-induced micronemal secretion, which was needed for gliding motility, was altered or not. With both RH/ht^{-} and RH/

TgCDPK1^{G128M}Flag strains, no obvious change was observed (Fig. 3E lanes 1-3) compared with the control experiment with 1 μM staurosporine treatment (Fig. 3E lane 5). However, the subtle changes in M2AP secreted protein amount were observed in wild type parasites.

Discussion

The author used 1NM-PP1 as a specific inhibitor to the *T. gondii* ASKA and found that the inhibitor had toxoplasmocidal effect. From computational analyses, TgCDPK1 was thought to be the candidate target of this drug. This hypothesis was confirmed by the results that parasites expressing mutated analog insensitive TgCDPK1^{G128M} successfully gained resistance for 1NM-PP1. The invasion capacity of wild-type *T. gondii* was reduced with 1NM-PP1 treatment and the contribution of TgCDPK1 to the invasion agreed with the previous report described with KT5926 (inhibitor analog which has broader spectrum than 1NM-PP1) (Kieschnick et al., 2001). The effect of 1NM-PP1 on the invasion might be partly due to the inhibition of as-kinases other than TgCDPK1 (among them, TgPKG has been reported to play a role in invasion (Donald et al., 2002)). However, the difference between 1NM-PP1 effects on invasion of RH/ht^{-} and RH/TgCDPK1^{G128M}Flag clones suggested the role of TgCDPK1 in the invasion. In the invasion steps, microneme secretion was not inhibited by 1NM-PP1 so much as staurosporine. Data in the present report failed to detect the significant inhibition of micronemal secretion by 1NM-PP1 in the western blotting analysis. Lourido *et al.* (Lourido et al., 2010) showed that TgCDPK1 plays an important role in microneme secretion. Lourido et al. uses TgCDPK1 conditional knock out parasites to show the function, therefore, the micronemal secretion function is dependent on TgCDPK1 (Lourido et al., 2010). Lourido *et al.* also used chemical genetics inhibition using 3MB-PP1 and TgCDPK1_G128M expressing parasites, and high concentration of 5 μM 3MB-PP1 resulting in inhibition of 50% micronemal secretion, whereas conditional knock out diminished almost all micronemal secretion (Lourido et al., 2010). The time span of micronemal secretion assay using inhibitor in the present study might not be

enough for inhibiting TgCDPK1 function in micronemal secretion. Micronemal secretion was reported to induced by the another signaling pathway of cGMP-dependent protein kinase (TgPKG). Another pathway can complement the micronemal secretion in the assay condition of the present study. Because staurosporine has the broad band of inhibition spectrum for the protein kinases, besides TgCDPK1, other protein kinases were inhibited, which leads to the dramatic reduce of micronemal secretion.

Our data showed that TgCDPK1 could regulate gliding motility directly. Some glideosome complex members, which provide parasites with motor function, were reported to be phosphorylated (Gilk et al., 2009; Green et al., 2008). TgCDPK1 might phosphorylate glideosome complex and change its activity. Wt-TgCDPK1 and TgCDPK1^{G128M} showed compatible kinase activity under the condition without 1NM-PP1 *in vitro*. This guaranteed further that as-mutated kinases were displaceable with wt-kinase (Bishop et al., 2001). ASKAs in *T. gondii* kinome, for example TgCDPK1, hampered the analysis of single kinase function using small compounds in *T. gondii* because leaking effect of kinase inhibitors on them are unavoidable. RH/TgCDPK1^{G128M}FLAG clone in the present report successfully acquired the resistant for 1NM-PP1. Therefore, any as-kinases knocked-in to RH/ TgCDPK1^{G128M}FLAG can be selectively and instantly inhibited by 1NM-PP1.

ASKA strategy with *T. gondii* provides us short time span functional gene suppression with low leaking effect. If the assumption that host kinome contains few ASKAs is fulfilled, ASKA strategy can be used for the analysis in secretion kinases, such as ROP2 family, which have been reported to play a role in the host modifications and to be a virulence factor (Saeij et al., 2006; Taylor et al., 2006).

Figure legends

Figure. 1. Schematic diagram of the predicted amino acid sequence of TgCDPK1 and the constructions of the expression plasmids.

(A) Domain structure and the gate keeper residue for the inhibitor analog are shown. (B) pAcGHLT-TgCDPK1 for the expression in the baculovirus expression system. (C) pMini.TgCDPK1^{G128M}.3×Flag.ht is used for the construction of TgCDPK1^{G128M} stably expressing parasite.

Figure 2. Toxoplasmocidal properties of 1NM-PP1 and its putative targets.

(A) The reduction in OD_{600} values from mock-infected wells was calculated as the monolayer disruption capacity. Capacity in the absence of 1NM-PP1 was estimated to be 100%. The structure of 1NM-PP1 is also illustrated. The standard errors of the means from triplicate experiments are shown. (B) Alignment of subdomain V of 12 predicted as-kinases and the human protein kinase A (PKA) catalytic subunit alpha are shown. The gatekeeper residues are shown in the red box. Predicted secondary structures are indicated with an S (β-sheet) or H (α-helix) on the first line. (C) Kinetics properties of GST-TgCDPK1 with substrate peptide syntide-2 and effects of 1NM-PP1 on GST-TgCDPK1 and GST-TgCDPK1G128M. Reactions were performed with 1.0 ng of kinase in 30 μl of reaction buffer (20 mM HEPES [pH 7.5], 10 mM MgCl2, 1 mg/ml bovine serum albumin, 100 μM CaCl2, 2 μM dithiothreitol, 2 μM ATP, and 5.0 μCi [γ^{32}P]ATP). For the inhibitory assay, 100 μM syntide-2 was used.

Figure 3. 1NM-PP1-resistant strain RH/TgCDPK1^{G128M}FLAG.

(A) Confirmation of FLAG-tagged TgCDPK1G128M expression in RH/TgCDPK1G128MFlag based on western blotting. Vero cells infected with RH/ht$^-$, RH/TgCDPK1G128MFlag, or mock infected were subjected to a western blot assay with the anti-M2 FLAG antibody (upper panel) or anti-*T. gondii* aldolase rabbit antibody newly raised as described previously against maltose binding protein-TgALD1 expressed in *Escherichia coli* (Sugi et al., 2009), in order to load adequate amounts of parasites. (B) Effects of 1NM-PP1 on the overall life cycle with RH/ht$^-$ or RH/TgCDPK1G128MFlag in the host monolayer disruption assay. OD_{600} values in the absence of infection and without 1NM-PP1 were estimated as 100%. (C) Effects of 1NM-PP1 on RH/ht$^-$ and RH/TgCDPK1G128MFlag during parasite invasion. Invasion rates were calculated from the number of completely invaded parasites per number of whole parasites counted. Invasion rates of RH/ht$^-$ in the absence of 1NM-PP1 were estimated as 100%. (D) Effects of 1NM-PP1 on gliding motility with RH/ht$^-$ or RH/TgCDPK1G128MFlag. Gliding trails were visualized with anti-SAG1 antibody. (E) Effects of 1NM-PP1 on secretions. The 35-kDa bands of TgM2AP are shown.

In panels C to E, parasites were pretreated with 1NM-PP1, 1 μM staurosporine (S), or DMSO (D) at the listed concentrations. In panels B and C, the standard errors of the means from triplicate experiments are shown. **: $p < 0.01$, two-tailed Student's *t*-test.

Figures

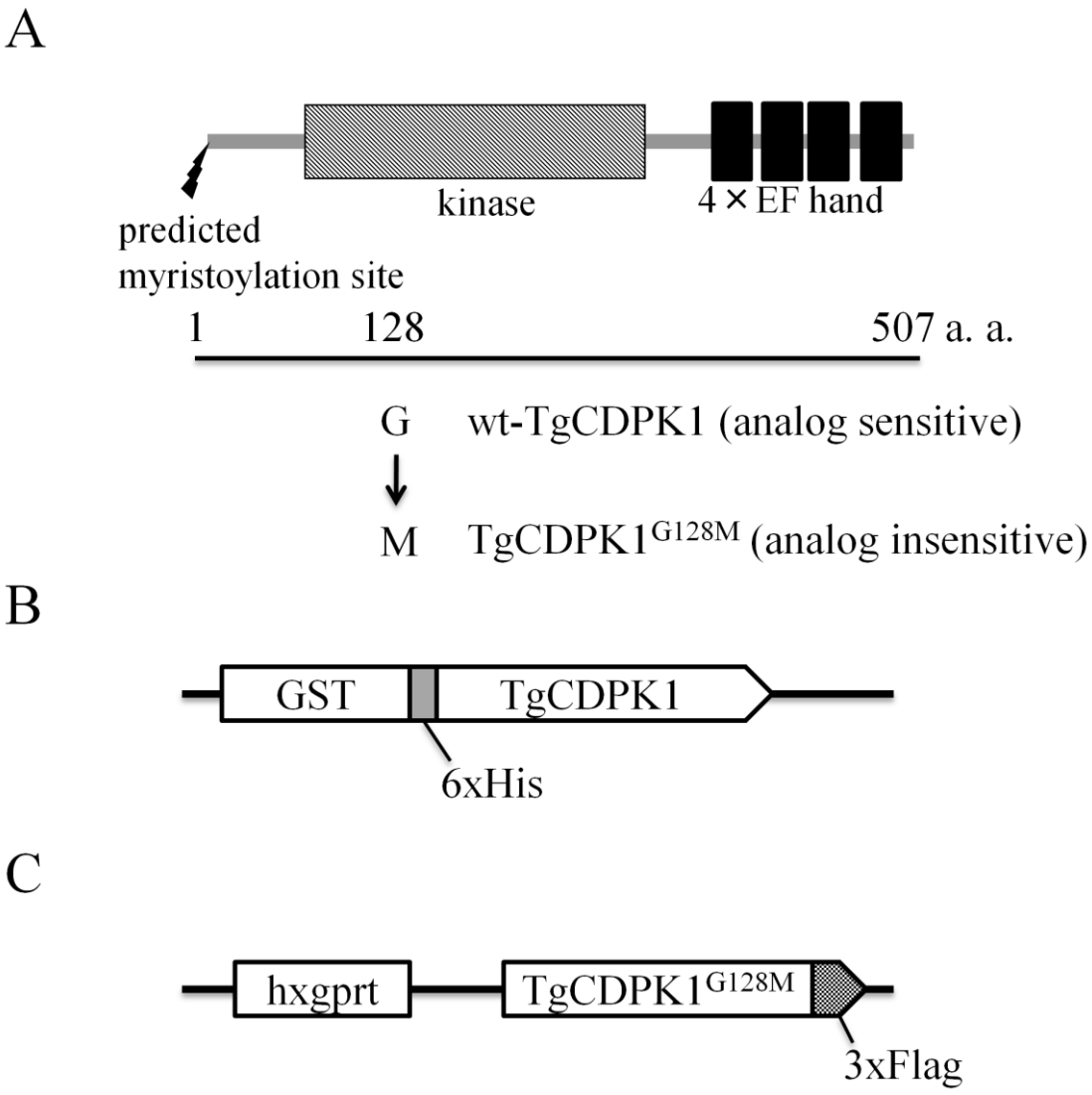

Figure 1

A

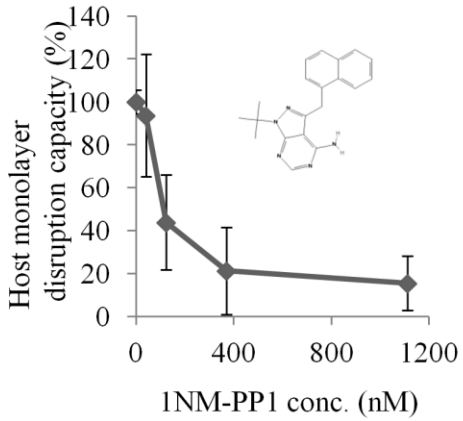

C

Properties of recombinant TgCDPK1	
*K*m (μ M)	136
*V*max (μ mol min^{-1} mg^{-1})	5
Molecular Weight (kDa)	87

IC_{50} of 1NM-PP1 (μM)	
GST-TgCDPK1	0.9
GST-TgCDPK1G128M	2400

B

```
2nd structure              - - S S S S S S - - - - - - - HHHHHHHH
hPKA_C alpha               - S N L Y M V M E Y V P G G E M F S H L R R I
                           - - - - - - - - - - - - - - - - - - - - - -
TgPKG1                     - E F L Y F L T E L V T G G E L Y D A I R K -
AGC like TGME49_039420     - Q K F Y F V S E K L E G G E L F D F L L T -
TgMAPK-1                   F E D I Y L V S D L M D T - D L H R V I - - -
TKL TGME49_037210          - - P L F M L T E L C A G G S L F D L L H K -
TKL TGME49_039130          - P L Y G L V T E Y V P A G S L F D L L H - -
TKL TGME49 104150          E R Y M Y M V S D L I L G G N L R Y H L N Q -
TKL TGME49_031070          - F D V W L V T N L V [ 3 ] D L H S R K Y S R
TgCDPK1                    K G Y F Y L V G E V Y T G G E L F D E I I S -
CamK TGME49_026540         - T D T Y L V A E Y A S G G E L F N E V A R V
CamK TGME49_035370         - - M S V L V T R K L S G P D F F D V I R T E
ROP36 TGME49_030470        - G N V Y M F T P L L Q G - D I R R V A V Q H
PfPK7 like TGME49_081430   - G K L I I I T N L Q [ 9 ] E R F V P A L K N
```

Figure 2

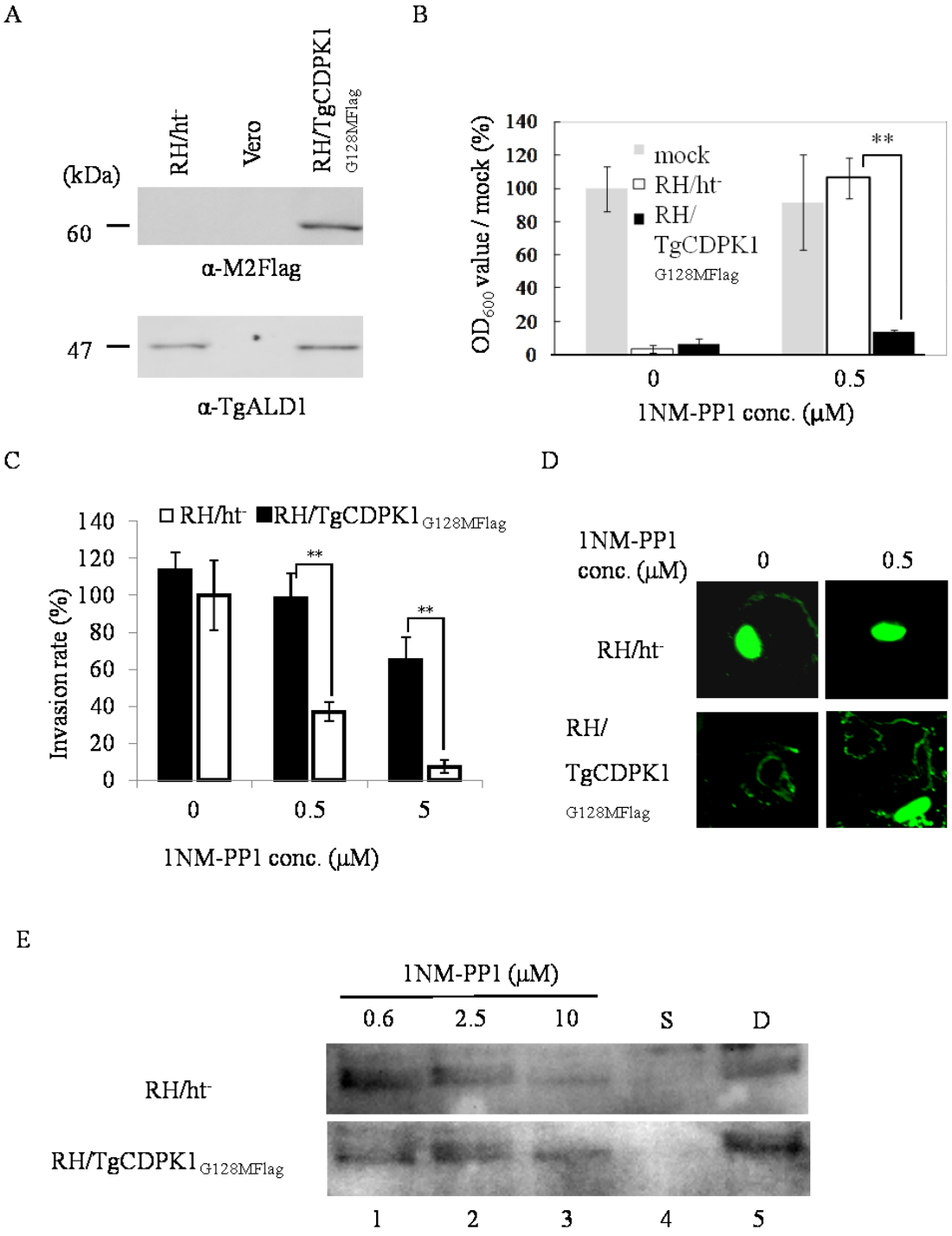
A
RH/ht-
Vero
RH/TgCDPK1 G128MFlag
(kDa)
60
α-M2Flag
47
α-TgALD1
B
OD600 value / mock (%)
mock
RH/ht-
RH/ TgCDPK1 G128MFlag
**
1NM-PP1 conc. (μM)
C
RH/ht-
RH/TgCDPK1 G128MFlag
Invasion rate (%)
**
**
1NM-PP1 conc. (μM)
D
1NM-PP1 conc. (μM)
RH/ht-
RH/ TgCDPK1 G128MFlag
E
1NM-PP1 (μM)
0.6
2.5
10
S
D
RH/ht-
RH/TgCDPK1 G128MFlag
1
2
3
4
5

Figure 3

Chapter 2

1NM-PP1 treatment of mice infected with *Toxoplasma gondii*

Submitted and Published in J. Vet. Med. Sci. 73(10): 1377–1379, 2011

Abstract

Bumped kinase inhibitors (BKIs) target analog-sensitive kinases, which the genomes of mammals rarely encode. Previously, the author demonstrated that a BKI effectively suppressed the *in vitro* replication of *Toxoplasma gondii* (*T. gondii*), the causative pathogen of toxoplasmosis, by targeting *T. gondii* calcium-dependent protein kinase 1 (TgCDPK1) (Eukaryotic Cell, 9:667-670). Here, the author examined whether the BKI 1NM-PP1 reduced parasite replication *in vivo*. A high dose of 1NM-PP1, by intraperitoneal injection, just before the parasite inoculation effectively reduced the parasite load in the brains, livers, and lungs of *T. gondii*-infected mice, however a low dose of 1NM-PP1 with oral administration didn't change survival rate of infected mice.

KEY WORDS

Bumped kinase inhibitor, drug, protein kinase, *Toxoplasma gondii*, 1NM-PP1.

Introduction

Bumped kinase inhibitor (BKI) inhibits the invasion steps of *T. gondii* (Lourido et al., 2010; Sugi et al., 2010). BKIs selectively inhibit analog-sensitive kinases, which contain a small amino acid at the gate site of the ATP binding pocket and are rare in mammalian genomes (Bishop et al., 2000). Using *in silico* prediction, we found that *T. gondii* has 12 potential BKI sensitive protein kinases (Sugi et al., 2010). *In silico* prediction, an *in vitro* culture assay using transgenic parasites, and a structural analysis of TgCDPK1 showed that TgCDPK1 is a main target of BKI (Lourido et al., 2010; Ojo et al., 2010; Sugi et al., 2010). TgCDPK1 is involved in parasite attachment, invasion, egress, and secretion *in vitro* (Kieschnick et al., 2001; Lourido et al., 2010). Thus, BKI and TgCDPK1 are a promising drug and drug target, if BKI can suppress parasite replication *in vivo*.

1NM-PP1 (Calbiochem, Darmstadt, Germany), one of the BKI previously published to inhibit analog sensitive mutated protein kinase expressed in the transgenic mouse *in vivo* (Wang et al., 2003). To evaluate the target validity of TgCDPK1, we checked the inhibition effect of 1NM-PP1 in the mouse infection models. The present study also focuses on the *in vivo* application of ASKA-GI technique to the *T. gondii* protein kinase analysis.

Materials and Methods

T. gondii culture

The parasites were maintained in monolayers of Vero cells, as described elsewhere (Sugi et al., 2009). Tachyzoites of *T. gondii* RH (kindly provided by Dr. X. Xuen), strains were used in this study. The parasites were maintained in monolayers of Vero cells cultured in Dulbecco's modified Eagle's medium (DMEM) that contained 1% fetal calf serum (FCS), 2 mM L-glutamine, 20 mM HEPES (pH 7.5), streptomycin, and penicillin. The host Vero cells were maintained in the same medium with 5% FCS. To purify the parasite, infected host monolayer were scraped at 48 h after parasite inoculation. Harvested infected cells were passed through 27G needle 3 times and filtered with 5 μm pore size filter ((Millipore, Billerica, MA, USA)), and counted with a hemocytometer.

Mouse infection

1.0×10^5 tachyzoites were inoculated into mice intraperitoneally. Five weeks old female ICR strain mice (SLC) were used throughout this study.

Chemicals

1NM-PP1 was purchased from Merck KGaA (Darmstadt, Germany).

Realtime qPCR

The parasite load per 1 mg of tissue was quantified using a quantitative real-time PCR system, as described elsewhere (Huynh and Carruthers, 2006). Tissues collected from the infected mice were weighed and used for genomic DNA isolation with QIAamp

(QIAGEN), according to the manufacturer's instructions. To detect *T. gondii*-specific DNA, the primer pair TOX-9 and TOX-11 was used (Reischl et al., 2003). To plot a standard curve, genomic DNA isolated from serial two times dilution of 1.0×10^6 tachyzoites was used.

Results and Discussion

Treatment of T. gondii infection by 1NM-PP1 in drinking water

The author treated mice with drinking water containing 5 μM 1NM-PP1 (low concentration) as described by Wang *et al.* (Wang et al., 2003), using the schedule shown in Figure 1A. From 24 h before the parasite inoculation to the end of this experiment, 1NM-PP1 was administered orally via the drinking water at a concentration of 5 μM, as described elsewhere (Wang et al., 2003). For the control group, the drinking water contained 0.1% DMSO, which was the solvent for 1NM-PP1. The mice were monitored twice daily for clinical signs of toxoplasmosis and mortality throughout the experiment. Five mice per group were used. All of the mice died between 5 and 10 days post inoculation in both the control and 1NM-PP1 groups (Fig. 1B). There was no marked difference between the symptoms in the groups (data not shown). A previous report suggested that the oral administration of 1NM-PP1 in the drinking water successfully inhibited the function of a mouse BKI-susceptible protein kinase, mutated CaMKII expressed in the brain, *in vivo* (Wang et al., 2003). The *in vitro* susceptibility of TgCDPK1 to 1NM-PP1 (IC_{50} = 0.02 μM) (Ojo et al., 2010) was not very different from that of susceptible mutated mouse CaMKII (IC_{50} = 0.03 μM) (Wang et al., 2003). TgCDPK1 was reported to localize in the parasite cytosol and not to be secreted (Pomel et al., 2008). 1NM-PP1 needs to pass through three membranes to reach TgCDPK1, the host cell membrane, parasitophorous vacuole membrane, and parasite cell membrane, whereas to reach CaMKII expressed in mouse brain cells, 1NM-PP1 needs to pass only through the cell membrane. Thus, the same administration conditions for 1NM-PP1 might not lead to a sufficient concentration of 1NM-PP1 where TgCDPK1 is active.

Intraperitoneal high dose treatment

To eliminate the possibility that 1NM-PP1 did not suppress parasite growth because of low drug concentrations in the mouse tissues, the author tested a dose of 3 mg/kg. In this test, 1,000 tachyzoites were inoculated intraperitoneally and 90 μg of 1NM-PP1 in 300 μL of phosphate-buffered saline (PBS) were inoculated daily intraperitoneally. Four days after the first drug injection, the mice were euthanized with ether and the lungs, liver, and brain were collected for parasite quantification.

When DMSO was administered as a control, the average parasite loads in the liver, lungs, and brain were $10^{4.8}$, $10^{4.7}$, and $10^{3.5}$ parasites/mg, respectively. 1NM-PP1 administration decreased the parasite loads in the liver and lungs by ~10-100-fold compared with the controls, while it decreased the load in the brain < 5-fold (Fig. 2A). However, when the drug was first administered 1 day post parasite inoculation, the parasite loads in tissues were the same in the experimental and control mice (Fig. 2B).

With high dose injection of 1NM-PP1, observation of survival rate and clinical signs and relation to the decrease of parasite loads should be needed in the future work. In this study genotype I RH strain only is used for the evaluation of 1NM-PP1. Efficacy of 1NM-PP1 to genotype II avirulent strain would be needed. Recently, Lourido *et al.* reported other BKIs 3MB-PP1 and PP1 derivatives had effect to gain the survival rate of type II avilulent Pru strain infected mouse (Lourido et al., 2013).

1NM-PP1 injected just before parasite inoculation could attack extracellular parasites through fewer barrier membranes. The first invasion of *T. gondii* inoculated in the mice was the only synchronous invasion event. One day after parasite inoculation, the parasite egress and re-invasion cycles are likely asynchronous in each parasitophorous vacuole. A

previous report showed that 1NM-PP1 injected intraperitoneally reached the brain within 10 min, but was cleared by 30 min (Wang et al., 2003). This suggests that 1NM-PP1 injected intraperitoneally is sustained at high concentration for only a very short time in mouse tissues. Thus, the day following parasite inoculation, invading parasites would rarely encounter a high concentration of 1NM-PP1, because the invasion time interval is very much shorter than the intracellular replication time.

Conclusion

Data in the present study showed that the BKI affected *T. gondii* invasion when the drug was present during the initial parasite invasion. Inhibiting the invasion step is a promising antimicrobial treatment. If the problem of drug delivery to TgCDPK1 can be resolved, BKIs may be a promising selective drug class for *T. gondii*.

The present study revealed the problems which need to be solved for the successful application of i*n vivo* ASKA-GI to the characteristics of *T. gondii* protein kinase function in the parasite infection to animal host. BKIs, which have better *in vivo* pharmacokinetics than 1NM-PP1, are needed. To avoid the membrane barrier of the host cell membrane, parasitophorous vacuole membrane, and parasite cell membrane, rhoptry protein kinases secreted into host cells are suitable for the target protein kinase.

Figure legends

Figure 1. **Oral administration of 1NM-PP1 to *T. gondii*-infected mice.**

(A) Schedule summary of the animal experiment. (B) Survival rates of mice infected with 1.0×10^5 parasites are shown. Squares show the group given drinking water containing 5 μM 1NM-PP1. Diamonds show the control group given drinking water containing only DMSO. Five mice were used per group.

Figure 2. **Intraperitoneal administration of a high concentration 1NM-PP1 to *T. gondii*-infected mice.**

Log_{10} parasite numbers in 1 mg of brain, lung, and liver 4 days after the first drug injection are shown. The first drug injection was administered (A) just before or (B) 1 day after inoculation with 1.0×10^3 parasites intraperitoneally. Parasite loads were measured with genomic DNA extracted from the infected tissue and the *T. gondii*-specific primers TOX-9 and TOX-11 (Reischl et al., 2003) by quantitative real-time PCR. Each experiment was performed with three mice and standard deviations (SD) are shown. * $p < 0.01$, by Student's *t*-test.

Figures

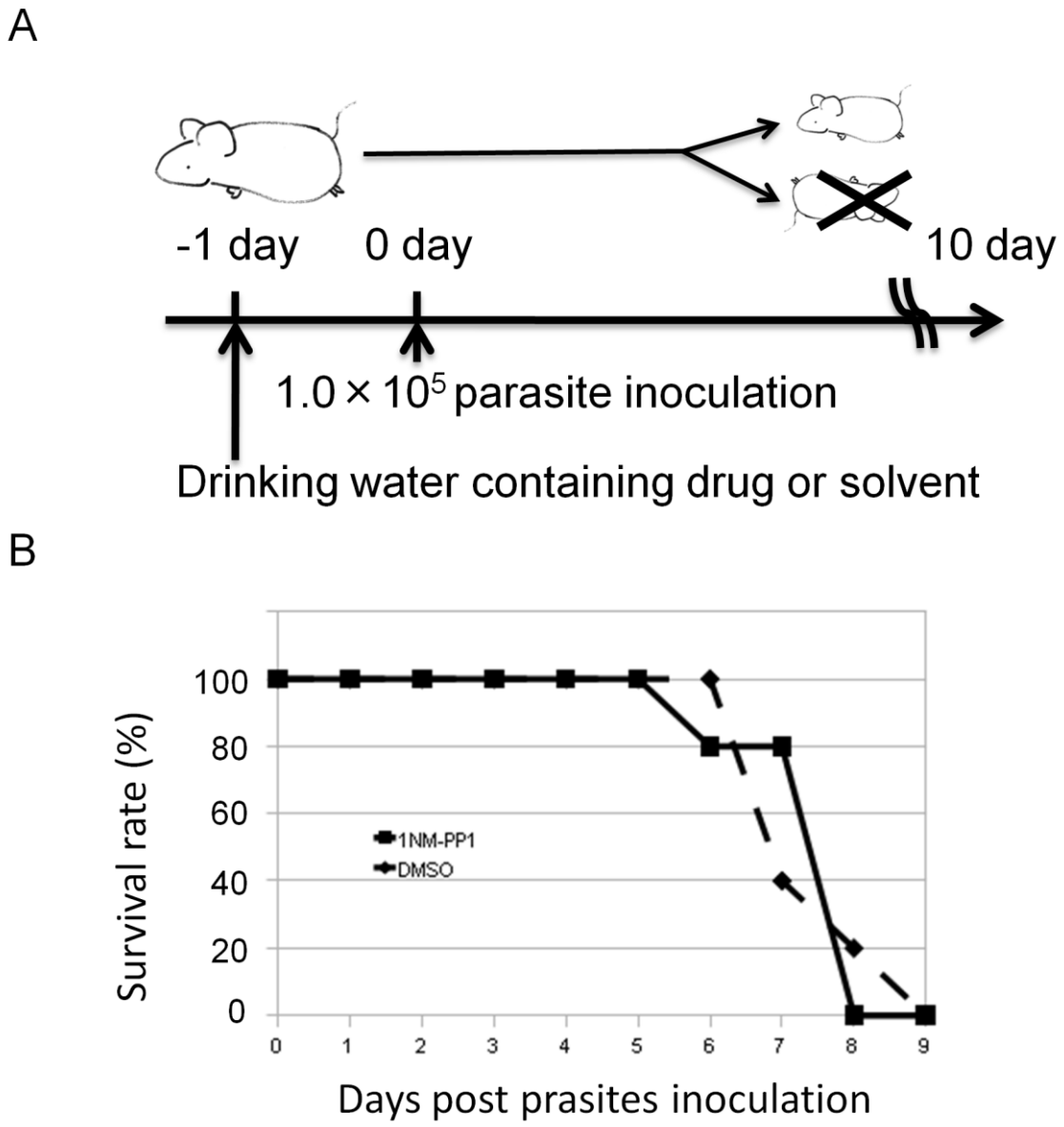

Figure 1

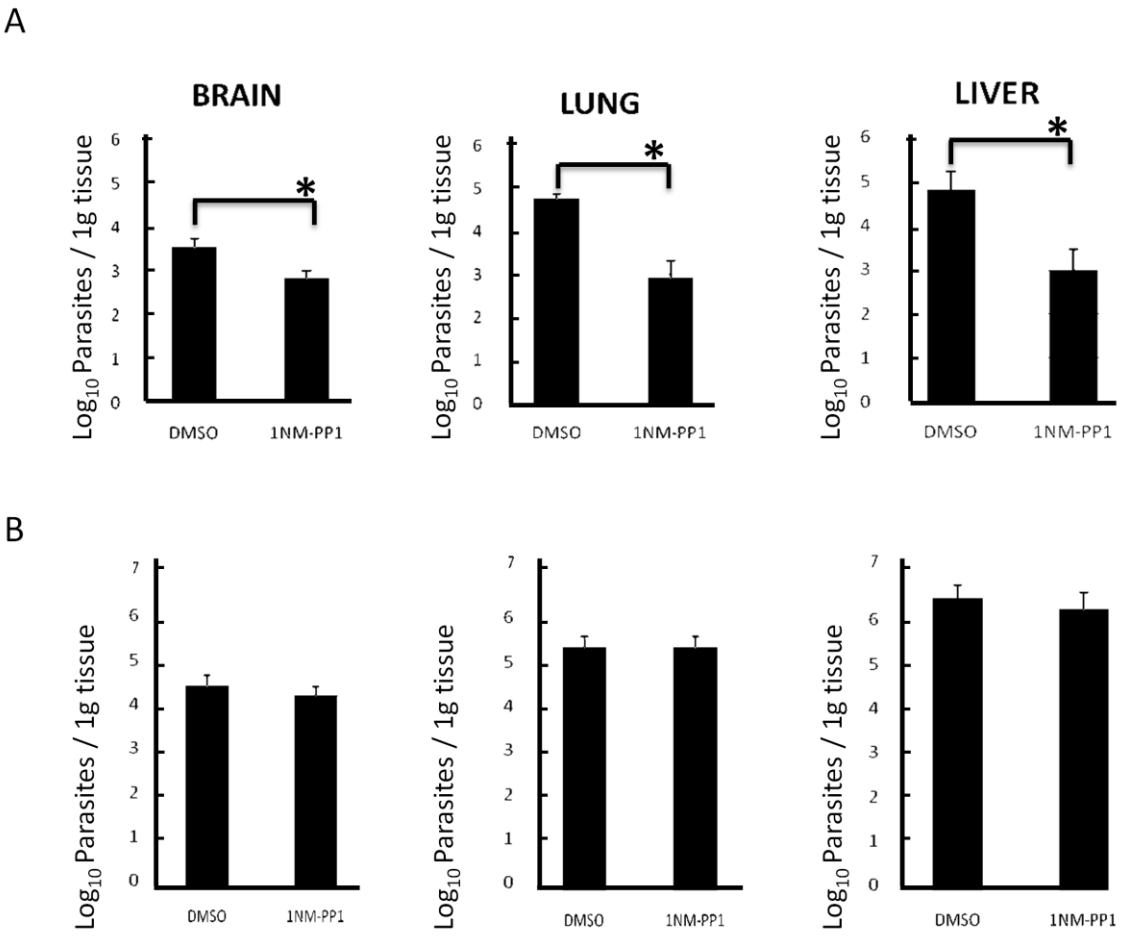
A
BRAIN
LUNG
LIVER
Log10 Parasites / 1g tissue
DMSO
1NM-PP1
B
Log10 Parasites / 1g tissue
DMSO
1NM-PP1

Figure 2

Chapter 3

Establishment of 1NM-PP1 resistant *T. gondii* clones and identification of responsible mutation site for the resistance

Part of a published report in International Journal for Parasitology: Drugs and Drug Resistance 3 (2013) 93–101

Abstract

Bumped kinase inhibitors (BKIs) have an antiparasitic effect on *T. gondii* tachyzoite growth by targeting *T. gondii* calmodulin-domain protein kinase 1 (TgCDPK1). To identify mutations that confer resistance to BKIs, chemical mutagenesis was performed, followed by selection in media containing either 250 or 1,000 nM 1NM-PP1. Whole-genome sequence analysis of resistant clones revealed single nucleotide mutations in *T. gondii* mitogen-activated protein kinase 1 (TgMAPK1) at amino acids 162 (L162Q) and 171 (I171N). Plasmid constructs having the TgMAPK1 L162Q mutant sequence successfully replace native TgMAPK1 genome locus in the presence of 1,000 nM 1NM-PP1. A plasmid construct expressing the full length TgMAPK1 splicing isoform with L162Q mutation successfully complemented TgMAPK1 function in the pressure of 250 nM 1NM-PP1 in plaque assay. 1NM-PP1-resistant clones showed resistance to other BKIs (3MB-PP1 and 3BrB-PP1) with different levels. Here the author identifies TgMAPK1 as a novel target for 1NM-PP1 activity. To characterize further the TgMAPK1 function in parasite cell signaling, the author tried to make conditional knockdown parasites by tagging of TgMAPK1 native locus by the destabilizing domain. The author made destabilizing domain fused TgMAPK1 (DD-TgMAPK1) expressing parasites and the DD-TgMAPK1 protein amount was regulated by the addition of low molecular ligand shield1 at concentration dependent manner. 1NM-PP1 resistant mutated DD-TgMAPK1 expression in parasite confers resistance to 250 nM 1NM-PP1. To check the native locus is accessible for the homologous recombination, the author first transfected knock-in construct replacing native locus with HA-tagged TgMAPK1. HA-tagged TgMAPK1 can knock-in native locus and the author confirmed that HA-TgMAPK1 was expressed in single band without proteolytic modification and

localized to parasite cytosol. Overexpression of HA-TgMAPK1 by GRA1 promoter expression could confer resistance to 1NM-PP1 and expression of 1NM-PP1 resistant mutated HA-TgMAPK1 conferred more resistance to 1NM-PP1 than wild type TgMAPK1. These data showed that N-terminal tagged TgMAPK1 is functional and native TgMAPK1 genome locus is accessible for the tagging. The strategy of DD-tagged TgMAPK1 knock-in instead of HA-tagged TgMAPK1 is promising to make the conditional knockdown and will contribute the analyses of the unique MAPK cell signaling in the *T. gondii*.

Introduction

Bumped kinase inhibitors (BKIs) have been shown to inhibit tachyzoite growth in *T. gondii* (Larson et al., 2012; Lourido et al., 2010; Ojo et al., 2010; Sugi et al., 2010), *Cryptosporidium parvum* infection (Murphy et al., 2010) and transmission of malaria from humans to mosquitoes (Ojo et al., 2012). BKIs are protein kinase inhibitor analogs which primarily affect analog-sensitive protein kinases containing a small amino acid at the gatekeeper position (Shokat and Velleca, 2002). Gatekeeper amino acids are found at the entrance of the protein kinase ATP-binding pocket; the size and shape of this amino acid greatly affects the susceptibility of protein kinases to kinase inhibitor analogs (Shokat and Velleca, 2002). Analog-sensitive protein kinases are rarely encoded in mammalian genomes.

The genomes of *Toxoplasma*, *Neospora*, and *Cryptosporidium* encode for calmodulin-domain protein kinase 1 (CDPK1) homologs (TGME49_101440, NCLIV_011980, and cgd3_920 in the EuPathDB http://eupathdb.org/eupathdb/) containing a glycine at the gatekeeper amino acid position. Both TgCDPK1 (Larson et al., 2012; Lourido et al., 2010; Murphy et al., 2010; Sugi et al., 2010) and CpCDPK1 (Murphy et al., 2010) have been confirmed as the primary targets of BKIs, however the *T. gondii* genome encodes for other analog-sensitive protein kinases containing a small amino acid such as alanine, serine, or threonine at the gatekeeper position, suggesting the possibility of multiple targets (Sugi et al., 2010). BKIs, therefore, represent a promising new class of antiparasitic compounds.

To predict the frequency at which BKI-resistant parasites may arise, identification of mutations conferring resistance to these inhibitors is required. Resistance to BKIs is predicted to occur through mutation of both the gatekeeper residue of the target protein

kinases, as well as other amino acids affecting the affinity of protein kinase inhibitors to their respective targets. Mutation of the gatekeeper residue of TgCDPK1 from wild-type (WT) glycine to methionine, which contains as larger side chain than that of glycine, has been shown to confer resistance in transfected parasites (Larson et al., 2012; Lourido et al., 2010; Murphy et al., 2010; Sugi et al., 2010). This effect is not limited to gatekeeper residues, as mutation at other sites within the protein kinase domain have been shown to confer resistance to ATP pocket binding inhibitors such as imatinib (Weisberg and Griffin, 2000) and nilotinib (Ray et al., 2007). Accordingly, the author chose to screen for all mutations conferring resistance to BKIs, including those not found at the gatekeeper residue, using randomly mutated parasites established in chapter 3. This strategy of using chemically mutated parasite lines, followed by whole-genome sequencing, has recently been validated in *T. gondii* as a means of identifying relevant mutations (Farrell et al., 2012).

In the present study, the author used whole genome re-sequence with random mutated resistant parasite clones to identify the single nucleotide polymorphism (SNP). SNPs detected in both resistant strains were further characterized by transgenic parasites making the candidate SNP in the parent strain. To check the resistance is restricted to 1NM-PP1 or other BKIs, the author checked that the identified mutation confers the resistance to other BKIs, 3MB-PP1 and 3BrB-PP1.

Materials and Methods

Tested reagents

1NM-PP1 was purchased from Merck KGaA (Darmstadt, Germany). 3BrB-PP1 and 3MB-PP1 were purchased from Toronto Research Chemicals (Ontario, Canada).

Parasite cultures

Tachyzoites of the *T. gondii* PLK/DUAL (Unno et al., 2009) strain (kindly provided by Dr. Y. Takashima, Gifu University, Gifu, Japan), PLK/hxgprt$^-$ strain (Roos et al., 1994) (NIH AIDS Reagent Program, Division of AIDS, NIAID, NIH #2860), RH/hxgprt$^-$ (kindly provided by Dr. X. Xuen) and RH/ku80$^-$/hxgprt$^-$ (ATCC® PRA-319) were used in this study. Parasites were maintained in monolayers of Vero cells cultured in Dulbecco's modified Eagle's medium (DMEM) (Nissui, Tokyo, Japan) containing 1% fetal calf serum (FCS) and 2 mM L-glutamine, streptomycin, and penicillin. Host Vero cells were maintained in the same medium containing 5% FCS. For assays, tested reagents or a DMSO control solvent were added to the same medium with 1% FCS (infection medium).

Chemical mutagenesis

Random mutagenesis was introduced using *N*-ethyl-*N*-nitrosourea (ENU) (Sigma-Aldrich, St. Louis, MO, USA) as previously described (Nagamune et al., 2007). PLK/DUAL tachyzoites (5.0×10^7) were inoculated onto Vero cells cultured in T75 flasks. At 2 h post inoculation (hpi), parasites were exposed to ENU (500 μg/mL) for 1 h in serum-free culture medium, then washed three times in infection medium. They were

then incubated at 37 °C for an additional 24 h, followed by 1NM-PP1 selection. Mutated parasites were selected using 1NM-PP1 at either 250 or 1,000 nM for 3 weeks with medium changes every 2 days. Parasites were passaged to a new host monolayer every 7 days with host cells ruptured by pass through a 25-G needle to remove uninfected cells. Resistant parasites were cloned by limiting dilution and designated as either PLK/DUAL res.1 for 250 nM selection or PLK/DUAL res.2 for 1,000 nM selection.

Sequence analysis and structure prediction of mutated TgMAPK1

The peptide sequence of the TgMAPK1 (GenBank: AY684849) protein kinase domain (from amino acid 81 to 532) was aligned with HsErk5 (GenBank: NP_002740.2), and CpCDPK1 (GenBank: 3NCG_A). Subdomain prediction was performed according to the method of Hanks and Hunter (Hanks and Hunter, 1995). ATP-binding sites were predicted by NCBI conserved domain search (Marchler-Bauer et al., 2011). 1NM-PP1-binding sites were predicted from the structure of 1NM-PP1 bound CpCDPK1 (Murphy et al., 2010) (PDB: 3NCG). For homology modeling, the TgMAPK1 protein kinase domain (amino acid residues 81–532) was used for structure calculation by SWISS-MODEL automated mode (Arnold et al., 2006) using the crystal structure of Homo sapiens MAPK7 (HsErk5) bound with inhibitor (PDB: 4B99) as a template. The predicted structure was superimposed over the 1NM-PP1-bound CpCDPK1 structure (PDB: 3NCG) using UCSF Chimera (Pettersen et al., 2004).

Assay for BKIs inhibition of parasite growth

The growth of PLK/DUAL and resistant clones was evaluated using the DsRed-Express reporter gene expressed under the control of SAG1 promoter. Parasites

were pre-incubated with various concentrations of 1NM-PP1, 3BrB-PP1, and 3MB-PP1 or the control solvent (DMSO) for 10 min at room temperature. 5×10^3 parasites per well were inoculated on confluent Vero cell monolayers in 48-well plates, and cultured with the tested reagent for 6 days. After incubation, media were aspirated and cells were lysed using phosphate buffered saline (PBS) containing 0.5% sodium dodecyl sulfate to reduce background fluorescence. Cell lysates were moved to 96-well plates and measured using an SH-9000 fluorimeter (Corona Electronic, Ibaraki, Japan) with an excitation wave length of 540 nm and an emission wave length of 590 nm. Background fluorescence intensities were detected using mock infected wells, and subtracted from the values of all wells.

Whole-genome sequencing and single nucleotide variants (SNV) identification

SOLiD sequencing libraries were generated from genomic DNA of PLK/DUAL, PLK/DUAL res.1, and PLK/DUAL res.2 strains. Libraries were sequenced using a 5500xl SOLiD system (Life Technologies, Carlsbad, CA) according to the manufacturer's instructions using 75-bp single-end reads. Sequencing data have been submitted to DDBJ (DDBJ: DRA000618). Reads were mapped to the *T. gondii* ME49 genome (ToxoDB http://toxodb.org/version 2008_07_23) using alignment software BWA (Li et al., 2009). SNVs were called with SAMTOOLS (Li et al., 2009) and filtered using a minimal coverage of 10, a maximum coverage of 100, and an alternative bases positive rate of > 80%. The average depth was calculated with a 100-kbp window. SNVs were further filtered using a predicted gene model in ToxoDB version 7.2.

Transgenic parasites

Approximately 2-kbp sequences of TgMAPK1 adjacent to the mutated sites, and lacking a promoter and start codon were amplified from genomic DNA of parent and resistant clones. Primers TgMAPK1_F1 and TgMAPK1cla1_R2 (Table 1) were used to generate the first-half fragment, and primers TgMAPK1_R1 and TgMAPK1cla1_F2 (Table 1) were used to generate the second-half fragment. The first-half fragment was digested with *Eco*RI and *Cla*I, while the second-half fragment was digested with *Cla*I and *Sma*I. The two fragments were inserted into the *Eco*RI and *Sma*I sites of pBluescript KS(-) to produce a *Cla*I site without affecting the TgMAPK1 coding sequence. Plasmids containing sequences from PLK/DUAL, PLK/DUAL res.1, and PLK/DUALres.2 were designated pTgMAPK1_WT, pTgMAPK1_LQ, and pTgMAPK1_IN, respectively. Twenty micrograms of each plasmid was transfected, either separately or in combination, into 1.8×10^7 freshly purified PLK/DUAL cells with Nucleofection™ and basic parasite Nucleofector® kit 1, using Nucleofector® II device program U-33 (Lonza, Basel, Switzerland). Following transfection, cells were incubated at 37 °C for 24 h, and treated with 1,000 nM 1NM-PP1. After 3 weeks of selection, genomic DNA from parasites was purified using a QIAamp DNA mini kit (QIAGEN) according to the manufacturer's instructions. PCR of the genomic locus containing TGME49_112570 was performed using KOD Fx Neo (TOYOBO, Osaka, Japan) and 35-mer primers genomic_Locus_primer_F and genomic_Locus_primer_R (Table 1) with step-down PCR under the following conditions: initial denaturation at 94 °C for 2 min, 5 cycles of 98 ^{0}C for 10 s and 74 °C for 10 min, 5 cycles of 98 °C for 10 s and 72 °C for 10 min, 5 cycles of 98 °C for 10 s and 70 °C for 10 min, and 25 cycles of 98 °C for 10 s and 68 °C for 10 min, followed by a final extension at 68 °C for 10 min. Amplified PCR products were used for the restriction enzyme cut assay. Sequence analysis of mutation sites was performed

using primers Mutation_screen_F and Mutation_screen_R (Table 1). Resistant parasites were cloned by limiting dilution; sequence analysis was performed as described above. For the functional expression of TgMAPK1, a TgMAPK1 splicing variant was investigated. Gene modeling in ToxoDB suggests the presence of eight exons in TgMAPK1, and is supported by RNAseq data demonstrating mRNA containing eight exons. Splicing at intron 7 was confirmed by RT-PCR using primers Splicing_confirm_F and Splicing_confirm_R (Table 1). Because of the long mRNA sequence, we could not amplify the TgMAPK1 full-length isoform in a single PCR reaction. Accordingly, we divided the gene into two parts; we amplified the 1st half from total RNA using primers 1st_half_F and 1st_half_R (Table 1), and the 2nd half using primers 2nd_half_F and 2nd_half_R (Table 1). The TgMAPK1 full-length isoform was then amplified by overlapping PCR using the 1st half and 2nd half PCR products as templates with primers 1st_half_F and 2nd_half_R. This full-length isoform was then cut using *Eco*RI and *Eco*RV restriction enzymes, and inserted into the *Eco*RI and *Eco*RV site of pMini.ht.3x-FLAG (Sugi et al., 2010). The resulting plasmid expressed TgMAPK1 tagged with a C-terminal 3xFLAG driven by a GRA1 promoter. Plasmids containing the WT sequence and L162Q mutation were designated pTgMAPK1-FLAG and TgMAPK1L162Q-FLAG, respectively. As a control, GFP was amplified from the pMini.GFP.ht (Karasov et al., 2005) using primers GFP_F and GFP_R (Table 1), and inserted into the *Bgl*II and *Eco*RV site of pMini.ht.3xFLAG to express C-terminal 3xFLAG-tagged GFP. Plasmids were transfected into *T. gondii* strain PLK/hxgprt$^-$, selected with 25 μg/ml Mycophenolic acid and 50 μg/ml Xanthine, as described (Karasov et al., 2005), and cloned by limiting dilution. Cloned parasites stably expressing WT and L162Q mutated TgMAPK1 or GFP tagged with 3xFLAG were designated to

PLK/TgMAPK1-FLAG, PLK/TgMAPK1L162Q-FLAG and PLK/GFP-FLAG, respectively.

For the overexpression of DD-tagged TgMAPK1, the author amplified DD tag with primers AGAAATCAAGCAAGATGGGAGTGCAGGTGGAAAC (underlined sequence is for InFusion® cloning)and CTCTGTGAATTCGCATGCATTTCCAGTTCTAGAAGCTC (underlined sequence is for *Eco*RI cut) from pTunerC vector (Takara clontech). Amplified fragment was cut with *Eco*RI and was inserted into *Eco*RI and *Eco*T22I sites of pTgMAPK1-FLAG-[WT/L162Q] with ligation and InFusion cloning and resultant plasmids were designated to pDD-TgMAPK1$^{[WT/L162Q]}$-FLAG (Fig. 7A). Plasmids encode N-terminal DD-tagged and C-terminal 3xFLAG-tagged TgMAPK1. pDD-TgMAPK1^{L162Q}-FLAG was transfected into *T. gondii* strain RH/hxgprt^{-}, selected with 25 μg/ml Mycophenolic acid and 50 μg/ml Xanthine, as described (Karasov et al., 2005), and cloned by limiting dilution.

For the endogenous tagging of native locus of TgMAPK1 with double homologous recombination, the author amplified 4,720 bp 5' UTR of TgMAPK1 with primers CGGTATCGATAAGCTCAAGAAAAGCAACGAGAGAT and CGTGCTGATCAAGCTATGGTGGCGAAGAGTTGAG (underlined sequences are homologous sequence to vector for the InFusion cloning) and inserted into *the HindIII site* of pDD-TgMAPK1 $^{[WT/L162Q]}$ -FLAG with InFusion cloning and designed to pKnockIn-DD-TgMAPK1 $^{[WT/L162Q]}$.

To replace the DD tag with epitope tag HA tag, HA tag was PCR amplified with GAAATGCATACCATGTACCCATACGATGT and TGTGAATTCGCGTAATCTGGAACATCGT (underlined sequences are restriction

enzyme site) from pMini.ht.HA (Takemae et al. unpublished). PCR fragment was cut with *Eco*RI and *Eco*T22I and inserted into *Eco*T22I and *Eco*RI site of pTgMAPK1-FLAG-[WT/L162Q] and 5'UTR of TgMAPK1 was inserted as described above to make knock-in construct.

Knock-in constructs were transfected into RH/ku80^{-}/hxgprt^{-} strain. Briefly knock-in constructs were linearized with *Bsi*WI and *Hpa*I (Fig. 2A) and purified with nucleospin Gel&PCR cleanup following agarose electrophoresis. 2 μg DNA were transfected with 10^6 parasites in 400 μL complete cytomix as described in (Karasov et al., 2005).

Selection and establishment of clones were performed as described above.

PCR restriction fragment length polymorphism (PCR-RFLP)

To confirm the homologous recombination at the TgMAPK1 locus, the author performed PCR-RFLP. The author designed the primers outer the transfected DNA as described in Fig. 8A (forward: TATTTCTTCTGACCGCACGACCTTTCGCAGTTCAG and reverse: CCGACAGAAGTCAAAAGGGAATGAGATGCCAGGTAT). Step down PCR were performed as described above. PCR fragments were purified with NucleoSpin Gel and PCR Cleanup column and cut with *Cla*I. DNA fragments were separated by electrophoresis with 0.7 % agarose gel.

Plaque assay

To evaluate the resistance to 1NM-PP1, plaque formation were observed with parasite clones. Vero monolayers in 12-well plates were inoculated with 1,000 parasites per well. After 2 h, media were changed to media containing various concentration of 1NM-PP1,

and incubated for 7 days. After incubation, cells were washed with PBS three times, fixed with methanol for 5 min, and stained with crystal violet.

Western blotting

Parasites infected host cells were harvested and purified as follows, cells were scraped, passed through with a 27G needle three times and filtered with 5 μm pore size filter. Purified parasites were washed with PBS three times and resuspended in PBS at 4×10^5 parasites/μl. Suspended parasites were lysed with addition of an equal volume of 2 × SDS-PAGE buffer. Lysates from 1.0×10^6 parasites/lane were loaded and separated by 5-20% gradient gels (ATTO), and transferred to PVDF membrane. For the loading control, TgALD1 were detected with rabbit antisera raised with MBP-TgALD1 (Sugi et al., 2010). For the detection of HA tagged protein, anti-HA tag rat monoclonal antibody (Roche: clone 3F10) was used. Secondary antibody detecting rabbit or rat IgG conjugated with horseradish peroxidase (GE healthcare) were used for ECL detection.

Immunofluorescence assay

32 h post parasites inoculation, infected Vero cells on the coverslips were washed with ice cold PBS and fixed with 4% paraformaldehyde in PBS for 20 min, followed by a twice wash with PBS. Fixed cells were permiabilized with 0.2% TritonX-100 in PBS for 10 min and excess fixative was quenched with 0.25 M Glycine in PBS 5 min and washed extensively twice with PBS. Cells were blocked with 3% milk in PBS with 0.1% Tween 20 for 30 min. Antibody reaction was performed in the blocking buffer. Anti-HA 1st antibody (Roche: rat mAb 3F10) was used in a dilution of 1:200 and anti-rat 2nd antibody conjugated to Alexa 546 (Invitrogen) was used in a dilution of

1:1000. DAPI at the final concentration of 1 μg/ml was added to the 2nd antibody reaction buffer. After each antibody reaction, cells were washed with PBS three times. Stained cells were mounted with a fluorescence mounting medium (DAKO) and sealed with nail polish. Slides were observed with confocal laser microscope TCS SP5 (Leica).

Host cell monolayer disruption assay

Host cell monolayer disruption assay was performed as essentially described in chapter 1. Briefly, Vero cells were seeded in 96 well plates and were allowed to form a monolayer. 1,000 parasites per wells were inoculated and after 2 h, the media were changed to the tested media containing various concentrations of 1NM-PP1. After 6 days incubation, plates were washed with PBS and fixed and stained with 5% methanol 0.1% crystal violet solution. After staining, plates were washed with water and dried. Viable host cells stained with crystal violet were measured as OD_{600} value. Reduction of OD_{600} value from the control was calculated as a host disruption value and the host disruption rate of no treatment control was estimated to 100%.

Results

Generation of 1NM-PP1-resistant parasites by $_N$-ethyl-$_N$-nitrosourea (ENU)-induced random mutagenesis

To identify mutations conferring resistance to BKI 1NM-PP1, *T. gondii* strain PLK/DUAL was mutagenized by treatment with ENU, and selected with either 250 nM or 1,000 nM 1NM-PP1. Two independent 1NM-PP1-resistant parasite clones were generated, designated PLK/DUAL res.1 and PLK/DUAL res.2. Sensitivity of resistant clones to 1NM-PP1 was determined using a tachyzoite growth assay. IC_{50} values for clones PLK/DUAL res.1 and PLK/DUAL res.2 were 290 and 210 nM, respectively, compared to 84 nM for parental strain PLK/DUAL (Fig. 1A). The effect of 1NM-PP1 treatment was reduced in resistant clones, especially at 250 nM and 500 nM (Fig. 1A).

Identification of SNPs in the resistant clones

To identify mutations conferring resistance to 1NM-PP1, the genomes of PLK/DUAL, PLK/DUAL res.1, and PLK/DUAL res.2 were sequenced using a 5500xl SOLiD system. Total reads of 16,618,344, 11,514,716, and 16,263,909 from PLK/DUAL, PLK/DUAL res.1, and PLK/DUAL res.2, respectively, were mapped to the *T. gondii* ME49 reference genome. Coverage throughout the genome was 97, 96, and 97%, respectively (Fig. 1B). The mapped sequence reads showed unbiased coverage and depth throughout the genome (Fig. 1C). Putative SNVs detected in each of the three strains are summarized in Table 2. Among them, 5 and 13 SNVs resulting in amino acid substitutions were found in PLK/DUAL res.1 and res.2, respectively (Table 3). Putative SNVs were distributed throughout the genome (Fig. 1C), however both resistant clones contained mutations in gene TGME49_112570 (Table 3).

Sequence analysis of mutated TgMAPK1

The region surrounding the mutation sites of TGME49_112570 (*T. gondii* mitogen activated protein kinase 1: TgMAPK1) was aligned with HsErk5 and CpCDPK1 to identify the ATP binding site. Structural homology was also used to predict the relationship between TgMAPK1 mutations and their effect on 1NM-PP1 binding (Fig. 2 and Fig. 3A). PLK/DUAL res.1 contained a Leu 162 to Gln mutation which falls within protein kinase subdomain III. Superposing the predicted structure of TgMAPK1 on 1NM-PP1-bound CpCDPK1 (PDB: 3NCG) showed that the mutated Leu 162 faced the naphthyl group of 1NM-PP1 (Fig. 2). The Ile 171 to Asn mutation in clone PLK/DUAL res.2 mapped to protein kinase subdomain IV, the putative ATP binding site, and the predicted target of 1NM-PP1.

Construction of parasites containing a mutated locus in TgMAPK1

To confirm that the mutations in TgMAPK1 were responsible for the resistance to 1NM-PP1, the author generated replacement constructs containing a sense mutation encoding for a *Cla*I restriction site to distinguish the inserted construct from the native genomic sequence (Fig. 3B). To determine whether the mutated TgMAPK1 sequence was selected by 1NM-PP1 treatment, plasmids pTgMAPK1_WT, pTgMAPK1_LQ, and pTgMAPK1_IN were nucleofected into WT strain PLK/DUAL and cultured for 3 weeks in the presence of 1,000 nM 1NM-PP1, or for 1 week without 1NM-PP1 as a control. Nucleofected control parasites showed no detectable *Cla*I digested bands after 1 week without selection (Fig. 4A), indicating a small population possessing homologous recombination at the TgMAPK1 genomic locus. Following selection in the presence of

1,000 nM 1NM-PP1, no propagating parasites were obtained from parasites nucleofected with pTgMAPK1_WT, though propagating parasites were obtained from parasites nucleofected with pTgMAPK1_LQ, and pTgMAPK1_IN. PCR-RFLP analysis showed that PCR products generated using genomic DNA from parasites nucleofected with pTgMAPK1_LQ, and pTgMAPK1_IN were readily cleaved by *Cla*I (Fig. 4B), confirming that double homologous recombination had occurred in the TgMAPK1 genomic locus. Sequence analysis confirmed the insertion of the *Cla*I and L162Q mutations in 1NM-PP1-selected parasites nucleofected with pTgMAPK1_LQ (Fig. 4C upper panels), and the *Cla*I and I171N mutations in 1NM-PP1-selected parasites nucleofected with pTgMAPK1_IN (Fig. 4C middle panels).

To identify the mutation that conferred the highest gain of fitness in the presence of 1NM-PP1, the PLK/DUAL parent strain was transfected with a mixture of WT and mutant constructs containing the TgMAPK1 genomic sequences from PLK/DUAL, PLK/DUAL res.1, and PLK/DUAL res.2, followed by selection with 1,000 nM 1NM-PP1. Sequence chromatograms from 1NM-PP1 selected parasites showed the presence of a *Cla*I restriction site, consistent with double homologous recombination at the TgMAPK1 genomic locus. Sequence chromatograms of the L162Q mutation site showed that the main population of selected parasites contained the L162Q mutation, with only a small population possessing the I171N mutation (Fig. 4C lower panels). Selected parasites were cloned by limiting dilution, and the resulting clone containing the TgMAPK1 Leu 162 to Gln mutation was designated PLK/DUAL TgMAPK1^{L162Q}.

Genomic replacement at the loci of TgMAPK1 in chromosome XI was confirmed by PCR followed by cleavage using a restriction enzyme. The TgMAPK1 genomic loci from PLK/DUAL and PLK/DUAL TgMAPK1^{L162Q} were amplified using primers

genomeLocusPrimer_F and genomeLocusPrimer_R (Fig. 3B and Table 1), resulting in a 16.6-kbp product; *Bam*HI digestion of the PCR products produced fragments approximately 7.8 and 8.8 kbp in length (Fig. 3C). The PCR fragment from PLK/DUAL TgMAPK1^{L162Q} was cut by *Cla*I, resulting in 11- and 5.6-kbp fragments, whereas the PCR fragment from PLK/DUAL was not cut, resulting in a fragment 16.6 kbp in length (Fig. 3C).

PLK/DUAL TgMAPK1^{L162Q} showed an IC_{50} of 300 nM for 1NM-PP1 in tachyzoite growth assays (Fig. 3D). To confirm that resistance was conferred by expression of the mutated TgMAPK1 protein, the author transfected a TgMAPK1 overexpression construct (Fig. 5A) into PLK/hxgprt- parasites. Established clones were checked for protein expression by western blotting using an anti-FLAG antibody. Proteins from PLK/TgMAPK1-FLAG and PLK/TgMAPK1^{L162Q}-FLAG showed TgMAPK1-FLAG bands at ~150 kDa (Fig. 5B). Bands were slightly higher than the calculated molecular weight of 3xFLAG tagged TgMAPK1 (140 kDa). Protein from the PLK/GFP-FLAG control showed a GFP-FLAG band at approximately 31 kDa. Western blotting with anti-TgALD1 antibody (Sugi et al., 2010) was used to confirm equivalent loading.

PLK/TgMAPK1-FLAG, PLK/TgMAPK1^{L162Q}-FLAG, and PLK/GFP-FLAG were examined by plaque assay with or without 1NM-PP1. PLK/GFP-FLAG showed no plaque at 250 nM 1NM-PP1 (Fig. 5C). PLK/TgMAPK1-FLAG showed a small plaque at 250 nM 1NM-PP1 (Fig. 5C), while PLK/TgMAPK1^{L162Q}-FLAG showed a medium sized plaque at 250 nM 1NM-PP1 (Fig. 5C). These results suggest that overexpression of TgMAPK1 is sufficient to confer modest resistance to 1NM-PP1, while overexpression of TgMAPK1 L162Q confers higher resistance to 1NM-PP1 than WT TgMAPK1 or control GFP expression alone.

Effect of TgMAPK1 mutations on susceptibility to other BKIs

TgMAPK1 mutants L162Q and I171N were next examined for cross resistance to other BKIs. 3BrB-PP1 inhibited clones PLK/DUAL, PLK/DUAL res.1, PLK/DUAL res.2, and PLK/DUAL TgMAPK1^{L162Q} at IC_{50} values of 41, 81, 30 and 95 nM, respectively (Fig. 6A). Inhibitor 3MB-PP1 elicited a similar pattern of sensitivity, with IC_{50} values for PLK/DUAL, PLK/DUAL res.1, PLK/DUAL res.2, and PLK/DUAL TgMAPK1^{L162Q} of 73, 146, 90 and 176 nM, respectively (Fig. 6B). Parasite clones harboring the L162Q mutation showed consistently higher IC_{50} values for both 3BrB-PP1 and 3MB-PP1 compared to the parental strain PLK/DUAL. On the other hand, parasite clones expressing the I171N mutation (PLK/DUAL res.2) showed similar IC_{50} value to 3BrB-PP1 and 3MB-PP1 as PLK/DUAL, demonstrating selective resistance to BKI 1NM-PP1.

Expression of DD-TgMAPK1

To characterize further the TgMAPK1 function in the parasite growth and to provide the tool for the identification of upstream and downstream signals of TgMAPK1, inducible knockdown or knock-out parasites are needed.

To make the inducible knockdown parasites, recent works on ku80 knock out parasites enables us to easily make the transgenic parasite with homologous recombination (Fox et al., 2011; Huynh and Carruthers, 2009). Low molecule ligand triggerd protein level regulation was introduced to *T. gondii* (Herm-Götz et al., 2007). The strategy using insertional tagging of native locus by the DD-tag with double homologous recombination provides us an instant establishment of inducible knock

down parasites. For the first, to confirm the DD-tag is applicable for the functional analysis of TgMAPK1, the DD-TgMAPK1^{L162Q}-FLAG expressing plasmid was transfected into the RH/hxgprt$^-$ parasites and the resultant clone was designated to RH/DD-TgMAPK1^{L162Q}-FLAG. The DD-TgMAPK1-FLAG protein amount was upregulated with shield1 treatment with concentration dependent manner at 250, 500, 1000 nM (Fig. 7B). However, RH/DD-TgMAPK1^{L162Q}-FLAG expressed DD-TgMAPK1-FLAG at low level without shield1 (Fig. 7B). Without shield-1 RH/DD-TgMAPK1^{L162Q}-FLAG formed plaque when treated with 250 nM 1NM-PP1, whereas parent RH/hxgprt$^-$ didn't (Fig. 7C).

Tagging of endogenous TgMAPK1 by DD or HA tag.

When the DD-TgMAPK1-FLAG expressing plasmid was transfected to RH/hxgprt$^-$, a copy number of DD-TgMAPK1-FLAG, which is integrated into the genome or maintained in the episome, may be different among the clones established and DD-tagged TgMAPK1 was not completely proteolysed even without shield-1 in the clone assayed in the present thesis. And native TgMAPK1 gene locus expresses wild type TgMAPK1 which may compete the exogenous expressed TgMAPK1. To resolve these problems, the author knocked in the tagged TgMAPK1 mini gene in the TgMAPK1 genome locus to replace the native TgMAPK1.

HA-TgMAPK1 knock-in plasmid (Fig. 8A) construct were transfected in the RH/ku80$^-$/hxgprt$^-$ strain and double homologous recombinated clones were screened with PCR-RFLP. The PCR fragment from parent RH/ku80$^-$/hxgprt$^-$ genome DNA showed no cut with *Cla*I (Fig. 8B), whereas the fragments amplified from the gDNA of

knock-in clones showed *Cla*I cut (Fig. 8B). Resultant knock-in clones were designated to RH/ku80^{-}/HA-TgMAPK1^{WT} and RH/ku80^{-}/HA-TgMAPK1L^{162Q}.

Western blotting of parasite lysate showed a single band around 150 kDa with HA antibody (Fig. 9A). The single band expression means no proteolytic processing after translation. Immunofluorescence assay was performed with host cells infected with parasites at 32 h post inoculation. The author observed that the HA-tagged TgMAPK1 localized in the parasite cytosol (Fig. 9B).

To check whether knock-inned HA-TgMAPK1 is functional or not, we performed 1NM-PP1 resistance acquisition assay. Parent clone RH/ku80^{-}/hxgprt^{-}, RH/ku80^{-}/HA-TgMAPK1^{WT} and RH/ku80^{-}/HA-TgMAPK1^{L162Q} were cultured with various concentrations of 1NM-PP1. At 250 and 500 nM treatment, parent RH/ku80^{-}/hxgprt^{-} showed significant decrease in the host disruptions compared to HA-TgMAPK1 $^{[WT/L162Q]}$ expressing parasites (Fig. 10). At 750 nM, HA-TgMAPK1^{L162Q} expressing parasites significantly retained its host lysis capacity compared to the HA-TgMAPK1^{WT} expressing parasite (Fig. 10).

Discussion

In *T. gondii*, the main target of 1NM-PP1 is TgCDPK1 (Larson et al., 2012; Lourido et al., 2010; Ojo et al., 2010; Sugi et al., 2010). This report represents the first description of mutations in TgMAPK1 capable of conferring resistance to 1NM-PP1. Mutants were generated using random mutagenesis followed by whole-genome sequencing. Considering the hundreds of SNVs detected by whole-genome sequencing, a lower concentration of ENU may be sufficient for whole genome mutagenesis. By decreasing the number of SNVs in a given sequence, identification of the mutation responsible for a desired phenotype becomes much easier. Surprisingly neither resistant clone had mutations in TgCDPK1. As this study failed to identify the known target of 1NM-PP1, higher concentration of ENU or larger starting parasites number may be useful for developing more robust target identification.

The method we chose for generating resistant clones in this study was somewhat slower than the usual selection time of 3 days to 1 week using the standard selectable marker HXGPRT to isolate transgenic parasites. Instead we selected for 3 weeks (three passages) to screen for resistant parasites. However, after screening, parasites were cloned and propagated in the absence of selection pressure, meaning the time necessary to establish clones after the screening was almost the same as with standard transgenic parasites.

Considering that TgMAPK1 has been shown to function in stress responses (Brumlik et al., 2011), inhibition of TgMAPK1 could affect the parasite's ability to respond to different stresses caused by 1NM-PP1, including TgCDPK1 inhibition. The PLK/DUAL reporter strain is an excellent system for measuring bradyzoite differentiation using a fluorescent reporter (Unno et al., 2009). Our resistant clones and BKIs may represent a

valuable tool to study the function of TgMAPK1 in bradyzoite differentiation.

Among the putative SNVs detected, both resistant clones had a mutation in TgMAPK1. PLK/DUAL res.2 carried a mutation at the predicted ATP and 1NM-PP1 binding site (Ile171). Protein kinase activity may be altered by this mutation; however, no significant change in tachyzoite growth was observed in the absence of 1NM-PP1. Furthermore, the mutated site in PLK/DUAL res.1 (Leu162) was predicted to face the nonpolar naphthyl group of 1NM-PP1 (Fig. 2). The polar characteristics of Gln 162 in these resistant parasites might disrupt the nonpolar interaction, decreasing the affinity between 1NM-PP1 and TgMAPK1.

Generation of the active recombinant enzyme will be necessary for *in vitro* kinase assays. *In vitro* assays will allow for detailed analyses of protein kinase activity in the presence of inhibitors such as 1NM-PP1, as well as the effect of mutations on enzyme activity. Preliminary efforts to isolate the active form of TgMAPK1 were unsuccessful. A truncated isoform of TgMAPK1 containing entire protein kinase domain (GenBankID:AY684849) fused with maltose binding protein or glutathione S transferase was expressed in *E. coli* or using a baculovirus system; however, the resulting protein did not exhibit sufficient enzymatic activity for use in drug inhibition assays. One possible explanation for this deficiency may be tied to enzyme regulation. MAPKs from other species require activation by corresponding MAPKKs for full enzyme activity. Identification of protein kinases which can activate TgMAPK1 may therefore be necessary.

The full-length isoform of TgMAPK1, which is predicted by both RNA-seq and gene modeling data in ToxoDB, alters the susceptibility of parasites to 1NM-PP1 when expressed in parasites, suggesting that this isoform may contribute to kinase activity.

Attempts at expressing the full-length TgMAPK1 isoform in *E. coli* were also unsuccessful; an alternative system suitable for the expression of large proteins will therefore be needed.

Parasite clones expressing an L162Q mutation in TgMAPK1 exhibited cross resistance to other BKIs (3BrB-PP1 and 3MB-PP1), suggests a more universal role for TgMAPK1 in BKI resistance. The possibility of mutations beyond TgCDPK1 should therefore be considered when BKI resistance is observed. Alternatively, clones possessing the I171N mutation in TgMAPK1 (PLK/DUAL res.2) showed similar susceptibilities to 3MB-PP1, along with slightly higher susceptibilities to 3BrB-PP1. The specificity of this mutation to 1NM-PP1 suggests structural differences between this and other BKIs, which may provide insight into the activity of this compound.

BKI derivatives with enhanced activity against TgCDPK1 have been reported recently (Larson et al., 2012). This activity is mediated through substitutions at the R2 position of the PP-based inhibitor. TgMAPK1 mutations described here aligned to the naphthyl group at the R1 position (Fig. 2). Resistant clones in the present report may not be cross resistant to R2 substituted derivatives; however, use of resistant parasite clones is necessary to predict the occurrence of BKI resistance in *T. gondii*.

The mutation in TgMAPK1 conferring resistance to 1NM-PP1 did not occur at the gatekeeper residue, suggesting the likelihood of similar mutations that may confer resistance in other analog sensitive kinases. Genome-wide screening these and other non-gatekeeper mutation conferring resistance to BKIs is therefore warranted. This work demonstrates the usefulness of random mutagenesis followed by whole-genome sequencing for the screening of such mutations.

In the prediction of the genome sequence, *Toxoplasma gondii* lacks MAPKK and MAPKKK which are the upstream protein kinases for the MAPK (Miranda-Saavedra et al., 2012). Albeit the lack of the typical activation cascade, the author showed in this chapter that TgMAPK1 was important for the tachyzoite growth. Another report by Brumlik *et al* suggested that the parasite who expresses antisense RNA against TgMAPK1 showed slow growth rate and change in the host cell signal manipulations (Brumlik et al., 2013).

Inhibition of TgMAPK1 both in the present thesis and the study by Brumlik leads to parasite growth arrest. However, direct data suggesting that TgMAPK1 is the regulator of parasite cell differentiation and that TgMAPK1 is the regulator of host cell signals is lack in both studies. Inhibitor based off-target effect prevents the present thesis from suggesting the inhibition of TgMAPK1 is the cause of cell division arrest, and antisense RNA based TgMAPK1 constitutively knockdown parasites which grow more slowly than parent parasites prevent Brumlik's study from suggesting the TgMAPK1 inhibition is the cause of the host cell signal change. To characterize further the TgMAPK1 function in the parasite growth the author attempted to make inducible knock out parasites. The author showed that DD-TgMAPK1-FLAG is functional and the protein amount of DD-TgMAPK1-FLAG can be regulated by the shield1 treatment.

By knock-in of HA-tagged TgMAPK1, the author confirmed that TgMAPK1 is localized in the parasite cytosol. The author suggested that the direct manipulation of host cell signals by TgMAPK1 was not occurring. Several GRAs are reported to manipulate the host cell signals (Braun et al., 2013). Parasites with down regulated TgMAPK1 in the Brumliks's study did change parasite growth rate in the host cells (Brumlik et al., 2013), which might result in the reduction of secreted effector proteins,

such as ROPs and GRAs, and which could explain the change in the host cell signal manipulation. Brumlik et al. reported that several splicing variants of TgMAPK1 were expressed at protein level (Brumlik et al., 2013). Another possibility is that some splicing variants, which are different from our full length functional isoform, can be translocated to host cells. N-terminal tagging of TgMAPK1 might change the localization, therefore the possibility that the native TgMAPK1 may translocate to the host cell should be considered.

The author observed that knock-inned HA-TgMAPK1 give parasites the resistance to 1NM-PP1. HA-TgMAPK1 was driven by the GRA1 promoter and might be stronger than the native TgMAPK1 promoter. Therefore, hyper expression of TgMAPK1 may result in the acquisition of resistance to 1NM-PP1. The resistance from the hyper expression of the target protein was usually observed and used in the drug target screening in the yeast as "multi-copy suppression profiling" (Hoon et al., 2008). These data suggest that HA-tagged full length isoform TgMAPK1 was sufficient for parasite growth and enough for the acquisition of resistance to 1NM-PP1. If the mutated TgMAPK1, which is more susceptible for the 1NM-PP1 than wild type TgMAPK1 or is more resistant for 1NM-PP1 than L162Q mutated TgMAPK1, will be knocked in, 1NM-PP1 treatment will further elucidate the effect of TgMAPK1 inhibition. Such mutated TgMAPK1 will be prepared through changing the gatekeeper amino acid from wild type serin to alanine and glycine (susceptible mutation) OR to threonine, fenylalanine and methionine (resistant mutation).

Success in the HA-tagging of TgMAPK1 with double homologous recombination meant that the genomic locus of TgMAPK1 was accessible and N-terminally tagged full length TgMAPK1 was functional and can be replace the native genome locus. By the

use of destabilizing domain instead of the HA tag for the N-terminal tagging, the author suggests that TgMAPK1 conditional knockdown parasite can be established. Conditional knock down parasites further reveals the role of TgMAPK1 in the future.

Tables

Table 1. Primers used in this study

Primer	Sequence (5' - 3')[(a)]
genomeLocusPrimer_F	ccgacagaagtcaaaagggaatgagatgccaggtat
genomeLocusPrimer_R	caagaaaagcaacgagagatttcagagtctccattg
TgMAPK1_F1	ct*GAATTC*cagagcacgagtgccgga
TgMAPK1_R1	agtccaggctccttgctttc
TgMAPK1cla1_F2	tgatttgatcgaTgccaaacgca
TgMAPK1cla1_R2	tgcgtttggcAtcgatcaaatca
Splicing_confirm_F	tccattctgctactctaagc
Splicing_confirm_R	acgatctcgggatgataaga
1st_half_F	ct*GAATTC*acagagcacgagtgccgga
1st_half_R	ctgcagcaggcgtttcgttgggacgaagtt
2nd_half_F	ccaacgaaacgcctgctgcagaacaaggt
2nd_half_R	aa*GATATC*agctgttgctggccatgct
GFP_F	gt*AGATCT*catgcataaaggagaagaa
GFP_R	tt*GATATC*ttgtatagttcatccatg
Mutation_screen_F	ttttgcaggtcggaagtg
Mutation _screen_R	agtccaggctccttgctttc

[(a)]Characters in italics show restriction enzyme site. Underline shows mutation positions introducing *Cla*I restriction site without amino acid change.

Table 2. Detected putative SNVs from reference strain ME49 genome

parasite line	chromosome	position	ref	alt	QUAL
PLK/DUAL	Ia	6974	A	C	159
	Ia	8040	C	T	148
	Ia	10725	T	C	175
	Ia	1405961	A	G	222
	Ib	756379	T	C	222
	Ib	1613012	A	G	7.79
	Ib	1613199	T	G	222
	Ib	1621370	A	G	172
	II	74351	G	T	222
	II	74399	T	A	222
	II	74400	A	C	222
	II	924571	G	A	190
	II	2016101	A	C	222
	II	2243782	C	G	222
	II	2248638	G	C	222
	II	2302022	T	G	222
	III	815556	G	A	213
	III	1373147	A	G	222
	III	2304884	C	G	123
	III	2311447	A	G	222
	IV	10985	A	G	127
	IV	299993	G	C	222
	IV	347380	G	A	222
	IV	905053	A	G	222
	IV	1108217	G	A	192
	IV	2155523	T	C	222
	V	28263	C	G	154
	V	32474	A	G	146
	V	135986	C	G	222
	V	2579862	T	G	222
	V	2694441	A	C	221
	V	2815964	A	G	222

PLK/DUAL cont.	V	3125550	C	A	222
	V	3150122	A	G	222
	VI	270306	G	A	181
	VI	912404	A	C	222
	VI	1163791	T	G	34
	VI	1163796	C	T	39
	VI	1689698	G	A	139
	VI	1709179	A	G	222
	VI	1800292	T	C	215
	VIIa	916215	A	C	222
	VIIb	63	C	A	222
	VIIb	1506886	C	A	222
	VIIb	1506894	T	A	222
	VIIb	2340306	G	T	54
	VIIb	2679698	T	C	213
	VIIb	3742319	T	A	222
	VIIb	4012005	G	T	222
	VIII	1874942	C	G	222
	VIII	2202435	C	A	222
	VIII	4486309	T	C	222
	VIII	5578688	C	G	222
	VIII	6811350	G	C	222
	IX	97569	C	G	136
	IX	99739	G	A	128
	IX	114085	T	C	222
	IX	142332	G	T	137
	IX	207411	A	C	222
	IX	243299	T	C	84
	IX	248082	G	A	222
	IX	1305716	A	G	161
	IX	2453680	T	A	222
	IX	3754204	C	G	222
	IX	4684529	A	G	222
	IX	5575273	T	C	222
	IX	6143610	T	C	200
	IX	6376931	T	C	222

PLK/DUAL cont.	X	62055	A	G	102
	X	1601940	C	G	222
	X	1857308	T	G	222
	X	1924988	G	T	165
	X	3390813	G	C	222
	X	4020019	A	C	222
	X	4022598	G	C	222
	X	5613042	A	G	222
	X	6817013	A	T	222
	XI	45193	A	G	191
	XI	49704	T	C	222
	XI	946465	G	T	222
	XI	1799160	T	C	175
	XI	2913242	T	A	222
	XI	4192485	G	A	102
	XI	6618603	G	T	220
	XII	11406	T	G	140
	XII	539971	C	T	222
	XII	542042	G	A	222
	XII	543194	G	A	148
	XII	3544088	C	A	222
	XII	4267944	G	C	222
	XII	4798151	G	A	222
	XII	5060482	C	G	222
	XII	5323790	C	G	83.1
	XII	5532037	T	C	222
	XII	5679793	C	G	206
	XII	5679794	T	A	183
	XII	5796752	C	T	222
P/D res.1	Ia	346	G	C	208
	Ia	416	A	C	222
	Ia	10725	T	C	132
	Ia	1405961	A	G	222
	Ia	1867910	A	G	195
	Ib	756379	T	C	222

P/D res.1 cont.	Ib	1613199	T	G	222
	Ib	1621370	A	G	171
	II	74351	G	T	222
	II	74399	T	A	222
	II	74400	A	C	222
	II	924571	G	A	192
	II	2016101	A	C	222
	II	2243782	C	G,T	172
	II	2248638	G	C	220
	II	2302022	T	G	222
	III	35456	A	G	175
	III	815556	G	A	167
	III	1373147	A	G	158
	III	2311447	A	G	143
	IV	299993	G	C	222
	IV	347380	G	A	187
	IV	905053	A	G	214
	IV	2155523	T	C	222
	V	32474	A	G	144
	V	33970	A	G	226
	V	38525	G	T	108
	V	40364	C	A	222
	V	135986	C	G	222
	V	2579862	T	G	222
	V	2694441	A	C,G	129
	V	2815964	A	G	199
	V	3125550	C	A	212
	V	3150122	A	G	222
	VI	270306	G	A	145
	VI	912404	A	C	157
	VI	1163791	T	G	51
	VI	1163796	C	T	53
	VI	1689698	G	A	96
	VI	1709179	A	G	222
	VI	1800292	T	C	222
	VIIa	916215	A	C	222

P/D res.1 cont.	VIIb	63	C	A	222
	VIIb	1506886	C	A	222
	VIIb	1506894	T	A	222
	VIIb	2679698	T	C	177
	VIIb	3741299	G	A	99
	VIIb	3742319	T	A	222
	VIIb	4012005	G	T	222
	VIIb	5004031	A	G	189
	VIII	655444	C	T	222
	VIII	1874942	C	G	221
	VIII	2202435	C	A	222
	VIII	4486309	T	C	222
	VIII	5168296	C	T	214
	VIII	5578688	C	G	174
	VIII	6811350	G	C	222
	VIII	6901890	C	T	99
	IX	97569	C	G	123
	IX	114085	T	C	212
	IX	207411	A	C	222
	IX	243299	T	C	110
	IX	248082	G	A	222
	IX	1305716	A	G	153
	IX	2453680	T	A	216
	IX	2714202	C	T	222
	IX	3050049	C	T	222
	IX	3754204	C	G	194
	IX	4487896	T	G	222
	IX	4684529	A	G	222
	IX	5337145	T	C	184
	IX	5575273	T	C	206
	IX	6143610	T	C	155
	IX	6376931	T	C	222
	IX	6385452	A	G	222
	X	62055	A	G	112
	X	63289	A	G	95
	X	1601940	C	G	222

P/D res.1 cont.	X	1857308	T	G	222
	X	1924988	G	T	191
	X	3390813	G	C	222
	X	4020019	A	C	222
	X	4022598	G	C	222
	X	4708598	G	A	222
	X	5613042	A	G	222
	X	6817013	A	T	222
	XI	45193	A	G	174
	XI	49704	T	C	222
	XI	946465	G	T	211
	XI	1069788	A	C	222
	XI	1799160	T	C	135
	XI	2180362	T	C	132
	XI	2783306	A	T	222
	XI	2913242	T	A	222
	XI	4192485	G	A	160
	XI	6618603	G	T	222
	XII	11406	T	G	98
	XII	542042	G	A	222
	XII	543194	G	A	178
	XII	2128556	T	A	222
	XII	3544088	C	A	222
	XII	4267944	G	C	222
	XII	4798151	G	A	222
	XII	5060482	C	G	222
	XII	5323786	C	T	102
	XII	5323787	T	C	111
	XII	5323790	C	G	94.2
	XII	5532037	T	C	222
	XII	5679793	C	G	220
	XII	5679794	T	A	219
	XII	5796752	C	T	175
P/D res.2	Ia	346	G	C	219
	Ia	8040	C	T	140

P/D res.2 cont.	Ia	311694	T	A	222
	Ia	1405961	A	G	222
	Ib	756379	T	C	222
	Ib	1387776	T	C	222
	Ib	1483250	A	G	211
	Ib	1613199	T	G	222
	Ib	1621370	A	G	183
	II	74351	G	T	222
	II	74399	T	A	222
	II	74400	A	C	222
	II	924571	G	A	192
	II	1894639	A	T	222
	II	2016101	A	C	222
	II	2096102	T	C	222
	II	2243782	C	G	222
	II	2248638	G	C	222
	II	2302022	T	G	222
	III	815556	G	A	178
	III	1373147	A	G	153
	III	1650508	A	G	145
	III	2079977	A	C	222
	III	2311447	A	G	222
	IV	299993	G	C	222
	IV	347380	G	A	222
	IV	896263	C	T	172
	IV	905053	A	G	189
	IV	979711	T	C	222
	IV	1108217	G	A	222
	IV	1495705	A	T	222
	IV	2155523	T	C	222
	V	31569	G	C	184
	V	32474	A	G	172
	V	40364	C	A	211
	V	135986	C	G	222
	V	2194859	A	T	220
	V	2579862	T	G	222

P/D res.2 cont.	V	2694441	A	C	157
	V	2815964	A	G	192
	V	3038327	A	C	222
	V	3125550	C	A	222
	V	3150122	A	G	222
	VI	270306	G	A	144
	VI	912404	A	C	177
	VI	1163791	T	G	43
	VI	1163796	C	T	46
	VI	1689698	G	A	161
	VI	1709179	A	G	222
	VI	1800292	T	C	222
	VI	2684711	A	G	222
	VI	2768809	G	A	222
	VIIa	403643	A	T	222
	VIIa	916215	A	C	222
	VIIa	1662948	A	G	222
	VIIa	3302226	T	A	222
	VIIa	3386982	T	C	172
	VIIa	3775004	T	C	222
	VIIa	3845346	T	A	222
	VIIa	4109150	T	A	222
	VIIb	63	C	A	222
	VIIb	1506886	C	A	222
	VIIb	1506894	T	A	222
	VIIb	2679698	T	C	179
	VIIb	3437846	A	G	222
	VIIb	3449675	A	T	222
	VIIb	3742319	T	A	189
	VIIb	4012005	G	T	222
	VIIb	4408633	T	A	222
	VIIb	4859821	A	G	222
	VIIb	5004031	A	G	181
	VIII	191113	A	G	222
	VIII	1452641	A	G	222
	VIII	1731366	A	T	222

P/D res.2 cont.	VIII	1874942	C	G	222
	VIII	2202435	C	A	222
	VIII	4486309	T	C	222
	VIII	5578688	C	G	222
	VIII	5884619	T	C	222
	VIII	5943975	T	A	222
	VIII	6811350	G	C	222
	IX	53461	G	A	191
	IX	97569	C	G	145
	IX	114085	T	C	222
	IX	142332	G	T	148
	IX	207411	A	C	222
	IX	243299	T	C	148
	IX	243569	G	T	80.1
	IX	248082	G	A	222
	IX	340275	A	G	222
	IX	804970	T	A	222
	IX	964139	T	A	222
	IX	1305716	A	G	222
	IX	2453680	T	A	222
	IX	2833714	A	T	222
	IX	2981058	A	G	222
	IX	3500681	A	G	221
	IX	3754204	C	G	215
	IX	4365569	A	T	222
	IX	4684529	A	G	222
	IX	5575273	T	C	222
	IX	6143610	T	C	181
	IX	6274115	G	C	222
	IX	6376931	T	C	222
	IX	6385452	A	G	222
	X	62055	A	G	90
	X	1601940	C	G	222
	X	1737926	A	T	222
	X	1857308	T	G	222
	X	1924988	G	T	184

P/D res.2 cont.	X	2088273	A	T	222
	X	2876018	A	T	195
	X	2927056	A	G	222
	X	3390813	G	C	222
	X	3620643	T	C	222
	X	4020019	A	C	222
	X	4022598	G	C	222
	X	4028432	T	G	222
	X	5613042	A	G	222
	X	6817013	A	T	222
	X	7400683	A	G	222
	XI	45193	A	G	199
	XI	49704	T	C	222
	XI	485591	A	T	215
	XI	946465	G	T	222
	XI	1257204	A	T	222
	XI	1799160	T	C	173
	XI	2423586	A	G	222
	XI	2751672	G	T	210
	XI	2783279	A	T	222
	XI	2913242	T	A	222
	XI	3272838	A	G	222
	XI	3503376	T	C	222
	XI	3776848	A	G	210
	XI	4692538	A	C	222
	XI	4734610	T	A	222
	XI	5623774	C	T	144
	XI	6588297	A	C	222
	XI	6618603	G	T	222
	XII	11406	T	G	138
	XII	539971	C	T	222
	XII	542042	G	A	222
	XII	543194	G	A	149
	XII	799202	A	G	221
	XII	1029418	C	A	222
	XII	3544088	C	A	222

P/D res.2 cont.	XII	4267944	G	C	222
	XII	4300598	A	T	222
	XII	4798151	G	A	222
	XII	5060482	C	G	222
	XII	5088893	A	T	222
	XII	5112575	T	C	222
	XII	5323790	C	G	123
	XII	5532037	T	C	222
	XII	5663583	A	C	222
	XII	5679793	C	G	222
	XII	5679794	T	A	222
	XII	5796752	C	T	222
	XII	5957517	A	T	222
	XII	6713079	A	T	222

QUAL column shows quality score of SNP detected with samtools.

Table 3. Putative missense SNPs detected only in the resistant clones

	Chromosome	SNP position	ref[a]	alt[b]	gene id	A. A.	ref A.A.	alt A.A.	[c]gene annotation in ToxoDB [pfam domain search]
PLK/DUAL res.1	Ia	416	A	C	TGME49_095210	7	K	T	hypothetical protein [N/D]
	VIII	655444	C	T	TGME49_030170	1005	S	N	hypothetical protein [N/D]
	IX	3050049	C	T	TGME49_089070	28	S	L	P-Type cation-transporting ATPase, putative
	XI	2783306	A	T	TGME49_112570	162	L	Q	CMGC kinase, MAPK family (ERK) TgMAPK-1
	XII	2128556	T	A	TGME49_017830	608	I	F	hypothetical protein [N/D]

	Chromosome	SNP position	ref[a]	alt[b]	gene id	A. A.	ref A.A.	alt A.A.	[c]gene annotation in ToxoDB [pfam domain search]
PLK/DUAL res.2	Ib	1387776	T	C	TGME49_009660	124	N	D	hypothetical protein [coiled_coil_region, Telomerase_RBD]
	V	31569	G	C	TGME49_096340	35	R	G	hypothetical protein [N/D]
	VIIa	3386982	T	C	TGME49_002330	62	D	G	hypothetical protein [N/D]
	VIIa	3845346	T	A	TGME49_001640	247	E	V	hypothetical protein [coiled_coil_region]
	VIIb	4408633	T	A	TGME49_056790	550	K	M	hypothetical protein [ABC_transp_aux]
	VIII	5884619	T	C	TGME49_069330	17	L	P	hypothetical protein, conserved [coiled_coil_region]
	IX	2981058	A	G	TGME49_088970	97	L	P	hypothetical protein [N/D]

X	1737926	A	T	TGME49_026110	424	N	I	copper-transporting ATPase 1, putative
X	2927056	A	G	TGME49_024550	296	F	S	hypothetical protein [N/D]
XI	2751672	G	T	TGME49_112520	237	H	N	tRNA delta(2)-isopentenylpyrophosphate transferase, putative
XI	2783279	A	T	TGME49_112570	171	I	N	CMGC kinase, MAPK family (ERK) TgMAPK-1
XII	1029418	C	A	TGME49_019220	922	V	F	hypothetical protein [coiled_coil_region]
XII	5957517	A	T	TGME49_078640	305	V	D	protein inhibitor of activated STAT protein, putative

Chromosomal positions are shown for the ME49 genome model. [(a)]Reference bases and [(b)] alternative bases on the positive strand of chromosomes are shown. [(C)] For genes annotated as hypothetical proteins in ToxoDB, pfam domain search hits are shown in parentheses. N/D; not detected.

Figure legends

Figure 1. Establishment of 1NM-PP1 resistant clones and whole-genome sequence

(A) Tachyzoite growth inhibition by 1NM-PP1 was calculated based upon expression of a DsRed Express fluorescent reporter driven by a SAG1 promoter. Cells were cultured for 6 days; fluorescent signals from cell lysates were detected using a fluorimeter, and expressed as relative fluorescent units. Error bars indicate the standard deviations across three independent experiments. IC_{50} values for three clones are inset. (B) Summary of sequence reads that could be aligned to the *T. gondii* genome. (C) Genome-wide average sequence depths of a 100-kbp window from PLK/DUAL (black), PLK/DUAL res.1 (red), and PLK/DUAL res.2 (blue) are plotted. The horizontal red line shows ×10 depth. Scale bar = 10 Mbp. Putative SNVs in PLK/DUAL res.1 (red triangle) and PLK/DUAL res.2 (blue triangle), based on the coding sequence of PLK/DUAL, are plotted.

Figure 2. Predicted TgMAPK1 protein kinase domain structure superimposed on the structure of 1NM-PP1-bound CpCDPK1 (PDB:3NCG).

Homology modeling of a TgMAPK1 peptide spanning residues 81 to 670 was performed using SWISS-MODEL in automated mode using PDB:4B99 as a template. The predicted structure of TgMAPK1 superimposed on 1NM-PP1-bound CpCDPK1 (PDB:3NCG) is shown in (A); structures near the 1NM-PP1 binding site are shown in (B). The blue ribbon represents the predicted structure of TgMAPK1, the purple ribbon shows CpCDPK1, and the structure of 1NM-PP1 is shown in green. TgMAPK1 mutation sites Leu 162 and Ile 171 are shown in orange. 1NM-PP1 has a naphthyl group at the R1

position of PP1-based structure and a methyl group at the R2 position.

Figure 3. 1NM-PP1 selects for mutations in TgMAPK1.

(A) Alignment of the mutated region of TgMAPK1 with proteins HsErk5 and CpCDPK1. * indicates the ATP-binding amino acid position, + indicates the 1NM-PP1 bound amino acid position in CpCDPK1, and # indicates the position of the gatekeeper residue. (B) Schematic depicting the chromosomal DNA around TGME49_112570 and a replacement construct. The blue boxes show coding sequences for genes TGME49_112560 and TGME49_112580. The red box shows the TGME49_112570 exon on the negative strand of chromosome XI. Arrows represent primers genomeLocusPrimer_F and genomeLocusPrimer_R used in PCR-RFLP analysis. A *Cla*I restriction site is contained in all plasmids; mutations L162Q and I171N are encoded by plasmids pTgMAPK1_LQ and pTgMAPK1_IN, respectively. (C) PCR fragments of chromosome XI 2,772,456–2,789,052 from PLK/DUAL and PLK/DUAL TgMAPK1^{L162Q} were cut with *Cla*I or *Bam*HI and separated by 0.7% agarose gel electrophoresis. (D) Tachyzoite growth inhibition by 1NM-PP1 was determined by measuring DsRed Express fluorescent reporter expression. Cells were cultured for 6 days; fluorescent signals in cell lysates were detected using a fluorimeter, and expressed as relative fluorescent units. Error bars indicate the standard deviations across three independent experiments. IC_{50} values are inset.

Figure 4. Sequence analyses of PLK/DUAL transfected with TgMAPK1 genome locus replacement constructs and selected using 1NM-PP1.

(A, B) PCR fragments of chromosome XI 2,772,456–2,789,052 were cut with *Bam*HI

or *Cla*I and separated by 0.7% agarose gel electrophoresis. gDNA from PLK/DUAL was used as a control. PLK/DUAL parasites transfected with pTgMAPK1_WT, pTgMAPK1_LQ and pTgMAPK1_IN were cultured either without 1NM-PP1 for 1 week (A) or with 1000 nM 1NM-PP1 for 3 weeks (B), followed by gDNA purification. (A, B) Approximate sizes are shown in kbp. (C) Sequence chromatograms of 1NM-PP1 selected parasites transfected with pTgMAPK1_LQ (upper panels), pTgMAPK1_IN (middle panels), and a mixture of pTgMAPK1_WT, pTgMAPK1_LQ, and pTgMAPK1_IN (lower panels) are shown. Sequences flanking mutation sites resulting in *Cla*I, L162Q, and I171N mutations are shown. Base pair numbers denote the genomic position of mutated nucleotides relative to the TgMAPK1 start codon. Wild type sequences are A995 for the *Cla*I site, T1027 for the L162Q site, and T1054 for the I171N site.

Figure 5. Overexpression of L162Q mutated TgMAPK1 alters the susceptibility of parasites to 1NM-PP1.

(A) Schematic of TgMAPK1 gDNA, mRNA splicing, and expression constructs. Red boxes denote exonic regions of TgMAPK1, numbered E1-E8. Black arrows indicate primers used for splicing confirmation (Splicing_confirm_F and Splicing_confirm_R in Supplemental Table 1). Primers used for amplification of the first half of TgMAPK1 mRNA are shown in red; primers used for amplification of the second half of TgMAPK1 mRNA are shown in green. C-terminal tagged 3xFLAG sequences are shown in the black box. The full-length mRNA sequence was amplified by overlapping PCR and inserted into an expression plasmid containing an HXGPRT selection marker, resulting in a TgMAPK1 construct containing a C-terminal 3xFLAG tag under control of a GRA1 promoter. (B) Western blots of 3xFLAG tagged proteins from PLK/TgMAPK1-FLAG,

PLK/TgMAPK1^{L162Q}-FLAG, and PLK/GFP-FLAG. 3xFLAG tagged proteins were detected with anti-FLAG M2 mAb (Sigma-Aldrich) (upper panel). TgALD1 was detected using anti-TgALD rabbit antisera, and used as a loading control. Molecular weights are shown on the left (kDa). (C) Plaque assays of PLK/GFP-FLAG (left panels), PLK/TgMAPK1-FLAG (center panels), and PLK/TgMAPK1^{L162Q}-FLAG (right panels) clones are shown. Vero monolayers in 12-well plates were inoculated with 1,000 parasites per well. After 2 h, media were changed to media containing various concentration of 1NM-PP1, and incubated for 7 days. After incubation, cells were washed with PBS three times, fixed with methanol for 5 min, and stained with crystal violet. Scale bar shows 0.5 mm.

Figure 6. Cross resistance of 1NM-PP1 resistant parasite clones to 3BrB-PP1 and 3MB-PP1.

Inhibitory effects of 3BrB-PP1 (A) and 3MB-PP1 (B) were evaluated using a tachyzoite growth assay. Tachyzoite growth was assayed using DsRed-Express fluorescent reporter expression driven by a SAG1 promoter. Cells were cultured for 6 days; fluorescent signals from cell lysates were detected using a fluorimeter, and expressed as relative fluorescent units. Error bars indicate the standard deviation across three independent experiments. IC_{50} values for four clones are shown in the inset. Ct indicates the relative background fluorescence intensity of DMSO-treated controls.

Figure 7. Shield1 concentration dependent TgMAPK1 protein amount regulation.

(A) Schematic depiction of DD-TgMAPK1-FLAG expression plasmid. DD tag is inserted into N-terminal of TgMAPK1 and 3xFLAG tag is inserted into C-terminal TgMAPK1. (B) Shield1 concentration dependent DD-TgMAPK1-FLAG protein amount changes. Parent RH/hxgprt$^-$ and RH/DD-TgMAPK1^{L162Q}-FLAG were inoculated to Vero cells and incubated overnight. Infected host cells were incubated with media with various concentration shield1 or vehicle ethanol control for 4 h. After shield1 treatment, cells were washed with ice cold PBS and lysed in SDS-PAGE sample buffer and FLAG-tagged proteins were detected with anti-FLAG M2 mAb conjugated with horseradish peroxidase (Sigma). Loading controls are shown in the lower panels. (C) Plaque formation assay was performed with parent RH/hxgprt$^-$ and RH/DD-TgMAPK1^{L162Q}-FLAG parasites. Full monolayer Vero cells in 12 well plates were inoculated with 2,000 parasites/well and incubated for 7 days with media containing 250 nM 1NM-PP1 or DMSO control. After incubation, infected host cells were fixed with methanol and stained with crystal violet.

Figure 8. Endogeneous tagging at TgMAPK1 locus

(A) Schematic diagram of double homologous recombination for the knock-in experiments. Wild type sequence of parasite chromosome, transfected linearized DNA and recombinated chromosomal sequence are shown. Red arrows show the primers site for the PCR-RFLP assay. *Cla*I emzyme recognition site is shown.

(B) PCR was performed with primers in (A) and cut with *Cla*I. DNA ladder of 5, 6, 8 and 10 kbp was loaded at the 1st left lane.

Figure 9. Characteristics of HA-tagged TgMAPK1.

(A) Protein expression from the knock-in locus was confirmed by western blotting. Protein lysates from 10^6 parasites/lane were loaded and were detected with anti-HA mAb (left panel), or with anti-TgALD1 antibody (right panel). TgALD1 were detected as the loading control. Molecular weight is shown at left.

(B) Parasites infected host cells were stained at 32 h post infection. Red: HA-tagged protein. Blue: Nuclei. Scale bar shows 10 μm.

Figure 10. Functional TgMAPK1 was expressed from HA tagged TgMAPK1 locus.

Parent RH/ku80-/hxgprt-, RH/HA-TgMAPK1^{WT} and RH/HA-TgMAPK1^{L162Q} parasites were inoculated to host Vero cells in 96 well plates. Parasites were incubated with various concentrations of 1NM-PP1 for 6 days. Host cell disruption was evaluated by the staining with crystal violet. OD_{600} value was measured and the decreases of OD_{600} value from the mock infected wells were calculated as host monolayer disruption values. Wells infected with a parent strain without 1NM-PP1 was estimated to 100% disruption. Error bar means standard deviation from the independent triplicate experiments. Statistical analyses were performed by Student's t-test. * $p < 0.05$, ** $p < 0.01$.

Figures

A

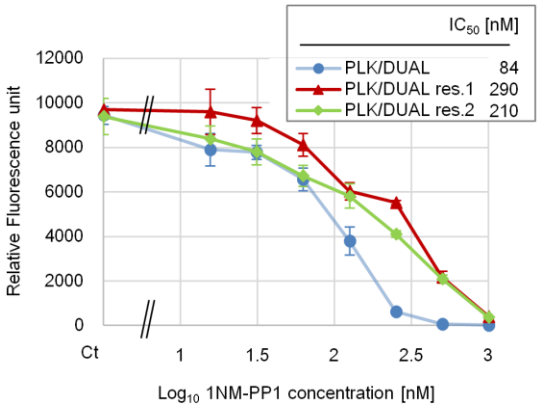

B

clone	Mapped reads	coverage (%)	Average depth
PLK/DUAL	16618344	96.86	20.17
PLK/DUAL res. 1	11514716	96.07	13.98
PLK/DUAL res.2	16263909	97.03	19.74

C

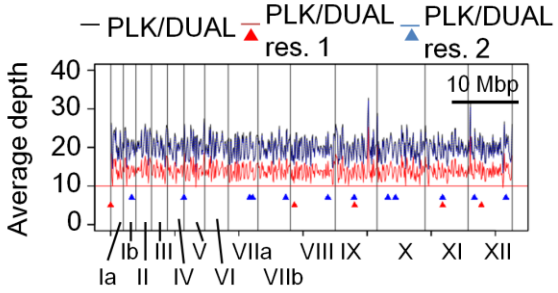

Figure 1

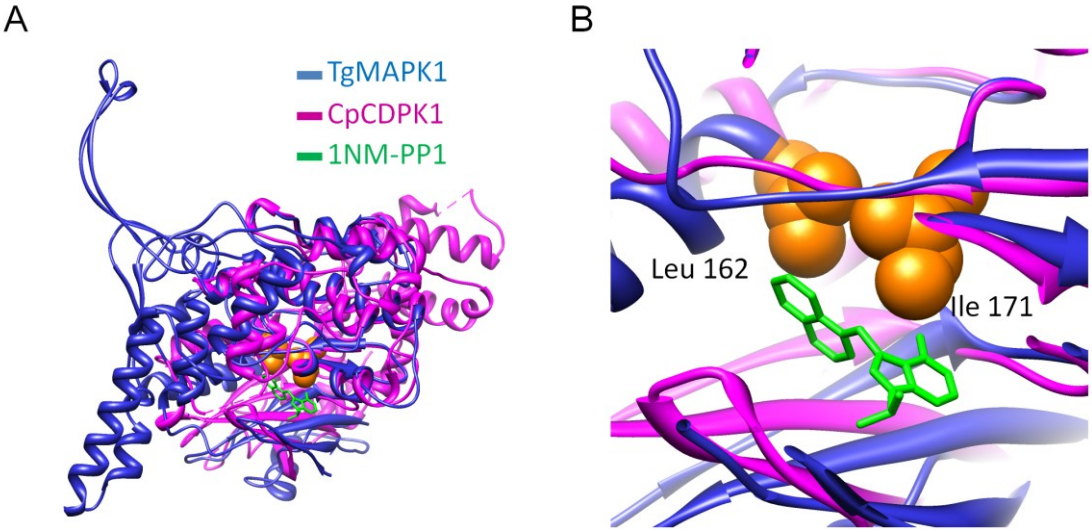

Figure 2

A

```
subdomain    ----III-------  -------IV---------  ---------V------------
ATP binding       *             *                   ****  * **
TgMAPK1 151:DAKRIYREIKILKELKHENIINLVEILDPLTPDF--EDIYLVSDLMDTDLHRVIYSRQ:216
HsERK5   95:NAKRTLRELKILKHFKHDNIIAIKDILRPTVPYGEFKSVYVVLDLMESDLHQIIHSSQ:152
CpCDPK1  64:DTSTILREVELLKKLDHPNIMKLFEILEDSSSFYIVGELYTGGELFDEIIKRKRFSEH:121
Mutation               Q        N
BKI interaction                 + +             + +  #
```

B

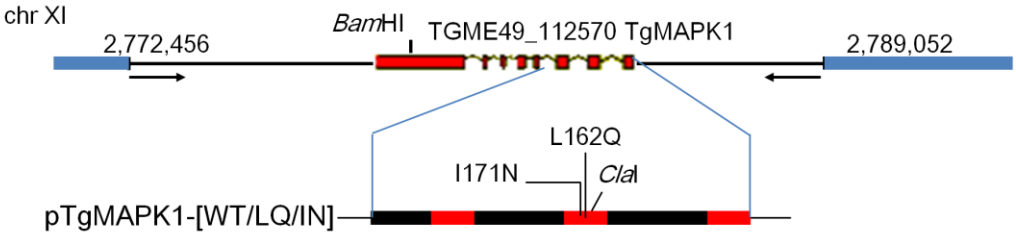

C

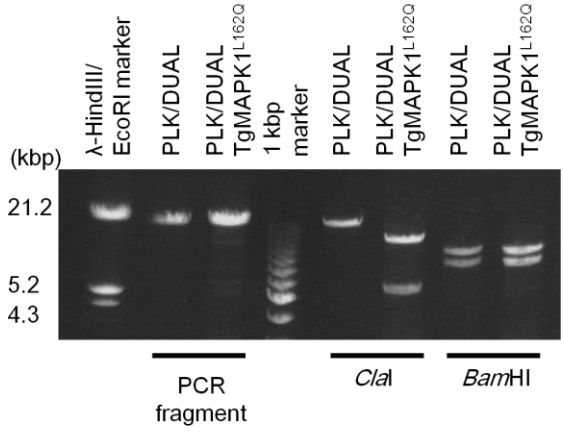

D

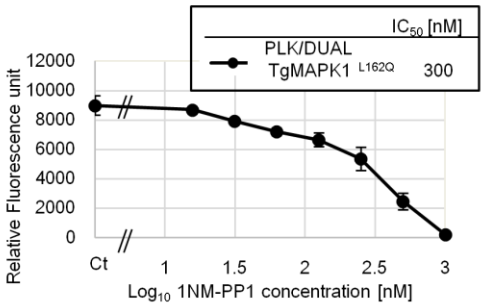

Figure 3

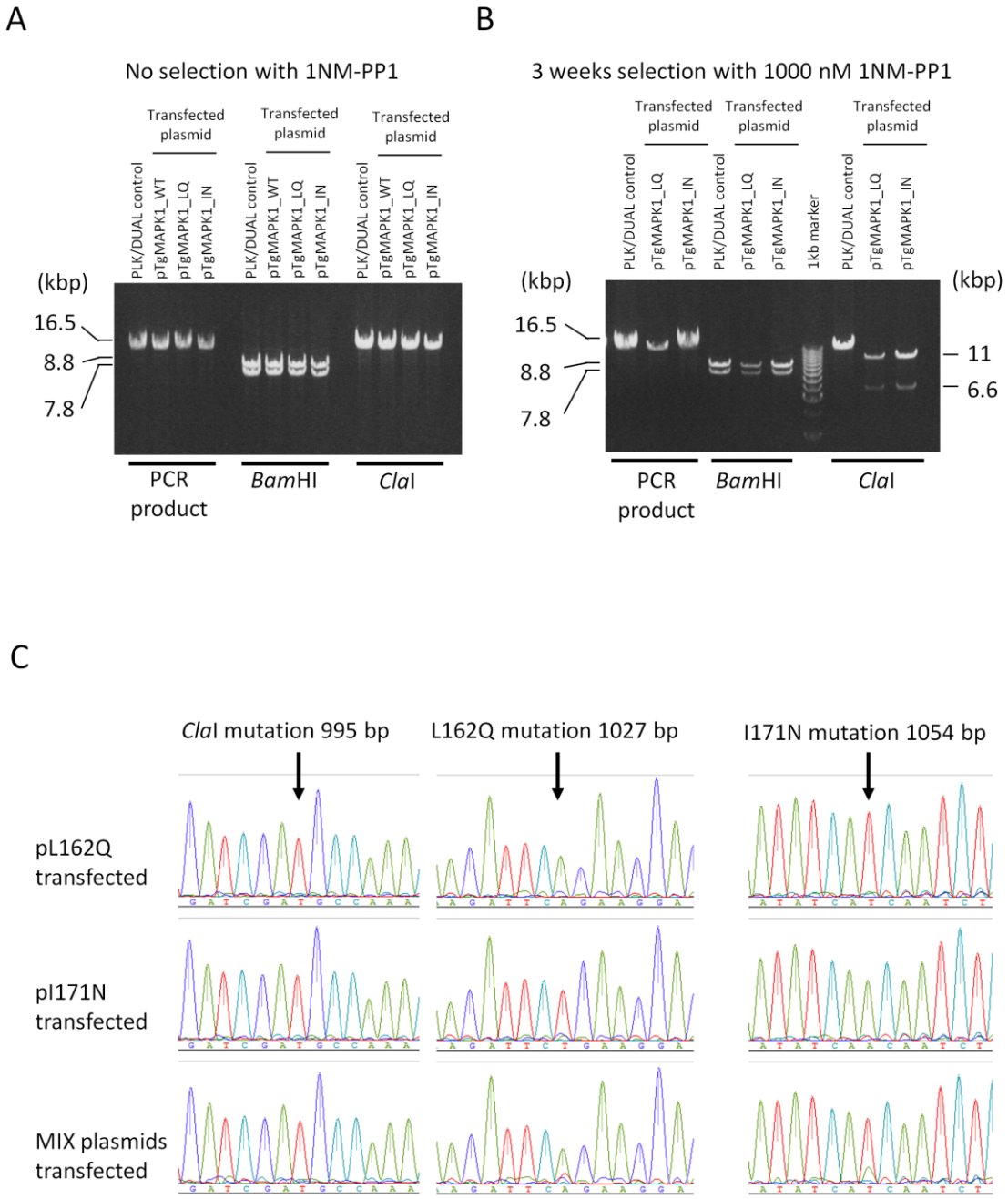
A
No selection with 1NM-PP1
Transfected plasmid
PLK/DUAL control
pTgMAPK1_WT
pTgMAPK1_LQ
pTgMAPK1_IN
(kbp)
16.5
8.8
7.8
PCR product
BamHI
ClaI
B
3 weeks selection with 1000 nM 1NM-PP1
1kb marker
11
6.6
C
ClaI mutation 995 bp
L162Q mutation 1027 bp
I171N mutation 1054 bp
pL162Q transfected
pI171N transfected
MIX plasmids transfected

Figure 4

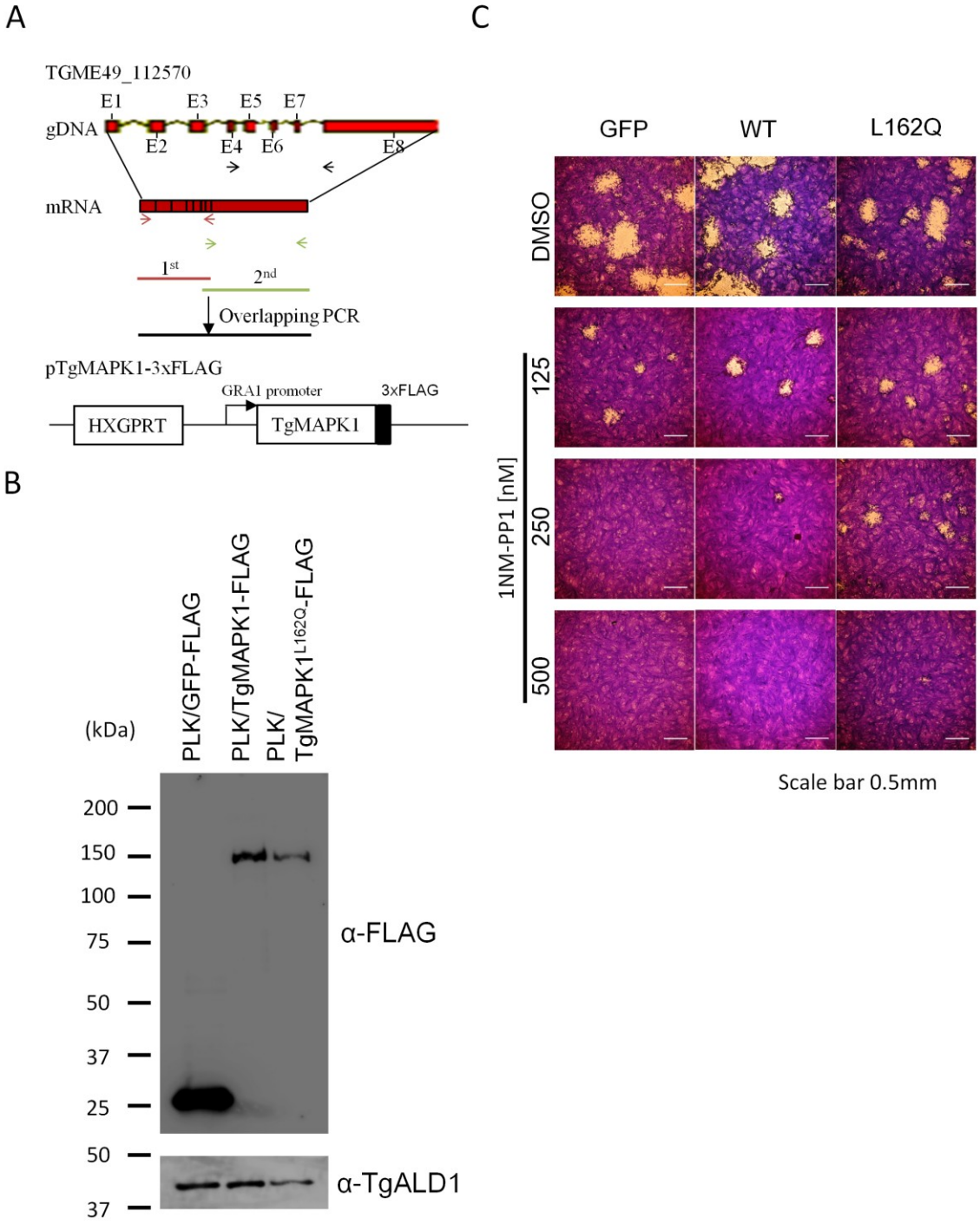
A
TGME49_112570
E1
E3
E5
E7
gDNA
E2
E4
E6
E8
mRNA
1st
2nd
Overlapping PCR
pTgMAPK1-3xFLAG
GRA1 promoter
3xFLAG
HXGPRT
TgMAPK1
B
(kDa)
PLK/GFP-FLAG
PLK/TgMAPK1-FLAG
PLK/
TgMAPK1L162Q-FLAG
200
150
100
75
50
37
25
50
37
α-FLAG
α-TgALD1
C
GFP
WT
L162Q
DMSO
1NM-PP1 [nM]
125
250
500
Scale bar 0.5mm

Figure 5

A

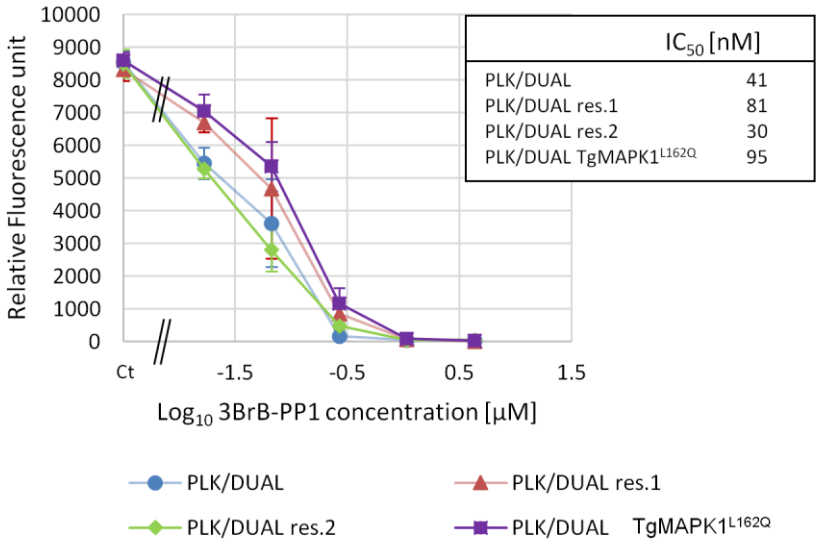
Relative Fluorescence unit
10000
9000
8000
7000
6000
5000
4000
3000
2000
1000
0
Ct
-1.5
-0.5
0.5
1.5
Log10 3BrB-PP1 concentration [µM]
IC50 [nM]
PLK/DUAL 41
PLK/DUAL res.1 81
PLK/DUAL res.2 30
PLK/DUAL TgMAPK1L162Q 95
PLK/DUAL
PLK/DUAL res.1
PLK/DUAL res.2
PLK/DUAL TgMAPK1L162Q

B

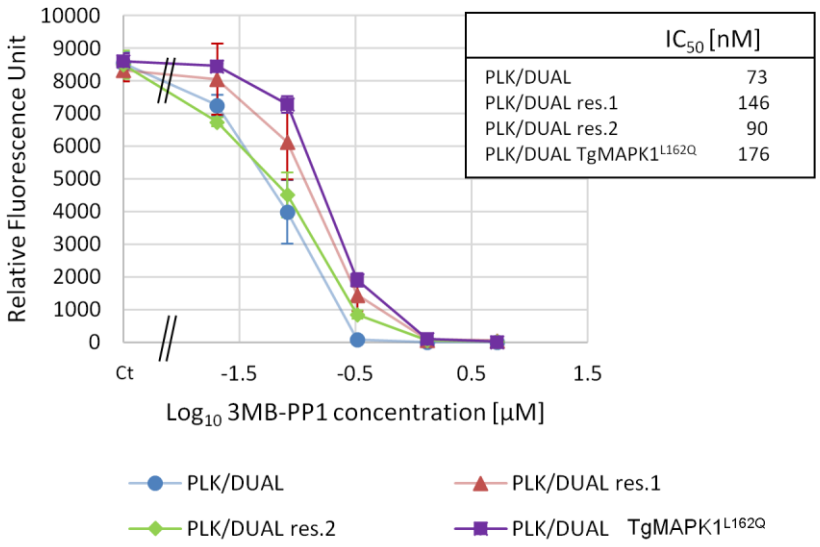
Relative Fluorescence Unit
10000
9000
8000
7000
6000
5000
4000
3000
2000
1000
0
Ct
-1.5
-0.5
0.5
1.5
Log10 3MB-PP1 concentration [µM]
IC50 [nM]
PLK/DUAL 73
PLK/DUAL res.1 146
PLK/DUAL res.2 90
PLK/DUAL TgMAPK1L162Q 176
PLK/DUAL
PLK/DUAL res.1
PLK/DUAL res.2
PLK/DUAL TgMAPK1L162Q

Figure 6

A
pDD-TgMAPK1-FLAG
HXGPRT cassette
GRA1 promoter
DD tag
3xFLAG
B
RH/hxgprt-
RH/DD-TgMAPK1L162Q-FLAG
(kDa)
250
150
100
75
50
37
α-FLAG
α-TgALD1
Shield1 (nM)
0
250
500
1000
0
250
500
1000
C
control
250nM 1NM-PP1
Parent
L162Q

Figure 7

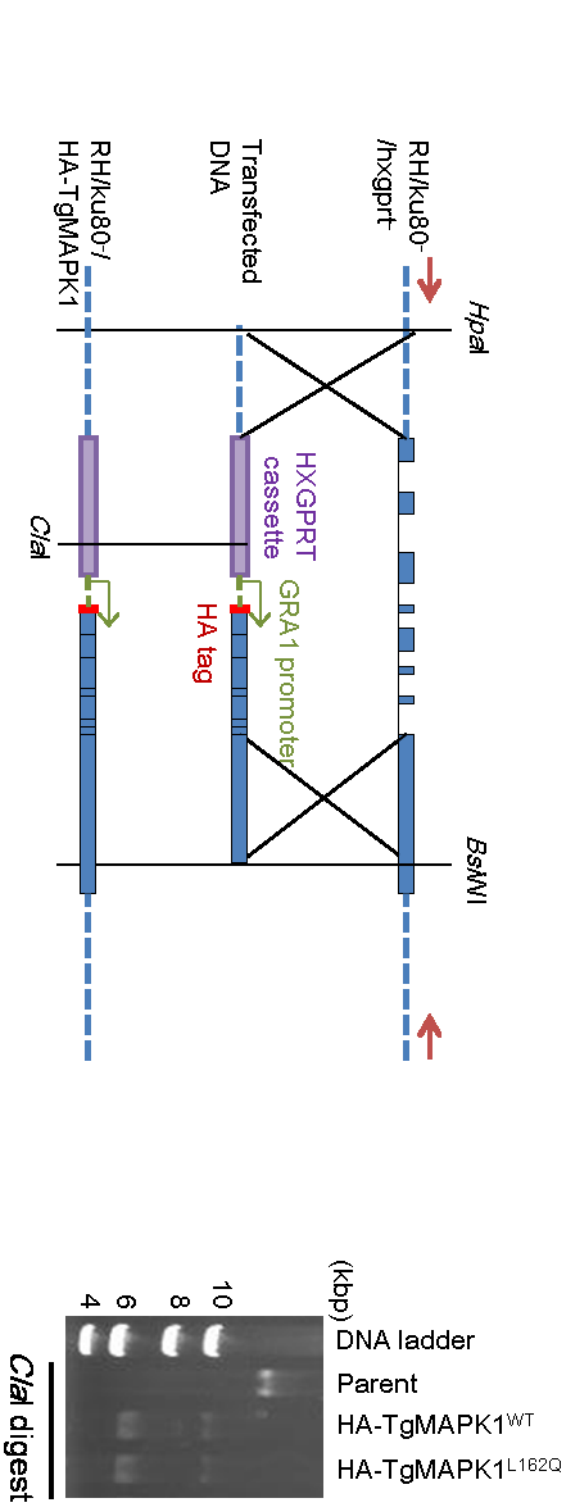
A
RH/ku80-/hxgprt
Transfected DNA
RH/ku80-/HA-TgMAPK1
HpaI
ClaI
BsmI
HXGPRT cassette
GRA1 promoter
HA tag
B
(kbp)
4
6
8
10
ClaI digest
DNA ladder
Parent
HA-TgMAPK1WT
HA-TgMAPK1L162Q

Figure 8

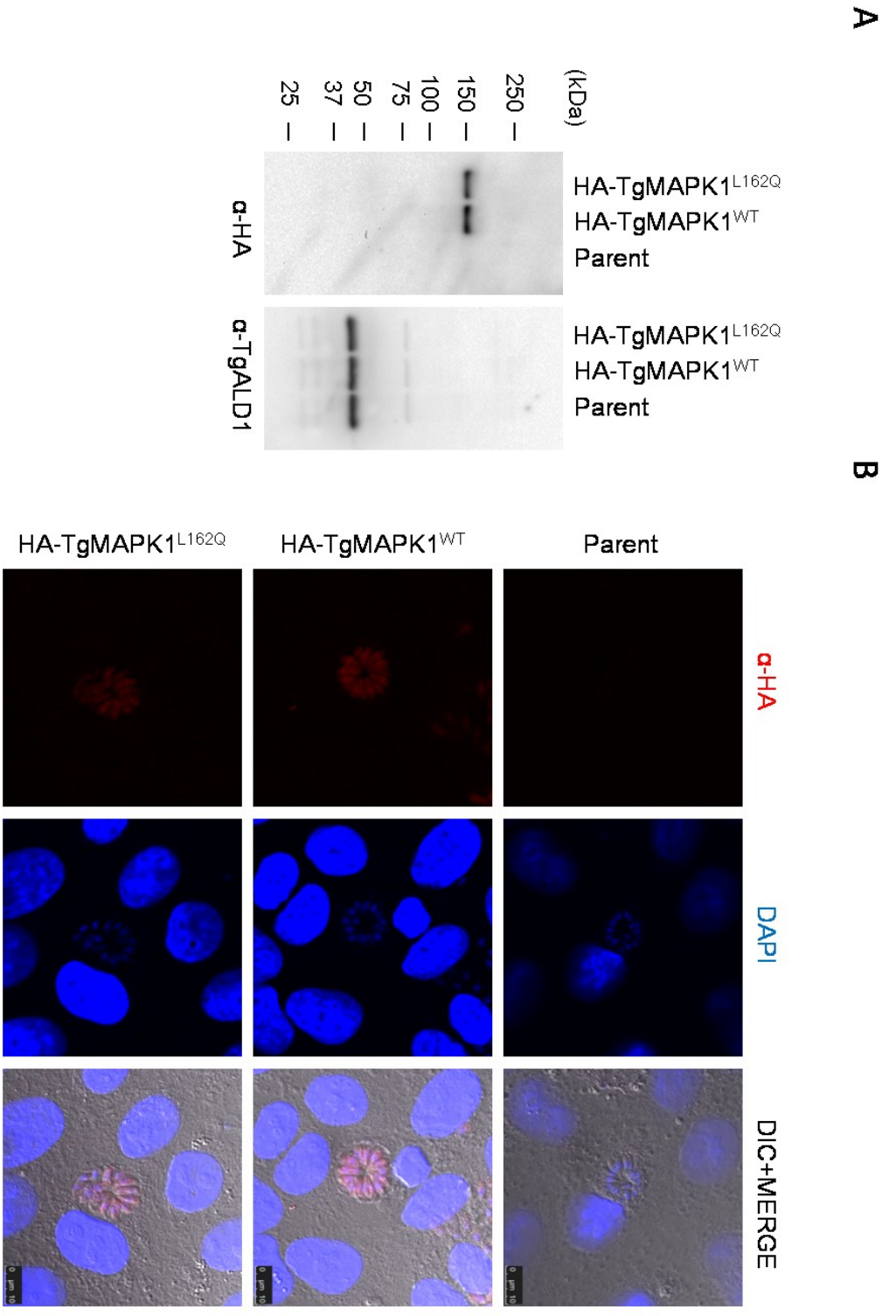
A
(kDa)
250 —
150 —
100 —
75 —
50 —
37 —
25 —
α-HA
HA-TgMAPK1L162Q
HA-TgMAPK1WT
Parent
α-TgALD1
HA-TgMAPK1L162Q
HA-TgMAPK1WT
Parent
B
HA-TgMAPK1L162Q
HA-TgMAPK1WT
Parent
α-HA
DAPI
DIC+MERGE

Figure 9

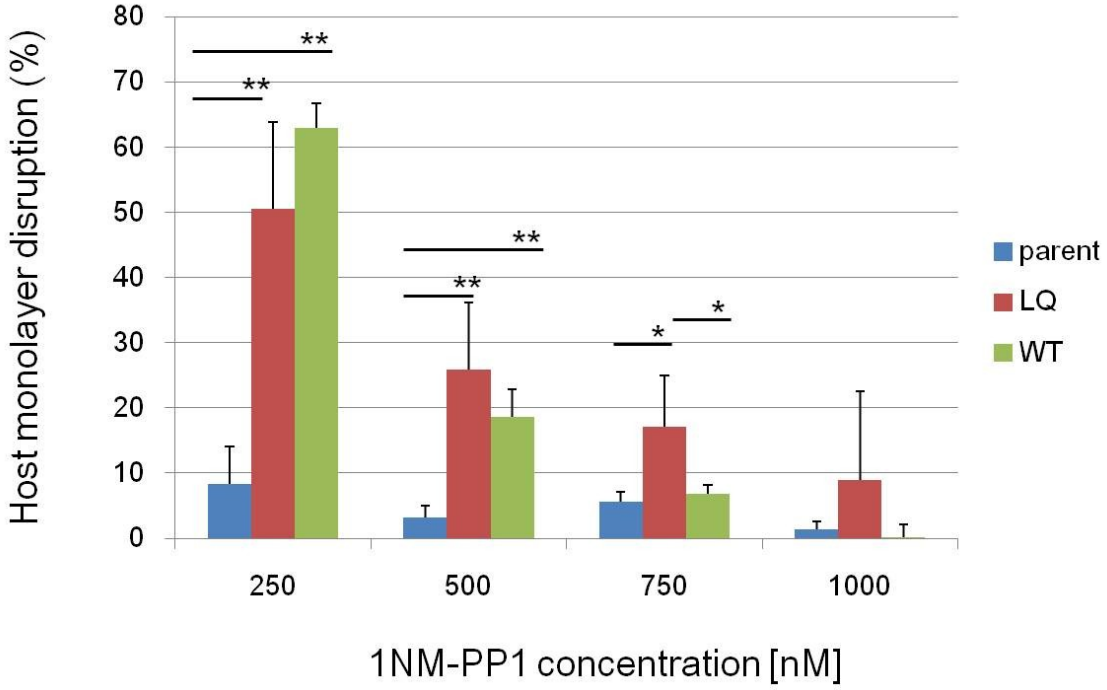
Host monolayer disruption (%)
80
70
60
50
40
30
20
10
0
**
**
**
**
*
*
250
500
750
1000
1NM-PP1 concentration [nM]
parent
LQ
WT

Figure 10

Chapter 4

TgMAPK1 bridges cell division and bradyzoite differentiation

Part of a published report in International Journal for Parasitology: Drugs and Drug Resistance 3 (2013) 93–101

Abstract

The author found the mutation in *Toxoplasma gondii* mitogen-activated protein kinase 1 (TgMAPK1) in 1NM-PP1 resistant clones (Chapter 3). To identify the resistant mechanisms and function of TgMAPK1 in parasite replication, the author characterized the 1NM-PP1-resistant parasites under the 1NM-PP1 treatment. The inhibitory effect of 1NM-PP1 on cell division observed in the parent clone was decreased in 1NM-PP1-resistant clones; however, effects on parasite invasion and calcium-induced egress were similar in both parent and resistant clones. 1NM-PP1 also induced bradyzoite differentiation to parent strain, whereas resistant clones were not induced bradyzoite differentiation. Bradyzoite inducing effect of 1NM-PP1 was not affected by the expression of 1NM-PP1-resistant TgCDPK1^{G128M}. The author revealed that TgMAPK1 is a member of the parasite protein kinase signals which regulates parasite cell division and cell differentiation.

Introduction

T. gondii differentiates into bradyzoite in the latent infection stage (Black and Boothroyd, 2000). Bradyzoite is a slow replicating parasite in the cyst. Bradyzoite is notorious for evading from the drugs usually used (Gormley et al., 1998). To disclose the mechanisms of differentiation between tachyzoite and bradyzoite will help the ideal vaccine or ideal drugs.

In vivo mechanisms of bradyzoite differentiation were not fully understood, however, we can induce bradyzoite differentiation in *in vitro* culture by several stress conditions (Ferreira da Silva et al., 2008). *In vitro* bradyzoite inducing system uses environmental stresses such as pH, NO and nutrient depletion, to make the parasite expressing bradyzoite specific transcription and to make the parasite replicate slowly (Bohne et al., 1994). Cell division is remarkably decreased in bradyzoite stages, and bradyzoite parasites are thought to be the differentiated cell state of G0 cell division cycle (Bohne et al., 1994). However, what genes and molecules are the sensors of the stress and what signala regulating the cell differentiation are remain unknown.

Recently, transcriptome aspect of bradyzoite differentiation was uncovered markedly (Behnke et al., 2008). In the time course of bradyzoite differentiation, several ApiAP2 transcription factor are reportedly to relate with the transition between tachyzoite gene expression and bradyzoite gene expression (Radke et al., 2013; Walker et al., 2013). eIF2 signals bridges stress condition to the bradyzoite differentiation (Narasimhan et al., 2008; Sullivan et al., 2004).

Inhibitor study using SB203580 and SB21090, which are mammalian p38α MAPK inhibitors, showed that protein kinase signals are related to the differentiation steps and cell division regulation (Wei et al., 2002). *T. gondii* has two MAPK homologs reported so

far, and *T. gondii* MAPK1 (TgMAPK1) was reported to related with the stress response (Brumlik et al., 2004). However, which of the parasite kinase or the host protein kinase is the target of the inhibitor and which gene and pathway is the target is not determined yet.

Putative BKI targets includes the TgMAPK1 (Sugi et al., 2010) which is suggested to relate with the bradyzoite differentiation (Brumlik et al., 2004). By the use of 1NM-PP1 resistant parasite clones having mutation in TgMAPK1 (Chapter 3), we can evaluate the function of TgMAPK1 in parasite growth steps, such as invasion, cell division in host cell and egress from host cell. We also checked that 1NM-PP1 can induce the bradyzoite differentiation. 1NM-PP1 and other BKIs mainly target the TgCDPK1, therefore the author checked whether bradyzoite differentiation induction effect was dependent on TgCDPK1 inhibition or not. To know the function and mechanisms of protein kinase signals in cell differentiation will lead to the more comprehensive understandings of the protein kinase signals in cell differentiation in *T. gondii*.

Materials and Methods

Tested reagent

1NM-PP1 was purchased from Merck KGaA (Darmstadt, Germany). Calcium ionophore A23187 was purchased from Sigma-Aldrich (St. Louis, MO, USA).

Parasite cultures

Tachyzoites of the *T. gondii* PLK/DUAL (Unno et al., 2009) strain (kindly provided by Dr. Y. Takashima, Gifu University, Gifu, Japan), PLK/DUAL derived 1NM-PP1 resistant clones (PLK/DUAL res.1 and res.2), PLK/DUAL TgMAPK1^{L162Q} in chapter 3, and PLK/hxgprt^{-} strain (Roos et al., 1994) (NIH AIDS Reagent Program, Division of AIDS, NIAID, NIH #2860) were used in this study. Parasites were maintained in monolayers of Vero cells cultured in Dulbecco's modified Eagle's medium (DMEM) (Nissui, Tokyo, Japan) containing 1% fetal calf serum (FCS) and 2 mM L-glutamine, streptomycin, and penicillin. Host Vero cells were maintained in the same medium containing 5% FCS. For assays, tested reagent or a DMSO control solvent was added to the same medium with 1% FCS (infection medium).

Transgenic parasites

For the strains PLK/CDPK1^{WT}3xFLAG and PLK/CDPK1^{G128M}3xFLAG, expression plasmids containing the CDPK1 ORF with a C-terminal 3xFLAG tag (pMini.CDPK1$_{WT}$3xFLAG.ht and pMini.CDPK1$_{G128M}$3xFLAG.ht) were constructed as described elsewhere (Sugi et al., 2010). These plasmids were used to transfect PLK/hxgprt^{-}, followed by selection of the transfected cells, as described elsewhere

(Karasov et al., 2005).

Invasion assay

Invasion assays were performed as described previously (Sugi et al., 2010). Briefly, freshly harvested and purified parasites were incubated in the tested reagent for 10 min at room temperature and inoculated onto a monolayer of Vero cells for 30 min at 37 °C with 500 nM 1NM-PP1 or with DMSO. Following invasion, cells were washed three times with ice cold PBS, and extracellular parasites stained with anti-SAG1 monoclonal antibodies (1:1,000 dilution) [TP3] (Santa Cruz Biotechnology, Santa Cruz, CA) in PBS containing 2% FCS for 30 min. After staining, the cells were washed three times with PBS containing 2% FCS, fixed with 4% paraformaldehyde in PBS, and stained with ALEXA 633 conjugated goat anti-mouse antibodies. Stained cells were visualized with a Zeiss LSM510 system. Microscopic fields were chosen at random; extracellular parasites were detected using anti-SAG1 antibodies and total parasites detected by DsRed-Express.

Calcium-induced egress assay

A calcium-induced egress assay was performed as described (Lourido et al., 2010). Briefly, purified parasites were inoculated onto a monolayer of Vero cells and allowed to invade for 2 h. At 2 hpi, the cells were washed with PBS to remove non-invaded parasites and incubated in infection medium overnight. At 30 hpi, the media were changed to media containing the reagent of interest and incubated for 10 min at room temperature. Calcium elevation was induced by the addition of media containing 5 μM A23187 along with the reagent of interest. Cells were incubated at 37 °C for 5 min, and egress stopped by addition of 4% paraformaldehyde in PBS for 10 min on ice.

Cell division assay

Cell division assays were performed as described elsewhere (Kurokawa et al., 2011). Briefly, parasites were inoculated into an 8-well chamber slide containing Vero cells grown in a monolayer, and incubated at 37 °C for 1 h. Following incubation, cells were washed with warm infection medium three times to remove non-invaded parasites, followed by incubation in infection medium with 250 nM 1NM-PP1 or DMSO. After incubation for 12 and 24 h, the cells were fixed with 4% paraformaldehyde in PBS for 10 min at room temperature, washed three times with PBS, dried at room temperature, and mounted with Fluorescence Mounting Medium (Dako, Glostrup, Denmark). Cells were observed by fluorescence microscopy (Olympus, Tokyo, Japan). Microscopic fields were chosen at random to count parasitophorous vacuoles. Average numbers of tachyzoites per vacuole were calculated.

Bradyzoite induction assay

Bradyzoite induction was performed under conditions of chemical stress by incubating the parasites in DMEM supplemented with 1% FCS and the tested reagent. As a control, DMSO was added to the medium. Parasites were inoculated to the monolayer of Vero cells in 12-well plate at 0.1 M.O.I. After 2 hpi, medium were changed to the medium with tested reagent and incubated for 4 days. Infected cells were lysed at 4 dpi to extract total RNA with an SV Total RNA Isolation System (Promega, Madison, WI), followed by real-time quantitative RT-PCR (qRT-PCR) analysis.

Real-time qRT-PCR analysis

Total RNA was used for cDNA synthesis with a SuperScript III First-Strand Synthesis System (Invitrogen, Carlsbad, CA), according to the manufacturer's instructions. The resulting cDNA was amplified using Go-Taq qPCR Master Mix (Promega). The primers for TUB1 and BAG1 were used as described elsewhere (Narasimhan et al., 2008).

Results

Inhibitory effect of 1NM-PP1 on invasion, egress, and cell division of TgMAPK1 mutant L162Q

Previous reports have demonstrated an inhibitory effect of BKIs on invasion and calcium-induced egress through targeting of TgCDPK1; the author therefore examined whether these mechanisms might also be contributing to 1NM-PP1 inhibition of TgMAPK1.

500 nM 1NM-PP1 reduced invasion of PLK/DUAL parasites by >40% relative to untreated controls (Fig. 1A). PLK/DUAL res.1, PLK/DUAL res.2, and PLK/DUAL TgMAPK1^{L162Q} showed similar levels of 1NM-PP1 susceptibility in terms of invasion inhibition, with no significant differences observed.

Calcium-induced egress was also examined. Parasites were treated with A23187, a calcium ionophore that causes increased Ca^{2+} concentration in parasites leading to egress of parasites from infected cells, with or without 1NM-PP1. All constructs (PLK/DUAL, PLK/DUAL res.1, PLK/DUAL res.2, and PLK/DUAL TgMAPK1^{L162Q}) showed a similar decrease in A23187-induced egress. Egress rates were approximately 80% for all constructs in the absence of drug; this rate dropped to <20% upon addition of 250 nM 1NM-PP1 (Fig. 1B).

As a final step we examined tachyzoite cell division. At 12 h, the average numbers of parasites per vacuole of PLK/DUAL, PLK/DUAL res.1, PLK/DUAL res.2, and PLK/DUAL TgMAPK1^{L162Q} were 1.58, 1.61, 1.60, and 1.60 without 1NM-PP1 treatment and 1.31, 1.53, 1.43, and 1.54 with 250 nM 1NM-PP1 treatment, respectively (Fig. 2A). At 24 h the average numbers of parasites per vacuole of PLK/DUAL, PLK/DUAL res.1, PLK/DUAL res.2, and PLK/DUAL TgMAPK1^{L162Q} were 4.85, 4.83, 4.62 and 4.81

without 1NM-PP1 treatment and 3.53, 4.38, 4.33, and 4.56 with 250 nM 1NM-PP1 treatment, respectively (Fig. 2A). These results demonstrate a significant change in parasite numbers between the WT PLK/DUAL strain and resistant clones in the presence of 250 nM 1NM-PP1 at both 12 and 24 h (Fig. 2A), suggesting that TgMAPK1 mutational resistance to 1NM-PP1 is mediated through cell division regulation in drug susceptibility.

Effect of 1NM-PP1 on bradyzoite differentiation

In the presence of 1NM-PP1, all three resistant clones showed a significant decrease in BAG1 upregulation compared with the response in the parent PLK/DUAL strain (Fig. 3). However, all three resistant clones showed the expected upregulation of BAG1 expression under the NO stress condition by the use of 75 μM SNP (Fig. 3). Thus, although the resistant clones were capable of bradyzoite specific gene expression change, 1NM-PP1 did not induce this response in the resistant clones.

Construction of 1NM-PP1 refractory TgCDPK1$_{G128M}$-expressing PLK parasites

Considering that TgCDPK1 has been reported to be the main target of the toxoplasmocidal effect of BKIs (Lourido et al., 2010; Ojo et al., 2010; Sugi et al., 2010), the author evaluated TgCDPK1 as the target of 1NM-PP1 for bradyzoite induction. The author constructed a 1NM-PP1-refractory TgCDPK1$_{G128M}$-expressing type II PLK parasite, designated as PLK/CDPK1$_{G128M}$3xFLAG, and a control TgCDPK1$_{WT}$-expressing parasite, designated as PLK/CDPK1$_{WT}$3xFLAG. The presence of 3xFLAG-tagged CDPK1 in the lysates of PLK/CDPK1$_{G128M}$3xFLAG and PLK/CDPK1$_{WT}$3xFLAG was confirmed as a band of approximately 60 kDa on a western

blot (Fig. 4A). No band was detected in lysates of the parent PLK/hxgprt$^-$ strain (Fig. 4A, upper panel). Equal loading of parasite lysates of all three samples was verified by the equivalent intensity of the TgALD1 band from each sample (Fig. 4A, lower panel). The localization of FLAG-tagged CDPK1 in the parasites was checked by immunofluorescence assay. Expressed TgCDPK1$_{WT}$3xFLAG (Fig. 4B, upper panel) and TgCDPK1$_{G128M}$3xFLAG (Fig. 3B, lower panel) were localized to the cytosol at 24 hpi. In a host lysis assay, PLK/CDPK1$_{G128M}$3xFLAG was resistant to treatment with 100 and 250 nM 1NM-PP1, compared with the parent PLK/hxgprt$^-$ strain (Fig. 4C). The response of PLK/CDPK1$_{WT}$3xFLAG to treatment with 100 and 250 nM 1NM-PP1 was not significantly different from that of the parental strain (Fig. 4C).

Bradyzoite induction by 1NM-PP1 in TgCDPK1$_{G128M}$-expressing parasites

The author tested whether 1NM-PP1 could induce bradyzoite formation in parasites expressing 1NM-PP1-refractory TgCDPK1$_{G128M}$. Parental PLK/hxgprt-, PLK/CDPK1$_{WT}$3xFLAG and PLK/CDPK1$_{G128M}$3xFLAG were treated with 250 nM 1NM-PP1 and 75 μM SNP. In 1NM-PP1 treatment and SNP treatment, BAG1 mRNA levels were upregulated in all three parasite clones without significant difference (Fig. 5).

Discussion

The resistant clones did not demonstrate resistance to 1NM-PP1 at invasion or egress where TgCDPK1 has been shown to play an important role (Lourido et al., 2010). Instead, resistance was mediated through altered susceptibility during cell division and bradyzoite differentiation. This alternative pattern of resistance may not be achieved through complementation of TgCDPK1 function directly, but by rescuing a different inhibitory effect of 1NM-PP1 on cell division which had not previously been evaluated.

The tachyzoite cell cycle is regulated by several protein kinase signals, including a PKA signal inhibited by a cAMP analog (Eaton et al., 2006), PKA specific inhibitors (Kurokawa et al., 2011), TgNEK1 (Gubbels et al., 2008), TPK2 (Khan et al., 2002), and a MAPK signal inhibited by p38 MAPK inhibitors (Wei et al., 2002). Analysis of the *T. gondii* genome suggests that the MAPK signaling cascade lacks the canonical upstream protein kinase STE group (Miranda-Saavedra et al., 2012). While its role in the cell cycle is not yet clear, TgMAPK1 may interact with the protein kinase signals described above instead of STE.

By the use of the chemical inhibitor of 1NM-PP1 and the genetically mutated clones having mutated TgMAPK1, the author can evaluate the role of TgMAPK1 in cell divisions and cell differentiations for the first time. TgMAPK1 is reported to be upregulated by the high pH stress (Brumlik et al., 2004) and can complement the osmotic stress responsible yeast MAPK hog1 in budding yeast when it is exogenetically expressed (Brumlik et al., 2004). The present report showed that TgMAPK1 is functional in parasites and regulating the cell division and cell differentiation, which is also important for the *T. gondii* stress responses (Sullivan et al., 2004). Recent report showed that expressional reduction of TgMAPK1 by antisense RNA leads to the differential host

protein kinase signal manipulation from the wild type parasites (Brumlik et al., 2013). The present report showed that TgMAPK1 function is needed for the cell division maintenance and Brumlik *et al.* (Brumlik et al., 2013) also showed the reduction of parasite growth in TgMAPK1 knock down parasites. The author cannot exclude the possibility that parasite cell division arrest and cell differentiation by inhibiting TgMAPK1 with 1NM-PP1 came from the preventing the host cell manipulation directly by TgMAPK1. However, the parasites load in host cells also affect the host cell manipulation, because parasite has many other host signaling manipulating factors, such as dense granule proteins (Bougdour et al., 2013; Braun et al., 2013; Yang et al., 2013) and a rhoptry protein (Yamamoto et al., 2009). For further understanding of the way how the TgMAPK1 regulates cell division and cell differentiation, the author suggests that the understandings of parasite protein kinase signal relating TgMAPK1 and host cell responsive signals is needed.

MAPK signals are the target of drugs among many human pathogenesis such as cancer (Wagner and Nebreda, 2009) and hyper immune responses (Thalhamer et al., 2008). Therefore, if the parasite MAPKs are inevitable for parasite growth, parasite MAPKs are promising drug target. Here, the author showed that TgMAPK1 is needed for the parasite replication. However, inhibition of TgMAPK1 results in bradyzoite differentiation. If prevention of reactivation of *T. gondii* from latent bradyzoite cyst to active tachyzoite, which has reported to be the promising targeting point by the inhibitors of eIF2α dephosphorylation (Konrad et al., 2013), is targeted, inhibition of TgMAPK1 is another way.

Figure legends

Figure 1. Parental PLK/DUAL and resistant clones had comparable susceptibility to 1NM-PP1 at invasion and calcium-induced egress.

(A) Parasites were allowed to invade for 30 min in the presence of 500 nM 1NM-PP1 or control solvent DMSO. Extracellular parasites were stained with anti-SAG1 antibodies. Invasion rate was determined by comparing the number of invaded parasites to total parasite counts. Invasion rates are reported as percentages relative to that of untreated PLK/DUAL parasites. More than 200 parasites were counted in each test. (B) The egress rate denotes the number of egressed vacuoles per total number of vacuoles as percentages. Calcium signal stimulation was performed using 5 μM A23187 for 5 min with or without 250 nM 1NM-PP1. More than 200 vacuoles were counted in each test. (A, B) Error bars indicate standard deviations across three independent experiments; statistical evaluations were performed using Student's *t*-test comparing PLK/DUAL and resistant parasite strains.

Figure 2. Tachyzoite cell division rates of resistant clones were not decreased in the presence of 1NM-PP1.

(A) Average parasite number per vacuole after 12 and 24 h incubation, with or without 250 nM 1NM-PP1, is shown. More than 200 vacuoles were counted in each test. Error bars indicate standard deviations across three independent experiments; statistical evaluations were performed using Student's *t*-test comparing PLK/DUAL and resistant parasites. * denotes $p < 0.05$; ** denotes $p < 0.01$

Figure 3 Effect of 1NM-PP1 in bradyzoite differentiation

Real-time qRT-PCR was used to monitor BAG1 mRNA levels induced by 75 μM SNP or 250 nM 1NM-PP1. At 96 hpi, total RNA from infected host cells was harvested and analyzed by real-time qRT-PCR. The fold change in each parasite strain compared with the DMSO control is shown. Blue bar, PLK/hxgprt$^-$; red bar, res.1; green bar, res.2; purple bar, res.3. Error bars are standard deviations of independent triplicate experiments. n.s., not significantly different. * $p < 0.05$, *** $p < 0.01$ by Student's *t*-test.

Figure 4 Expression of 1NM-PP1 insensitive TgCDPK1G128M did not alter the bradyzoite differention induction by 1NM-PP1.

(A) Western blot of total lysates from PLK/CDPK1$_{WT}$3xFLAG (lane 1), PLK/CDPK1$_{G128M}$3xFLAG (lane 2), and the parent strain PLK/hxgprt$^-$ (lane 3). Antibodies against FLAG (upper panel) and TgALD1 (lower panel) were used to detect protein expression. Molecular weight (kDa) is shown beside the panels. (B) Immunofluorescence analysis of the transgenic parasites PLK/CDPK1$_{WT}$3xFLAG (upper panels) and PLK/CDPK1$_{G128M}$3xFLAG (lower panels). Green, FLAG tag; blue, DNA; Scale bar = 10 μm. (C). Tachyzoite growth was evaluated with a host monolayer disruption assay. At 72 hpi, viable host cells were stained with crystal violet, and the areas of lysed host cells were measured. The lysed area of a control well of the parent strain was set as 100%. Blue diamond, PLK/CDPK1$_{WT}$3xFLAG; red square, PLK/CDPK1$_{G128M}$3xFLAG; green triangle, PLK/hxgprt$^-$. Error bars are standard deviations of independent triplicate experiments.

Figures

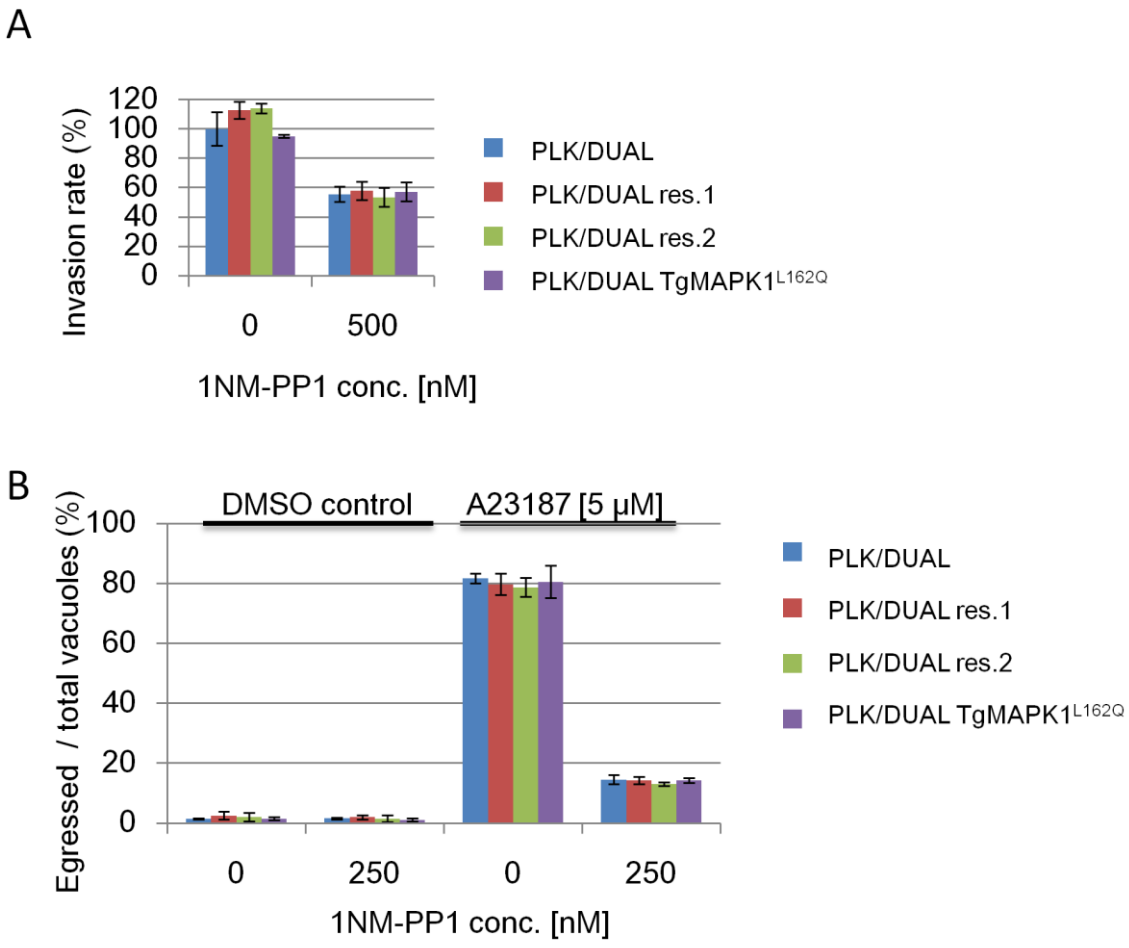

Figure 1

A

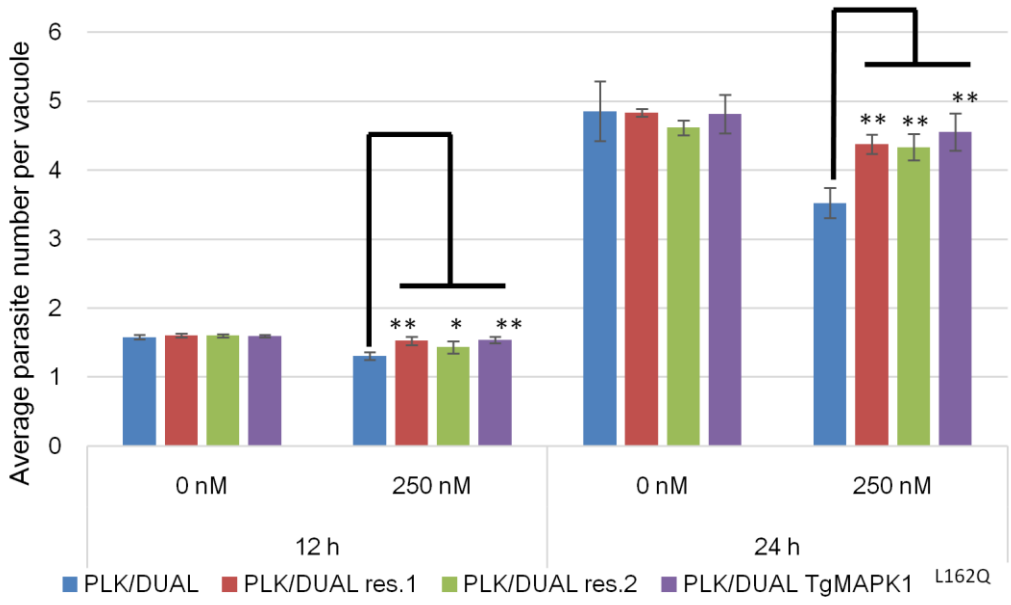
Average parasite number per vacuole
6
5
4
3
2
1
0
**
*
**
**
**
**
0 nM
250 nM
0 nM
250 nM
12 h
24 h
PLK/DUAL
PLK/DUAL res.1
PLK/DUAL res.2
PLK/DUAL TgMAPK1 L162Q

Figure 2

A

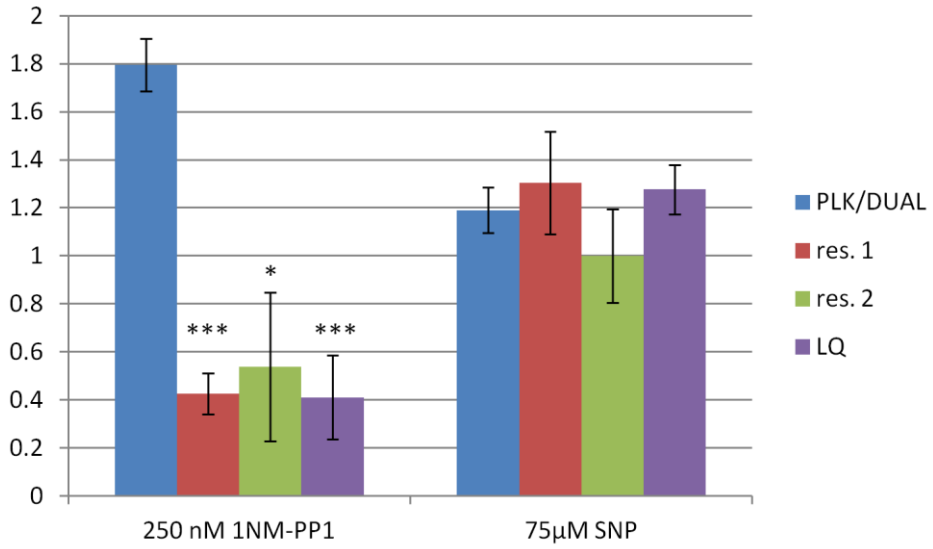
2
1.8
1.6
1.4
1.2
1
0.8
0.6
0.4
0.2
0
***
*
***
250 nM 1NM-PP1
75µM SNP
PLK/DUAL
res. 1
res. 2
LQ

Figure 3

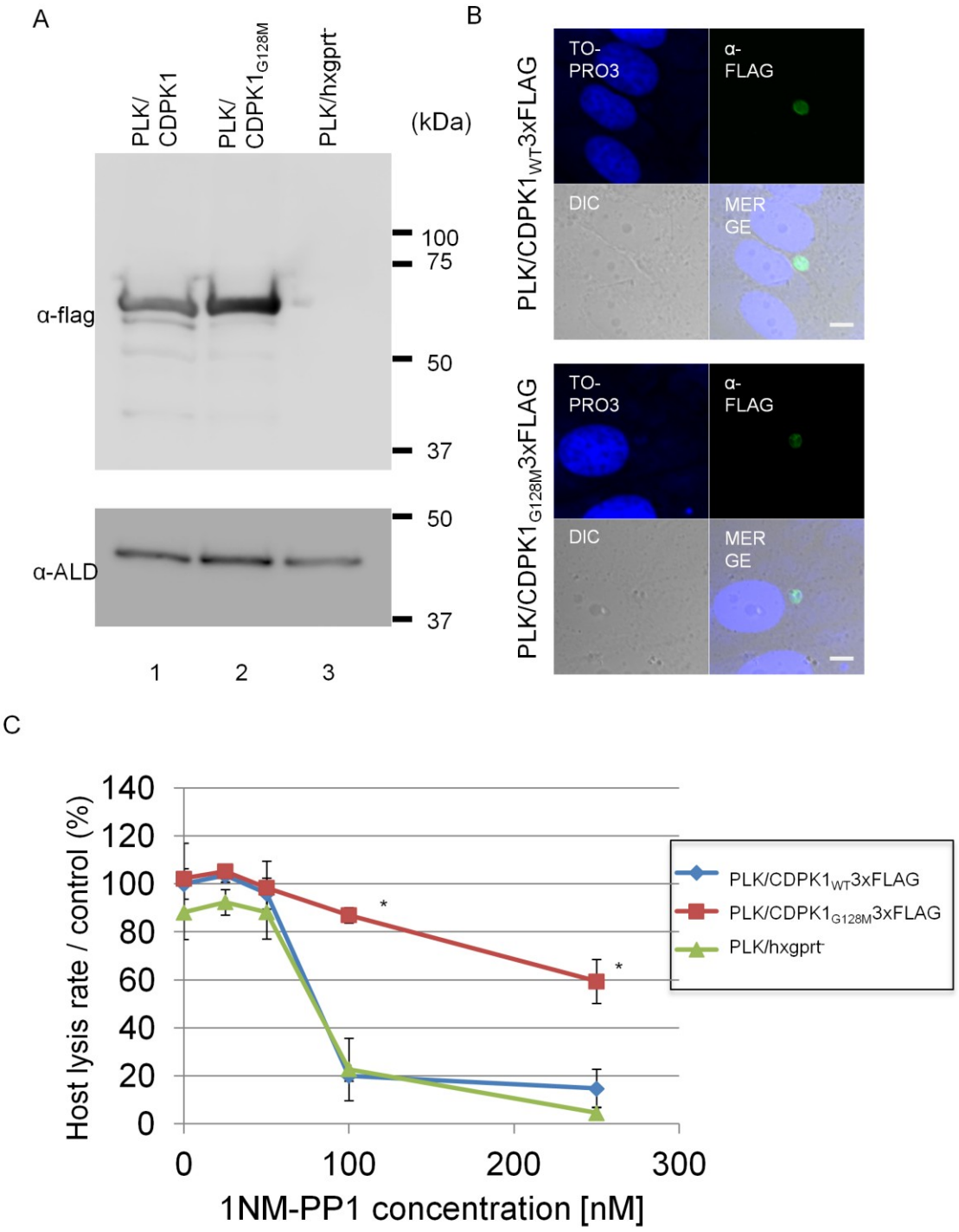
A
PLK/ CDPK1
PLK/ CDPK1G128M
PLK/hxgprt-
(kDa)
α-flag
100
75
50
37
α-ALD
50
37
1
2
3
B
PLK/CDPK1WT3xFLAG
TO-PRO3
α-FLAG
DIC
MERGE
PLK/CDPK1G128M3xFLAG
TO-PRO3
α-FLAG
DIC
MERGE
C
Host lysis rate / control (%)
140
120
100
80
60
40
20
0
0
100
200
300
1NM-PP1 concentration [nM]
*
*
PLK/CDPK1WT3xFLAG
PLK/CDPK1G128M3xFLAG
PLK/hxgprt-

Figure 4

A

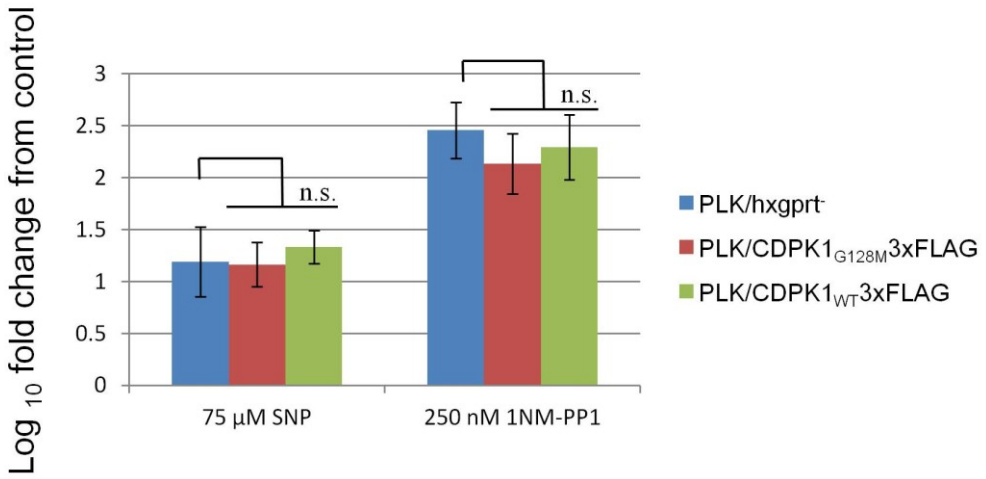
Log 10 fold change from control
3
2.5
2
1.5
1
0.5
0
n.s.
n.s.
75 µM SNP
250 nM 1NM-PP1
PLK/hxgprt-
PLK/CDPK1G128M3xFLAG
PLK/CDPK1WT3xFLAG

Figure 5

General Conclusion

Toxoplasma gondii (*T. gondii*) is a pathogen of Toxoplasmosis. Toxoplasmosis is still one of the neglected diseases, although more and more the risks of the congenital Toxoplasmosis have been revealed. Toxoplasmosis is accompanied by the parasite adroit parasitic strategy; opportune switching between fast replicating tachyzoites which make pathosis and dormant bradyzoites which become sources of infection. To reveal the parasite mechanisms regulating fast growth in tachzyotie will contribute to the identification of new drug target. To disclose the mechanism of differentiation will contribute to the identification of the target molecules for controlling the source of infection.

In this thesis, the author focused on molecular mechanisms of *T. gondii* growth and cell differentiation especially on the protein kinase signals which are the attractive druggable target in cancers and are suggested to relate with the parasite cell differentiation steps.

For a start, in chapters, 1 and 2, the author focused on the technique “analog sensitive kinase allele based gene inhibition (ASKA-GI)”, which makes it possible to analyze the precise protein kinase function in the cell. During the attempt to apply ASKA-GI to the protein kinase analysis in *T. gondii*, the author fortuitously found that the *T. gondii* genome encodes no less than twelve inhibitor-analog sensitive protein kinases, which are rare in the mammalian genomes. The author also found that *T. gondii* calcium dependent protein kinase 1 (TgCDPK1) is unique in the aspect of the high susceptibility

to inhibitor-analog “1NM-PP1”. To take advantage of an instant effect of the inhibitor and specificity by the 1NM-PP1-insensitive mutated TgCDPK1 expressing parasite, the author found that TgCDPK1 plays an important role in the parasite invasion step and that an inhibition of TgCDPK1 results in the parasite growth defect. The author also tested the effect by 1NM-PP1 on *T. gondii* in the *in vivo* mouse infection models. Although the effect was limited, 1NM-PP1 successfully inhibited parasite growth *in vivo*.

These results suggested that ASKA-GI is applicable for the *T. gondii* protein kinase analyses and *T. gondii* has the attractive drug targets, which include TgCDPK1 and the inhibitor-analog sensitive protein kinases.

Inhibitor-analogs including 1NM-PP1, has potentials for the drug that is specific to parasites. However, the sensitivity of the protein kinases to inhibitor-analog is easily changed by substituting a single amino acid. In order to make the inhibitor-analog to be the promising drug lead, it is needed to predict the occurrence of the resistance and revealing mechanisms of resistance acquisition by *T. gondii*. In chapter 3, the author established 1NM-PP1 resistant parasite clones and identified point mutations on *T. gondii* mitogen-activated protein kinase 1 (TgMAPK1) in the resistant clones. Resistant clones also had resistance to other inhibitor-analog 3BrB-PP1 and 3MB-PP1. The mutation in TgMAPK1 conferring resistance to 1NM-PP1 did not occur at the gatekeeper residue, suggesting the likelihood of similar mutations that may confer resistance in other analog sensitive kinases.

In chapter 4, by the use of parasite having the mutation in TgMAPK1 conferring

resistance to 1NM-PP1, the author characterized a role of TgMAPK1 in the parasite growth and cell differentiation. By the inhibition of TgMAPK1, *T. gondii* differentiated into bradyzoite and normal cell division was inhibited. These results suggested that the TgMAPK1 is the one of the signals regulating the cell division and cell differentiation.

In conclusion, the author elucidated the role of the protein kinase signals in parasite growth and cell differentiation in both aspects of a function in parasite and its validity as drug targets. The author suggests that ASKA-GI, which is applicable for *T. gondii*, is a strong technique to elucidate the parasite protein kinase function. Protein kinase inhibitor-analog, which is used in ASKA-GI, is promising for the anti-*T. gondii* drug lead, although the risk of resistant parasites should be considered. The resistant-point mutation reported in the present thesis will contribute to the development of drug with low risks of the resistance. The author used chemical random mutagenesis of parasites and following whole genome re-sequence, and successfully identified un-predicted resistant mutation. In order to find unpredicted mutations conferring resistance, further identification of resistant mutation by the same strategy is promising. The author conducted a structural analysis with computer calculated protein structure models. Experimental structural data are needed in the future for the fundamental analysis of the mechanisms of resistance acquisition. In the present thesis, the author revealed the function of TgMAPK1 in the parasite cell division and cell differentiation for the first time. The canonical MAPKKs and MAPKKKs, which is upstream MAPK regulator in eukaryotes, were not found in the *T. gondii* genome. The author suggests that TgMAPK1 is regulated by atypical MAPKKs. This is different from mammalian hosts. Therefore the author suggests that the unique cell differentiation mechanisms of *T.*

gondii is regulated by TgMAPK1. Further identification and analyses of upstream and downstream factors of TgMAPK1 will contribute to unveiling a parasite adroit mechanism of differentiation between tachyzoite and bradyzoite.

Acknowledgments

This study is supervised by Drs. H. Akashi and T. Horimoto (University of Tokyo) and Dr. K. Kato (Obihiro University of Agriculture and Veterinary Medicine). The author appreciates the dedicated instructions by the supervisors.

The author thanks Drs. Y. Nishikawa and X. Xuan (Obihiro University of Agriculture and Veterinary Medicine), Dr. Y. Takashima (Gifu University), Dr. G. Arrizabalaga, (University of Idaho), Dr. V. Carruthers (University of Michigan Medical School), Dr. D. S. Roos (University of Pennsylvania), and Dr. T. Masatani (Kagoshima Univ.) for the useful technical advises and help for the materials.

The author also thanks the members of BIBUTU for the dedicated discussion on science and life.

The author would like to express the gratitude to KANO = SAN (Department of Veterinary microbiology, University of Tokyo) and OKUYAMA = SAN (Obihiro University of Agriculture and Veterinary Medicine) for the indispensable helps over the whole works in the laboratory.

The author also thanks his family for the support throughout the study.

References

Al Riyahi, A., Al-Anouti, F., Al-Rayes, M., Ananvoranich, S., 2006. Single argonaute protein from *Toxoplasma gondii* is involved in the double-stranded RNA induced gene silencing. Int J Parasitol 36, 1003-1014.

Alford, C.A., Stagno, S., Reynolds, D.W., 1974. Congenital toxoplasmosis: clinical, laboratory, and therapeutic considerations, with special reference to subclinical disease. Bull N Y Acad Med 50, 160-181.

Arnold, K., Bordoli, L., Kopp, J., Schwede, T., 2006. The SWISS-MODEL workspace: a web-based environment for protein structure homology modelling. Bioinformatics 22, 195-201.

Behnke, M.S., Radke, J.B., Smith, A.T., Sullivan, W.J., White, M.W., 2008. The transcription of bradyzoite genes in *Toxoplasma gondii* is controlled by autonomous promoter elements. Mol Microbiol 68, 1502-1518.

Billker, O., Lourido, S., Sibley, L.D., 2009. Calcium-dependent signaling and kinases in apicomplexan parasites. Cell Host Microbe 5, 612-622.

Bishop, A.C., Buzko, O., Shokat, K.M., 2001. Magic bullets for protein kinases. Trends Cell Biol 11, 167-172.

Bishop, A.C., Ubersax, J.A., Petsch, D.T., Matheos, D.P., Gray, N.S., Blethrow, J., Shimizu, E., Tsien, J.Z., Schultz, P.G., Rose, M.D., Wood, J.L., Morgan, D.O., Shokat, K.M., 2000. A chemical switch for inhibitor-sensitive alleles of any protein kinase. Nature 407, 395-401.

Black, M.W., Boothroyd, J.C., 2000. Lytic cycle of *Toxoplasma gondii*. Microbiol Mol Biol Rev 64, 607-623.

Bohne, W., Heesemann, J., Gross, U., 1994. Reduced replication of *Toxoplasma gondii* is necessary for induction of bradyzoite-specific antigens: a possible role for nitric oxide in triggering stage conversion. Infect Immun 62, 1761-1767.

Bougdour, A., Durandau, E., Brenier-Pinchart, M.P., Ortet, P., Barakat, M., Kieffer, S., Curt-Varesano, A., Curt-Bertini, R.L., Bastien, O., Coute, Y., Pelloux, H., Hakimi, M.A., 2013. Host cell subversion by *Toxoplasma* GRA16, an exported dense granule protein that targets the host cell nucleus and alters gene expression. Cell Host Microbe 13, 489-500.

Braun, L., Brenier-Pinchart, M.P., Yogavel, M., Curt-Varesano, A., Curt-Bertini, R.L., Hussain, T., Kieffer-Jaquinod, S., Coute, Y., Pelloux, H., Tardieux, I., Sharma, A., Belrhali, H., Bougdour, A., Hakimi, M.A., 2013. A *Toxoplasma* dense granule protein, GRA24, modulates the early immune response to infection by promoting a direct and sustained host p38 MAPK activation. J Exp Med 210, 2071-2086.

Brumlik, M.J., Pandeswara, S., Ludwig, S.M., Jeansonne, D.P., Lacey, M.R., Murthy, K., Daniel, B.J., Wang, R.F., Thibodeaux, S.R., Church, K.M., Hurez, V., Kious, M.J., Zhang, B., Alagbala, A., Xia, X., Curiel, T.J., 2013. TgMAPK1 is a *Toxoplasma gondii* MAP kinase that hijacks host MKK3 signals to regulate virulence and interferon-γ-mediated nitric oxide production. Exp Parasitol 134, 389-399.

Brumlik, M.J., Pandeswara, S., Ludwig, S.M., Murthy, K., Curiel, T.J., 2011. Parasite mitogen-activated protein kinases as drug discovery targets to treat human protozoan

pathogens. Journal of signal transduction 2011, 971968.

Brumlik, M.J., Wei, S., Finstad, K., Nesbit, J., Hyman, L.E., Lacey, M., Burow, M.E., Curiel, T.J., 2004. Identification of a novel mitogen-activated protein kinase in *Toxoplasma gondii*. International Journal for Parasitology 34, 1245-1254.

Carruthers, V.B., Giddings, O.K., Sibley, L.D., 1999. Secretion of micronemal proteins is associated with toxoplasma invasion of host cells. Cell Microbiol 1, 225-235.

Carruthers, V.B., Sibley, L.D., 1999. Mobilization of intracellular calcium stimulates microneme discharge in *Toxoplasma gondii*. Mol Microbiol 31, 421-428.

Coombes, J.L., Charsar, B.A., Han, S.J., Halkias, J., Chan, S.W., Koshy, A.A., Striepen, B., Robey, E.A., 2013. Motile invaded neutrophils in the small intestine of *Toxoplasma gondii*-infected mice reveal a potential mechanism for parasite spread. Proc Natl Acad Sci U S A 110, E1913-1922.

Doerig, C., 2004. Protein kinases as targets for anti-parasitic chemotherapy. Biochim Biophys Acta 1697, 155-168.

Donald, R.G.K., Allocco, J., Singh, S.B., Nare, B., Salowe, S.P., Wiltsie, J., Liberator, P.A., 2002. *Toxoplasma gondii* cyclic GMP-dependent kinase: Chemotherapeutic targeting of an essential parasite protein kinase. Eukaryotic Cell 1, 317-328.

Dubey, J.P., 1997. Tissue cyst tropism in *Toxoplasma gondii*: a comparison of tissue cyst formation in organs of cats, and rodents fed oocysts. Parasitology 115 (Pt 1), 15-20.

Dubey, J.P., Miller, N.L., Frenkel, J.K., 1970. The *Toxoplasma gondii* oocyst from cat feces. J Exp Med 132, 636-662.

Eaton, M.S., Weiss, L.M., Kim, K., 2006. Cyclic nucleotide kinases and tachyzoite-bradyzoite transition in *Toxoplasma gondii*. International Journal for Parasitology 36, 107-114.

Farrell, A., Thirugnanam, S., Lorestani, A., Dvorin, J.D., Eidell, K.P., Ferguson, D.J., Anderson-White, B.R., Duraisingh, M.T., Marth, G.T., Gubbels, M.J., 2012. A DOC2 protein identified by mutational profiling is essential for apicomplexan parasite exocytosis. Science 335, 218-221.

Ferreira da Silva, M.F., Barbosa, H., Gross, U., Lüder, C., 2008. Stress-related and spontaneous stage differentiation of *Toxoplasma gondii*. Mol Biosyst 4, 824-834.

Fox, B.A., Falla, A., Rommereim, L.M., Tomita, T., Gigley, J.P., Mercier, C., Cesbron-Delauw, M.F., Weiss, L.M., Bzik, D.J., 2011. Type II *Toxoplasma gondii* KU80 knockout strains enable functional analysis of genes required for cyst development and latent infection. Eukaryot Cell 10, 1193-1206.

Frenkel, J.K., Dubey, J.P., Miller, N.L., 1970. *Toxoplasma gondii* in cats: fecal stages identified as coccidian oocysts. Science 167, 893-896.

Gajria, B., Bahl, A., Brestelli, J., Dommer, J., Fischer, S., Gao, X., Heiges, M., Iodice, J., Kissinger, J.C., Mackey, A.J., Pinney, D.F., Roos, D.S., Stoeckert, C.J., Jr., Wang, H., Brunk, B.P., 2008. ToxoDB: an integrated *Toxoplasma gondii* database resource. Nucleic Acids Res 36, D553-556.

Gilk, S.D., Gaskins, E., Ward, G.E., Beckers, C.J.M., 2009. GAP45 Phosphorylation Controls Assembly of the *Toxoplasma* Myosin XIV Complex. Eukaryotic Cell 8, 190-196.

Gormley, P.D., Pavesio, C.E., Minnasian, D., Lightman, S., 1998. Effects of drug therapy on *Toxoplasma* cysts in an animal model of acute and chronic disease. Invest Ophthalmol Vis Sci 39, 1171-1175.

Green, J.L., Rees-Channer, R.R., Howell, S.A., Martin, S.R., Knuepfer, E., Taylor, H.M., Grainger, M., Holder, A.A., 2008. The motor complex of *Plasmodium falciparum*: phosphorylation by a calcium-dependent protein kinase. J Biol Chem 283, 30980-30989.

Gregg, B., Taylor, B.C., John, B., Tait-Wojno, E.D., Girgis, N.M., Miller, N., Wagage, S., Roos, D.S., Hunter, C.A., 2013. Replication and distribution of *Toxoplasma gondii* in the small intestine after oral infection with tissue cysts. Infect Immun 81, 1635-1643.

Gubbels, M.J., Lehmann, M., Muthalagi, M., Jerome, M.E., Brooks, C.F., Szatanek, T., Flynn, J., Parrot, B., Radke, J., Striepen, B., White, M.W., 2008. Forward genetic analysis of the apicomplexan cell division cycle in *Toxoplasma gondii*. PLoS Pathog 4, e36.

Hanks, S.K., Hunter, T., 1995. Protein kinases 6. The eukaryotic protein kinase superfamily: kinase (catalytic) domain structure and classification. FASEB J 9, 576-596.

Hartmann, A., Arroyo-Olarte, R.D., Imkeller, K., Hegemann, P., Lucius, R., Gupta, N., 2013. Optogenetic modulation of an adenylate cyclase in *Toxoplasma gondii* demonstrates a requirement of the parasite cAMP for host-cell invasion and stage differentiation. J Biol Chem 288, 13705-13717.

Herm-Gotz, A., Agop-Nersesian, C., Munter, S., Grimley, J.S., Wandless, T.J., Frischknecht, F., Meissner, M., 2007. Rapid control of protein level in the apicomplexan *Toxoplasma gondii*. Nat Methods 4, 1003-1005.

Herm-Götz, A., Agop-Nersesian, C., Münter, S., Grimley, J.S., Wandless, T.J.,

Frischknecht, F., Meissner, M., 2007. Rapid control of protein level in the apicomplexan *Toxoplasma gondii*. Nat Methods 4, 1003-1005.

Hoon, S., St Onge, R.P., Giaever, G., Nislow, C., 2008. Yeast chemical genomics and drug discovery: an update. Trends Pharmacol Sci 29, 499-504.

Huang, H., Ma, Y.F., Bao, Y., Lee, H., Lisanti, M.P., Tanowitz, H.B., Weiss, L.M., 2011. Molecular cloning and characterization of mitogen-activated protein kinase 2 in *Toxoplasma gondii*. Cell Cycle 10, 3519-3526.

Huynh, M.H., Carruthers, V.B., 2006. *Toxoplasma* MIC2 is a major determinant of invasion and virulence. PLoS Pathog 2, e84.

Huynh, M.H., Carruthers, V.B., 2009. Tagging of endogenous genes in a *Toxoplasma gondii* strain lacking Ku80. Eukaryot Cell 8, 530-539.

Innes, E.A., Bartley, P.M., Maley, S., Katzer, F., Buxton, D., 2009. Veterinary vaccines against *Toxoplasma gondii*. Mem Inst Oswaldo Cruz 104, 246-251.

Jones, D.T., 1999. Protein secondary structure prediction based on position-specific scoring matrices. J Mol Biol 292, 195-202.

Jones, J.L., Dubey, J.P., 2012. Foodborne toxoplasmosis. Clin Infect Dis 55, 845-851.

Karasov, A.O., Boothroyd, J.C., Arrizabalaga, G., 2005. Identification and disruption of a rhoptry-localized homologue of sodium hydrogen exchangers in *Toxoplasma gondii*. Int J Parasitol 35, 285-291.

Kato, K., Kawaguchi, Y., Tanaka, M., Igarashi, M., Yokoyama, A., Matsuda, G., Kanamori, M., Nakajima, K., Nishimura, Y., Shimojima, M., Phung, H.T., Takahashi, E.,

Hirai, K., 2001. Epstein-Barr virus-encoded protein kinase BGLF4 mediates hyperphosphorylation of cellular elongation factor 1delta (EF-1delta): EF-1delta is universally modified by conserved protein kinases of herpesviruses in mammalian cells. J Gen Virol 82, 1457-1463.

Kato, N., Sakata, T., Breton, G., Le Roch, K.G., Nagle, A., Andersen, C., Bursulaya, B., Henson, K., Johnson, J., Kumar, K.A., Marr, F., Mason, D., McNamara, C., Plouffe, D., Ramachandran, V., Spooner, M., Tuntland, T., Zhou, Y., Peters, E.C., Chatterjee, A., Schultz, P.G., Ward, G.E., Gray, N., Harper, J., Winzeler, E.A., 2008. Gene expression signatures and small-molecule compounds link a protein kinase to Plasmodium falciparum motility. Nat Chem Biol 4, 347-356.

Khan, F., Tang, J.Z., Qin, C.L., Kim, K., 2002. Cyclin-dependent kinase TPK2 is a critical cell cycle regulator in *Toxoplasma gondii*. Molecular Microbiology 45, 321-332.

Kieschnick, H., Wakefield, T., Narducci, C.A., Beckers, C., 2001. *Toxoplasma gondii* attachment to host cells is regulated by a calmodulin-like domain protein kinase. J Biol Chem 276, 12369-12377.

Konrad, C., Queener, S.F., Wek, R.C., Sullivan, W.J., 2013. Inhibitors of eIF2α dephosphorylation slow replication and stabilize latency in *Toxoplasma gondii*. Antimicrob Agents Chemother 57, 1815-1822.

Krupa, A., Abhinandan, K.R., Srinivasan, N., 2004. KinG: a database of protein kinases in genomes. Nucleic Acids Res 32, D153-155.

Kurokawa, H., Kato, K., Iwanaga, T., Sugi, T., Sudo, A., Kobayashi, K., Gong, H., Takemae, H., Recuenco, F.C., Horimoto, T., Akashi, H., 2011. Identification of

Toxoplasma gondii cAMP Dependent Protein Kinase and Its Role in the Tachyzoite Growth. PLoS ONE 6, e22492.

Larson, E.T., Ojo, K.K., Murphy, R.C., Johnson, S.M., Zhang, Z., Kim, J.E., Leibly, D.J., Fox, A.M., Reid, M.C., Dale, E.J., Perera, B.G., Kim, J., Hewitt, S.N., Hol, W.G., Verlinde, C.L., Fan, E., Van Voorhis, W.C., Maly, D.J., Merritt, E.A., 2012. Multiple determinants for selective inhibition of apicomplexan calcium-dependent protein kinase CDPK1. J Med Chem 55, 2803-2810.

Letunic, I., Doerks, T., Bork, P., 2009. SMART 6: recent updates and new developments. Nucleic Acids Res 37, D229-232.

Li, H., Handsaker, B., Wysoker, A., Fennell, T., Ruan, J., Homer, N., Marth, G., Abecasis, G., Durbin, R., Subgroup, G.P.D.P., 2009. The Sequence Alignment/Map format and SAMtools. Bioinformatics 25, 2078-2079.

Lourido, S., Shuman, J., Zhang, C., Shokat, K.M., Hui, R., Sibley, L.D., 2010. Calcium-dependent protein kinase 1 is an essential regulator of exocytosis in *Toxoplasma*. Nature 465, 359-362.

Lourido, S., Zhang, C., Lopez, M.S., Tang, K., Barks, J., Wang, Q., Wildman, S.A., Shokat, K.M., Sibley, L.D., 2013. Optimizing small molecule inhibitors of calcium-dependent protein kinase 1 to prevent infection by *Toxoplasma gondii*. J Med Chem 56, 3068-3077.

Marchler-Bauer, A., Lu, S., Anderson, J.B., Chitsaz, F., Derbyshire, M.K., DeWeese-Scott, C., Fong, J.H., Geer, L.Y., Geer, R.C., Gonzales, N.R., Gwadz, M., Hurwitz, D.I., Jackson, J.D., Ke, Z., Lanczycki, C.J., Lu, F., Marchler, G.H.,

Mullokandov, M., Omelchenko, M.V., Robertson, C.L., Song, J.S., Thanki, N., Yamashita, R.A., Zhang, D., Zhang, N., Zheng, C., Bryant, S.H., 2011. CDD: a Conserved Domain Database for the functional annotation of proteins. Nucleic Acids Res 39, D225-229.

McLeod, R., Kieffer, F., Sautter, M., Hosten, T., Pelloux, H., 2009. Why prevent, diagnose and treat congenital toxoplasmosis? Mem Inst Oswaldo Cruz 104, 320-344.

Meissner, M., Schlüter, D., Soldati, D., 2002. Role of *Toxoplasma gondii* myosin A in powering parasite gliding and host cell invasion. Science 298, 837-840.

Miller, N.L., Frenkel, J.K., Dubey, J.P., 1972. Oral infections with Toxoplasma cysts and oocysts in felines, other mammals, and in birds. J Parasitol 58, 928-937.

Miranda-Saavedra, D., Gabaldón, T., Barton, G.J., Langsley, G., Doerig, C., 2012. The kinomes of apicomplexan parasites. Microbes Infect 14, 796-810.

Murphy, R.C., Ojo, K.K., Larson, E.T., Castellanos-Gonzalez, A., Perera, B.G., Keyloun, K.R., Kim, J.E., Bhandari, J.G., Muller, N.R., Verlinde, C.L., White, A.C., Jr., Merritt, E.A., Van Voorhis, W.C., Maly, D.J., 2010. Discovery of Potent and Selective Inhibitors of Calcium-Dependent Protein Kinase 1 (CDPK1) from *C. parvum* and *T. gondii*. ACS Med Chem Lett 1, 331-335.

Nagamune, K., Moreno, S.N., Sibley, L.D., 2007. Artemisinin-resistant mutants of Toxoplasma gondii have altered calcium homeostasis. Antimicrobial Agents and Chemotherapy 51, 3816-3823.

Narasimhan, J., Joyce, B.R., Naguleswaran, A., Smith, A.T., Livingston, M.R., Dixon, S.E., Coppens, I., Wek, R.C., Sullivan, W.J., 2008. Translation regulation by eukaryotic initiation factor-2 kinases in the development of latent cysts in *Toxoplasma gondii*.

Journal of Biological Chemistry 283, 16591-16601.

Nissapatorn, V., 2009. Toxoplasmosis in HIV/AIDS: a living legacy. Southeast Asian J Trop Med Public Health 40, 1158-1178.

O'Connell, E., Wilkins, M.F., Te Punga, W.A., 1988. Toxoplasmosis in sheep. II. The ability of a live vaccine to prevent lamb losses after an intravenous challenge with *Toxoplasma gondii*. N Z Vet J 36, 1-4.

Ojo, K.K., Larson, E.T., Keyloun, K.R., Castaneda, L.J., DeRocher, A.E., Inampudi, K.K., Kim, J.E., Arakaki, T.L., Murphy, R.C., Zhang, L., Napuli, A.J., Maly, D.J., Verlinde, C., Buckner, F.S., Parsons, M., Hol, W.G.J., Merritt, E.A., Van Voorhis, W.C., 2010. *Toxoplasma gondii* calcium-dependent protein kinase 1 is a target for selective kinase inhibitors. Nature Structural & Molecular Biology 17, 602-U102.

Ojo, K.K., Pfander, C., Mueller, N.R., Burstroem, C., Larson, E.T., Bryan, C.M., Fox, A.M., Reid, M.C., Johnson, S.M., Murphy, R.C., Kennedy, M., Mann, H., Leibly, D.J., Hewitt, S.N., Verlinde, C.L., Kappe, S., Merritt, E.A., Maly, D.J., Billker, O., Van Voorhis, W.C., 2012. Transmission of malaria to mosquitoes blocked by bumped kinase inhibitors. J Clin Invest 122, 2301-2305.

Pappas, G., Roussos, N., Falagas, M.E., 2009. Toxoplasmosis snapshots: global status of *Toxoplasma gondii* seroprevalence and implications for pregnancy and congenital toxoplasmosis. Int J Parasitol 39, 1385-1394.

Petersen, E., Liesenfeld, O., 2007. Clinical Disease and Diagnostics, in: Kim, W.a. (Ed.), *Toxoplasma gondii*. The Model Apicomplexan-Perspectives and Methods. Elsevier, pp. 81-100.

Pettersen, E.F., Goddard, T.D., Huang, C.C., Couch, G.S., Greenblatt, D.M., Meng, E.C., Ferrin, T.E., 2004. UCSF Chimera--a visualization system for exploratory research and analysis. J Comput Chem 25, 1605-1612.

Pomel, S., Luk, F.C., Beckers, C.J., 2008. Host cell egress and invasion induce marked relocations of glycolytic enzymes in *Toxoplasma gondii* tachyzoites. PLoS Pathog 4, e1000188.

Rabenau, K.E., Sohrabi, A., Tripathy, A., Reitter, C., Ajioka, J.W., Tomley, F.M., Carruthers, V.B., 2001. TgM2AP participates in *Toxoplasma gondii* invasion of host cells and is tightly associated with the adhesive protein TgMIC2. Mol Microbiol 41, 537-547.

Radke, J.B., Lucas, O., De Silva, E.K., Ma, Y., Sullivan, W.J., Weiss, L.M., Llinas, M., White, M.W., 2013. ApiAP2 transcription factor restricts development of the *Toxoplasma* tissue cyst. Proc Natl Acad Sci U S A 110, 6871-6876.

Radke, J.R., Donald, R.G., Eibs, A., Jerome, M.E., Behnke, M.S., Liberator, P., White, M.W., 2006. Changes in the expression of human cell division autoantigen-1 influence *Toxoplasma gondii* growth and development. Plos Pathogens 2, 964-974.

Ray, A., Cowan-Jacob, S.W., Manley, P.W., Mestan, J., Griffin, J.D., 2007. Identification of BCR-ABL point mutations conferring resistance to the Abl kinase inhibitor AMN107 (nilotinib) by a random mutagenesis study. Blood 109, 5011-5015.

Reischl, U., Bretagne, S., Kruger, D., Ernault, P., Costa, J.M., 2003. Comparison of two DNA targets for the diagnosis of Toxoplasmosis by real-time PCR using fluorescence resonance energy transfer hybridization probes. BMC Infect Dis 3, 7.

Remington, J.S., 1974. Toxoplasmosis in the adult. Bull N Y Acad Med 50, 211-227.

Roos, D.S., Donald, R.G., Morrissette, N.S., Moulton, A.L., 1994. Molecular tools for genetic dissection of the protozoan parasite *Toxoplasma gondii*. Methods Cell Biol 45, 27-63.

Saeij, J.P.J., Boyle, J.P., Coller, S., Taylor, S., Sibley, L.D., Brooke-Powell, E.T., Ajioka, J.W., Boothroyd, J.C., 2006. Polymorphic secreted kinases are key virulence factors in toxoplasmosis. Science 314, 1780-1783.

Sakikawa, M., Noda, S., Hanaoka, M., Nakayama, H., Hojo, S., Kakinoki, S., Nakata, M., Yasuda, T., Ikenoue, T., Kojima, T., 2012. Anti-*Toxoplasma* antibody prevalence, primary infection rate, and risk factors in a study of toxoplasmosis in 4,466 pregnant women in Japan. Clin Vaccine Immunol 19, 365-367.

Salomon, D., Bonshtien, A., Sessa, G., 2009. A chemical-genetic approach for functional analysis of plant protein kinases. Plant Signal Behav 4, 645-647.

Shokat, K., Velleca, M., 2002. Novel chemical genetic approaches to the discovery of signal transduction inhibitors. Drug Discov Today 7, 872-879.

Sugi, T., Kato, K., Kobayashi, K., Pandey, K., Takemae, H., Kurokawa, H., Tohya, Y., Akashi, H., 2009. Molecular analyses of *Toxoplasma gondii* calmodulin-like domain protein kinase isoform 3. Parasitology International 58, 416-423.

Sugi, T., Kato, K., Kobayashi, K., Watanabe, S., Kurokawa, H., Gong, H., Pandey, K., Takemae, H., Akashi, H., 2010. Use of the Kinase Inhibitor Analog 1NM-PP1 Reveals a Role for *Toxoplasma gondii* CDPK1 in the Invasion Step. Eukaryotic Cell 9, 667-670.

Sullivan, W.J., Narasimhan, J., Bhatti, M.M., Wek, R.C., 2004. Parasite-specific eIF2 (eukaryotic initiation factor-2) kinase required for stress-induced translation control.

Biochemical Journal 380, 523-531.

Taylor, S., Barragan, A., Su, C., Fux, B., Fentress, S.J., Tang, K., Beatty, W.L., El Hajj, H., Jerome, M., Behnke, M.S., White, M., Wootton, J.C., Sibley, L.D., 2006. A secreted serine-threonine kinase determines virulence in the eukaryotic pathogen *Toxoplasma gondii*. Science 314, 1776-1780.

Tenter, A.M., Heckeroth, A.R., Weiss, L.M., 2000. *Toxoplasma gondii*: from animals to humans. Int J Parasitol 30, 1217-1258.

Thalhamer, T., McGrath, M.A., Harnett, M.M., 2008. MAPKs and their relevance to arthritis and inflammation. Rheumatology (Oxford) 47, 409-414.

Unno, A., Suzuki, K., Batanova, T., Cha, S., Jang, H., Kitoh, K., Takashima, Y., 2009. Visualization of *Toxoplasma gondii* stage conversion by expression of stage-specific dual fluorescent proteins. Parasitology 136, 579-588.

Unno, A., Suzuki, K., Xuan, X., Nishikawa, Y., Kitoh, K., Takashima, Y., 2008. Dissemination of extracellular and intracellular *Toxoplasma gondii* tachyzoites in the blood flow. Parasitol Int 57, 515-518.

Vidal, J.E., Hernandez, A.V., de Oliveira, A.C., Dauar, R.F., Barbosa, S.P., Focaccia, R., 2005. Cerebral toxoplasmosis in HIV-positive patients in Brazil: clinical features and predictors of treatment response in the HAART era. AIDS Patient Care STDS 19, 626-634.

Wagner, E.F., Nebreda, A.R., 2009. Signal integration by JNK and p38 MAPK pathways in cancer development. Nat Rev Cancer 9, 537-549.

Walker, R., Gissot, M., Croken, M.M., Huot, L., Hot, D., Kim, K., Tomavo, S., 2013. The *Toxoplasma* nuclear factor TgAP2XI-4 controls bradyzoite gene expression and cyst formation. Mol Microbiol 87, 641-655.

Wang, H., Shimizu, E., Tang, Y.P., Cho, M., Kyin, M., Zuo, W., Robinson, D.A., Alaimo, P.J., Zhang, C., Morimoto, H., Zhuo, M., Feng, R., Shokat, K.M., Tsien, J.Z., 2003. Inducible protein knockout reveals temporal requirement of CaMKII reactivation for memory consolidation in the brain. Proc Natl Acad Sci U S A 100, 4287-4292.

Wei, S., Marches, F., Daniel, B., Sonda, S., Heidenreich, K., Curiel, T., 2002. Pyridinylimidazole p38 mitogen-activated protein kinase inhibitors block intracellular *Toxoplasma gondii* replication. International Journal for Parasitology 32, 969-977.

Weisberg, E., Griffin, J.D., 2000. Mechanism of resistance to the ABL tyrosine kinase inhibitor STI571 in BCR/ABL-transformed hematopoietic cell lines. Blood 95, 3498-3505.

Wetzel, D.M., Hakansson, S., Hu, K., Roos, D., Sibley, L.D., 2003. Actin filament polymerization regulates gliding motility by apicomplexan parasites. Mol Biol Cell 14, 396-406.

Wulf, M.W., van Crevel, R., Portier, R., Ter Meulen, C.G., Melchers, W.J., van der Ven, A., Galama, J.M., 2005. Toxoplasmosis after renal transplantation: implications of a missed diagnosis. J Clin Microbiol 43, 3544-3547.

Yamamoto, M., Standley, D.M., Takashima, S., Saiga, H., Okuyama, M., Kayama, H., Kubo, E., Ito, H., Takaura, M., Matsuda, T., Soldati-Favre, D., Takeda, K., 2009. A single polymorphic amino acid on *Toxoplasma gondii* kinase ROP16 determines the direct and

strain-specific activation of Stat3. Journal of Experimental Medicine 206, 2747-2760.

Yang, N., Farrell, A., Niedelman, W., Melo, M., Lu, D., Julien, L., Marth, G.T., Gubbels, M.J., Saeij, J.P., 2013. Genetic basis for phenotypic differences between different *Toxoplasma gondii* type I strains. BMC Genomics 14, 467.

Zhang, W., Liu, H.T., 2002. MAPK signal pathways in the regulation of cell proliferation in mammalian cells. Cell Res 12, 9-18.

List of publications

1. Kobayashi, K., Takano, R., Takemae, H., **Sugi, T.**, Ishiwa, A., Gong, H., Recuenco, F.C., Iwanaga, T., Horimoto, T., Akashi, H., Kato, K. Analyses of Interactions Between Heparin and the Apical Surface Proteins of *Plasmodium falciparum*. **Scientific Reports,** vol. 3, Article number: 3178, 2013.
2. Takemae, H., **Sugi, T.**, Kobayashi, K., Gong, H., Ishiwa, A., Recuenco, F.C., Murakoshi, F., Iwanaga, T., Inomata, A., Horimoto, T., Akashi, H., Kato, K. Characterization of the interaction between *Toxoplasma gondii* rhoptry neck protein 4 and host cellular ß-tubulin. **Scientific Reports**, vol. 3, Article number: 3199, 2013.
3. Ishiwa, A., Kobayashi, K., Takemae, H., **Sugi, T.**, Gong, H., Recuenco, F.C., Murakoshi, F., Inomata, A., Horimoto, T., Kato, K. Effects of dextran sulfates on the acute infection and growth stages of *Toxoplasma gondii*. **Parasitol Res,** vol. 112, pp4169-4176, 2013.
4. **Sugi, T.**, Kobayashi, K., Kurokawa, H., Takemae, H., Gong, H., Ishiwa, A., Murakoshi, F., Recuenco, FC., Iwanaga, T., Horimoto T., Akashi, H., Kato, K. Identification of mutations in TgMAPK1 of *Toxoplasma gondii* conferring resistance to 1NM-PP1. **Int J Parasitol Drugs Drug Resist**, vol. 4, pp93–101, 2013.
5. Iwanaga, T., **Sugi, T.**, Kobayashi, K., Takemae, H., Gong, H., Ishiwa, A., Murakoshi, F., Recuenco, FC., Horimoto T., Akashi, H., Kato, K. Characterization of *Plasmodium falciparum* cdc2-related kinase and the effects of a CDK inhibitor on the parasites in erythrocytic schizogony.

Parasitol Int, vol. 62(5), pp423-430, 2013.

6. Gong, H., Kobayashi, K., **Sugi, T.,** Takemae, H., Kurokawa, H., Horimoto, T., Akashi, H., Kato, K. A novel PAN/apple domain-containing protein from *Toxoplasma gondii*: characterization and receptor identification. **PLoS One**, vol. 7, pp e30169, 2012.
7. **Sugi, T.,** Kato, K., Kobayashi, K., Kurokawa, H., Takemae, H., Gong, H., Recuenco, FC., Iwanaga, T., Horimoto T., Akashi, H., 1NM-PP1 treatment of mice infected with *Toxoplasma gondii*. **J Vet Med Sci**., vol. 73, pp1377-1379, 2011.
8. Kurokawa, H., Kato, K., Iwanaga, T., **Sugi, T.**, Sudo, A., Kobayashi, K., Gong, H., Takemae, H., Recuenco, F.C., Horimoto, T., Akashi, H. Identification of *Toxoplasma gondii* cAMP dependent protein kinase and its role in the tachyzoite growth. **PLoS One.** vol. 6, pp e22492, 2011.
9. **Sugi, T.**, Kato, K., Kobayashi, K., Watanabe, S., Kurokawa, H., Gong, H., Pandey, K., Takemae, H. & Akashi, H. Use of the kinase inhibitor analog 1NM-PP1 reveals a role for *Toxoplasma gondii* CDPK1 in the invasion step. **Eukaryot Cell,** vol. 9, pp667-670, 2010.
10. Kobayashi, K., Kato, K., **Sugi, T.**, Takemae, H., Pandey, K., Haiyan, G., Tohya, Y. & Akashi, H. *Plasmodium falciparum* BAEBL binds to heparan sulfate proteoglycans on the human erythrocyte surface. **J Biol Chem**, vol. 285, pp1716-1725, 2010.
11. **Sugi, T.**, Kato, K., Kobayashi, K., Pandey, K., Takemae, H., Kurokawa, H., Tohya, Y. & Akashi, H. Molecular analyses of *Toxoplasma gondii* calmodulin-like domain protein kinase isoform 3. **Parasitol Int**, vol. 58,

pp416-423, 2009.

12. Kato, K., Sudo, A., Kobayashi, K., **Sugi, T.**, Tohya, Y. & Akashi, H. Characterization of *Plasmodium falciparum* calcium-dependent protein kinase 4. **Parasitol Int**, vol. 58, pp 394-400, 2009.
13. Kobayashi, K., Kato, K., **Sugi, T.**, Yamane, D., Shimojima, M., Tohya, Y. & Akashi, H. Application of retrovirus-mediated expression cloning for receptor screening of a parasite. **Anal Bio Chem**, vol. 389, pp80-82, 2009.

Review

14. **杉 達紀**、加藤健太郎 トキソプラズマのステージ変換制御とシグナル伝達 獣医寄生虫学会誌１２巻２号（2013 年 12 月 31 日発刊）(accepted)
15. Kato, K., **Sugi, T.**, Iwanaga, T. Roles of Apicomplexan protein kinases at each life cycle stage. **Parasitol Int**, vol. 61, pp224-34, 2012.

Summary in Japanese

論　文　の　内　容　の　要　旨

獣医学　専攻

平成 22 年度博士課程　入学

氏　　名　杉　達紀

指導教員名　堀本泰介

論文題目　Molecular analyses of *Toxoplasma gondii* protein kinase signals in parasite growth and differentiation

（トキソプラズマの増殖および分化に関わる
原虫プロテインキナーゼシグナルの分子生物学的解析）

Toxoplasma gondii (以下トキソプラズマ)は、トキソプラズマ症を引き起こす病原体である。本原虫はアピコンプレクサ門に属する原虫で、同門に属するマラリア原虫やクリプトスポリジウム、ネオスポラなどの病原原虫と近縁である。これらの原虫では、市販されている有効なワクチンが存在しない。薬剤による治療には、耐性原虫や副作用といった問題がある。本研究では、抗原虫作用を持つ薬剤の標的候補および、薬剤耐性に関わる機序について着目し、トキソプラズマが持つプロテインキナーゼが原虫の生存に果たす役割について解析を行った。

トキソプラズマのプロテインキナーゼが原虫の増殖や細胞の分化に関わることは、従来の阻害剤を利用した研究により証明されている。しかし、個別のプロテインキナーゼがどのような細胞機能を果たし、抗原虫薬剤の標的となりうるのかについては、未解明なところが多い。

第一章、第二章では、プロテインキナーゼの細胞内機能解析の手段として *ASKA-GI*（*Analog sensitive kinase allele based-Gene Inhibition*）をトキソプラズマでのプロテインキナーゼ解析に応用した。その結果として、*T. gondii C*alcium dependent protein kinase 1 (TgCDPK1) が原虫の侵入、ひいては効率的な原虫の増殖における重要な役割を果たすことを明らかにした。また、TgCDPK1 を主標的とする阻害剤である 1NM-PP1 が特異的な抗トキソプラズマ活性を示すことを明らかにした。第 2 章においては *ASKA-GI* が *in vivo* のマウス感染モデルにおいても適用可能であることを検証した。

ASKA-GI のトキソプラズマへの応用を検討する中で、1NM-PP1 を含む「こぶつきキナーゼ阻害剤」（*analog sensitive kinase allele* を選択的に阻害する低分子化合物）に感受性のプロテインキナーゼがトキソプラズマのゲノムに非常に多くコードされていることを発見した。これは哺乳類ゲノムにはない特徴である。「こぶつきキナーゼ阻害剤」がトキソプラズマに特異的な薬剤クラスと考えられることから、このクラスのさらなる薬剤妥当性を検討するため、原虫による薬剤耐性の獲得について解析した。第三章においては、化学無作為変異で得られた原虫ライブラリの中から薬剤耐性原虫を選択し、原因変異点として TgMAPK1 遺伝子内のアミノ酸置換を同定した。

トキソプラズマへの対策が困難である理由の一つとして、トキソプラズマによる潜伏感染が挙げられる。潜伏感染状態のトキソプラズマは環境抵抗性のシスト壁に包まれ、薬剤

による排除を受けない。また、食肉生産家畜において潜伏感染が成立することで、食肉中に含まれるシストが感染源として問題となる。トキソプラズマのプロテインキナーゼの中で *MAPK* ファミリーは潜伏感染への移行を司ることが示唆されているが、先行の研究では潜伏感染を引き起こす標的の具体的な遺伝子は未解明であった。第四章において、第三章で同定された *TgMAPK1* に変異を持つ原虫を用いて、*TgMAPK1* の原虫における役割について詳細な解析を行った。*1NM-PP1* は親株のトキソプラズマには、潜伏感染状態への細胞分化を誘導したが、*TgMAPK1* に耐性型の変異が導入されることで分化誘導が起こらなくなった。*TgMAPK1* の機能阻害がどのようにして分化誘導につながるかを明らかにするため、トキソプラズマの増殖における *TgMAPK1* の機能を解析した。その結果、細胞の分裂速度の維持に *TgMAPK1* が役割を果たしていることが明らかになった。

本論文において、筆者はトキソプラズマのプロテインキナーゼの原虫の増殖および細胞分化における役割について、その機能と薬剤標的としての妥当性の両面において解析を試みた。今回トキソプラズマに適用可能であることを示した *ASKA-GI* は、トキソプラズマが持つプロテインキナーゼの解析において強力な力を発揮する道具となる。また、こぶつきキナーゼ阻害剤は抗トキソプラズマ薬の有効な候補低分子クラスとして有望である。本論文で明らかになった細胞分化における *TgMAPK1* の機能は、トキソプラズマの「速い増殖と潜伏を切り替える」という寄生戦略に迫る足掛かりになる。また、トキソプラズマの潜伏感染状態を標的とする薬剤開発の標的候補分子を提供することが期待される。